THE EFFECTS OF cGAS-STING-TBK1 PATHWAY AND NKT CELL-ACTIVATING LIGAND ALPHA-GALACTOSYLCERAMIDE ON LEISHMANIA MAJOR INFECTION AND PROTECTION

A THESIS SUBMITTED TO
THE GRADUATE SCHOOL OF NATURAL AND APPLIED SCIENCES
OF
MIDDLE EAST TECHNICAL UNIVERSITY

BY

EMRE DÜNÜROĞLU

IN PARTIAL FULFILLMENT OF THE REQUIREMENTS
FOR
THE DEGREE OF MASTER OF SCIENCE
IN
MOLECULER BIOLOGY AND GENETICS

FEBRUARY 2022

Approval of the thesis:

THE EFFECTS OF cGAS-STING-TBK1 PATHWAY AND NKT CELL-ACTIVATING LIGAND ALPHA-GALACTOSYLCERAMIDE ON LEISHMANIA MAJOR INFECTION AND PROTECTION

submitted by **EMRE DÜNÜROĞLU** in partial fulfillment of the requirements for the degree of **Master of Science** in **Molecular Biology and Genetics, Middle East Technical University** by,

Prof. Dr. Halil Kalıpçılar
Dean, Graduate School of **Natural and Applied Sciences** _____

Prof. Dr. Ayşegül Gözen
Head of the Department, **Biological Sciences** _____

Prof. Dr. Mayda Gürsel
Supervisor, **Biological Sciences, METU** _____

Examining Committee Members:

Assoc. Prof. Dr. Yasemin Özsürekçi
Internal Medicine Sciences, Hacettepe Üniversity _____

Prof. Dr. Mayda Gürsel
Biological Sciences, METU _____

Asst. Prof. Dr. Banu Bayyurt Kocabaş
Biological Sciences, METU _____

Date: 08.02.2022

I hereby declare that all information in this document has been obtained and presented in accordance with academic rules and ethical conduct. I also declare that, as required by these rules and conduct, I have fully cited and referenced all material and results that are not original to this work.

Name Last name: Emre Dünüroğlu

Signature:

ABSTRACT

THE EFFECTS OF cGAS-STING-TBK1 PATHWAY AND NKT CELL-ACTIVATING LIGAND ALPHA-GALACTOSYLCERAMIDE ON LEISHMANIA MAJOR INFECTION AND PROTECTION

Dünüroğlu, Emre
Master of Science, Molecular Biology and Genetics
Supervisor: Prof. Dr. Mayda Gürsel

February 2022, 171 pages

Leishmaniasis is a multi-faceted group of diseases caused by various species of Leishmania protozoa. Depending on the infecting Leishmania species, the disease manifests as recurrent cutaneous, mucocutaneous or visceral leishmaniasis all of which can be devastating for infected individuals. Lack of a protective vaccine and the rise of drug resistances in Leishmania spp. prompted us to explore preventative vaccine candidates and novel drugs against Leishmania major.

In the first part of this thesis, we evaluated the role of cGAS-STING-TBK1 DNA-sensing pathway in the context of Leishmania major infection. Our findings showed that the absence of cGAS, STING or TBK1 proteins significantly diminished parasite loads of differentiated THP-1 macrophages. In contrast to STING-KO THP-1 cells, this effect was not due to reduced phagocytic capacities of cGAS- and TBK1-KO THP-1 cells. Similarly, gene expression analysis pointed to increased expression of genes which code for proteins that may aid in parasite control in KO cell lines. Furthermore, treatment of WT THP-1 cells with amlexanox, a TBK1 inhibitor, reduced both phagocytosis of Leishmania major promastigotes and replication of amastigotes inside phagolysosomes. Our results suggest that cGAS-STING-TBK1 pathway might be exploited by Leishmania major to promote a pro-parasitic

environment in macrophages which can partially be reversed with the TBK1 inhibitor, amlexanox.

In the second part of this thesis, we examined the degree of immunoprotection induced by Leishmania major exosomes, soluble Leishmania antigens (SLA) or whole lyophilized parasites combined with an NKT-cell inducing ligand, α-Galactosylceramide (α-GalCer), in BALB/c mice. While all of the vaccine candidates protected against Leishmania major, SLA and lyophilized parasites combined with α-GalCer were the most promising groups amongst them.

Keywords: Cutaneous leishmaniasis, DNA-sensing, Amlexanox, α-Galactosylceramide, Immunization

ÖZ

cGAS-STING-TBK1 YOLAĞININ VE DOĞAL KATİL T-HÜCRELERİ AKTİFLEŞTİREN LİGAND ALFA-GALAKTOSİLSERAMİD'İN LEISHMANIA MAJOR ENFEKSİYONU VE KORUNMASINDAKİ ETKİLERİ

Dünüroğlu, Emre
Yüksek Lisans, Moleküler Biyoloji ve Genetik
Tez Yöneticisi: Prof. Dr. Mayda Gürsel

Şubat 2022, 171 sayfa

Leishmaniasis, Leishmania tek hücreli parazitlerinin sebep olduğu çok yönlü bir hastalıktır. Enfeksiyona sebep olan Leishmania parazitlerinin suşuna bağlı olarak, hastalık kendini tekrarlı kutanöz, mukozal veya viseral olarak gösterebilir. Leishmaniasis hastalığına karşı uygulanan koruyucu bir aşının bulunmaması ve Leishmania parazitlerinin ilaçlara karşı direnç geliştirmeye başlaması, bizi koruyucu aşı adayları ve yeni ilaçları keşfetmeye yöneltmiştir.

Bu tezin ilk bölümünde, cGAS-STING-TBK1 DNA-algılama yolağının Leishmania enfeksiyonu üzerindeki etkisini inceledik. Sonuçlarımız, cGAS, STING veya TBK1 proteinlerinin yokluğunda enfekte edilen THP-1 tipi makrofajların parazit yüklerinde anlamlı ölçüde düşüş olduğunu gösterdi. Bu etkinin cGAS- ve TBK1-KO hücrelerin fagositoz mekanizmalarındaki bir yetersizlikten kaynaklanmadığını gösterdik. Bununla beraber, KO hücre hatlarında paraziti kontrol altında tutabilecek RNA'ların anlatım seviyelerinin artmış olduğunu gen anlatım analizi yaparak gözlemledik. Sonrasında, TBK1 inhibitörü amlexanox eşliğinde enfekte edilen vahşi tip THP-1 makrofajlarda, Leishmania major parazitlerinin fagositozunun ve fagolizozomlar içerisindeki replikasyonunun düştüğünü ortaya koyduk. Elde edilen

bulgular, cGAS-STING-TBK1 yolağının Leishmania major parazitleri tarafından suistimal edilerek makrofajların içerisinde çoğalabilecekleri bir ortam yaratmış olabileceklerine işaret etmekte ve bu etkinin TBK1 inhibitörü amlexanox ile engellenebileceğini göstermektedir.

Bu tezin ikinci bölümünde, Leishmania major eksozomlarının, çözünmüş Leishmania antijenlerinin (SLA) veya bütün olarak liyofilize edilmiş Leishmania parazitlerinin NKT-hücre aktive eden ligand α-Galaktosilseramid (α-GalCer) ile kombine edilmesi sonrasında aşılanan BALB/c farelerde yarattığı immünoprotektif etkileri araştırdık. Elde edilen bulgular, en güçlü etkinin α-GalCer ile kombine edilen SLA ve liyofilize edilmiş parazitler ile sağlandığını ortaya koymuştur.

Anahtar Kelimeler: Kutanöz leishmaniasis, DNA-algılama, Amlexanox, α-Galactosylceramide, Aşılama

To my family and my love

ACKNOWLEDGMENTS

Firstly, I would like to thank Prof. Dr. Mayda Gürsel for her supervision and support during my master's education. She has been supportive and understanding for all the mistakes I made in my experiments throughout my learning process. Our scientific discussions and her enthusiasm improved me as a researcher.

Secondly, I would like to thank Prof. Dr. İhsan Gürsel for his help and guidance during the vaccination studies. I, specially, thank him for teaching me how to remove the cap of an insulin syringe without stabbing myself.

Thirdly, I would like to express my gratitude for thesis examining committee; Assoc. Prof. Dr. Yasemin Özsürekçi and Asst. Prof. Dr. Banu Bayyurt Kocabaş for sparing their valuable time to evaluate this thesis.

In addition, I would like to thank Bilgi Güngör, İhsan Cihan Ayanoğlu and İsmail Cem Yılmaz for their previous work in the *Leishmania* project. I, specially, thank İhsan Cihan Ayanoğlu for teaching me the ways of a researcher and improving my critical thinking skills.

I, also, want to thank my lab friends Başak Kayaoğlu, Yağmur Aydın, Büşranur Geçkin, Esin Alpdündar, İlayda Baydemir, Emre Mert İpekoğlu, Asena Şanlı, Naz Yılmaz and Neşe Güvençli for their friendship. Special thanks to Başak Kayaoğlu and Yağmur Aydın for their help in my last days in the laboratory. Without their help, I would not be able to finish my experiments. Also, I will remember our conversations with Büşranur Geçkin with a smile on my face. Moreover, I would like to thank the members of IG group, especially Muzaffer Yıldırım, for their help whenever I needed.

Most importantly, I would like to thank my love, Hoşnaz Tuğral, for supporting me throughout the light and dark times, and helping me in the laboratory when I was overwhelmed. Without her love and friendship, I would not be able to pull through.

TABLE OF CONTENTS

LIST OF TABLES

TABLES

LIST OF FIGURES

FIGURES

LIST OF ABBREVIATIONS

AP-1	Activator protein 1
APC	Antigen Presenting cell
cGAS	Cyclic GMP-AMP synthase
DTH	Delayed-type hypersensitivity
EGFP	Enhanced green fluorescent protein
FcγRs	Fc gamma receptors
GFP	Green fluorescent protein
GILPs	Glycoinositol phospholipids
GP63	Leishmanolysin
ISGs	Interferon-stimulated genes
iNOS	Inducible nitric oxide synthase
KO	Gene knockout
LPG	Lipophosphoglycan
MAC	Membrane attack complex
MHC-I	Major histocompatibility complex I
MHC-II	Major histocompatibility complex II
NADPH oxidase	Nicotinamide adenine dinucleotide phosphate oxidase
NFkB	Nuclear factor kappa B
NK cells	Natural killer cells
NKT cells	Natural killer T cells

NO	Nitric oxide
SHP-1	Tyrosine-protein phosphatase non-receptor type 6
SLA	Soluble Leishmania antigens
STING	Stimulator of interferon genes
TBK1	TANK-binding kinase 1
αGalCer	α-galactosylceramide

CHAPTER 1

INTRODUCTION

1.1 Leishmaniasis

Leishmaniasis is a neglected tropical disease reported over 90 countries in Asia, Middle East, Africa, Central and South America. Currently, estimates of cutaneous Leishmaniasis ranges from 700,000 to 1.2 million cases per year while estimates of visceral Leishmaniasis is less than 100,000 cases per year (Centers for Disease Control and Prevention, 2020). The most important risk factors include poverty, malnutrition and an immunocompromised state, affecting the poor people most severely (*World Health Organziation. Leishmaniasis.*, 2022). With the rising temperatures at the global scale, Leishmaniasis cases are expected to geographically spread and rise in number (González et al., 2010).

1.1.1 Representation of the Disease

There are over 20 species of *Leishmania* parasites categorized under *Trypanosomatidae* family and *Leishmania* genus. The most common forms causing cutaneous Leishmaniasis are *L. major, L. tropica* and *L. aethiopica* in the Eastern Hemisphere, and *L. amazonensis, L. Mexicana, L. braziliensis,* and *L. guyanensis* in the Western Hemisphere. On the other hand, visceral Leishmaniasis is caused by *L. donovani* and *L. infantum* in the Eastern Hemisphere, and *L. chagasi* in the Western Hemisphere. Depending on the infecting *Leishmania* species, the disease manifests as recurrent cutaneous, mucocutaneous or visceral leishmaniasis. Upon parasite establishment, cutaneous lesions develop into painless ulcers which may take weeks, and spontaneously heal over months to years or cause severe scarring and

disfigurement. Mucocutaneous lesions can progress more aggressively, and progressively destroy nasal, oral and/or pharyngeal mucosa leading to mutilating disease and even death due to aspiration pneumonia or respiratory obstruction. Visceral Leishmaniasis, can cause infection of the liver, spleen, blood and lymphatic system, and leads to death in 95% of the cases in the absence of treatment (Mann et al., 2021).

1.1.2 Life Cycle of *Leishmania*

The vector insects responsible from transmission of *Leishmania spp.* are *Phlebotomus spp.* in the Eastern Hemisphere and *Lutzomyia spp.* in the Western Hemisphere, which are commonly known as sandflies.

The life cycle starts with ingestion of infected monocytes during the blood feeding by the sand fly. Amastigote to procyclic promastigote transition occur, and promastigotes start proliferating in the blood meal. Within 2 to 3 days, parasites slow down their replicative process and transform into highly motile nectomonad promastigotes with long cell bodies in order to escape peritrophic matrix-encased blood meal and move into the anterior thoracic midgut lumen, where they bind to epithelium of the midgut to avoid being excreted from the digestive tract and transform into replicative leptomonad promastigotes with shorter cell bodies. Parasite proliferation in the midgut of the sandfly continues as well as the transformation of a portion of leptomonad promastigotes to highly mobile, infective, non-dividing metacyclic promastigotes. Large numbers of leptomonad promastigotes and detached metacyclic promastigotes accumulate in the anterior midgut and produce filamentous proteophosphoglycan, a gel like substance obstructing the digestive tract. Yet another transformation of leptomonad promastigotes to haptomonad promastigotes take place. In this haptomonad form, promastigotes strongly attach to the chitin lining of the stomodeal valve, forming HSP (haptomonad parasite sphere), ultimately occluding it and causing damage to it possibly through secreted chitinase. Obstruction of the digestive tract coupled with

damaged stomodeal valve results in regurgitation of the parasites into the mammalian host during the blood feeding (Bates, 2008; Dostálová & Volf, 2012; Gossage et al., 2003; Rogers, 2012; Serafim et al., 2018). Inside the mammalian target of *Leishmania spp.*, metacyclic promastigotes infect their ultimate host cell, macrophage, and transform into amastigote form and replicate intracellularly until subsequent blood feeding by the sandfly, completing the life cycle. The interaction of the immune system of the mammalian host with the parasite is complex, and further explained in Section 1.2.

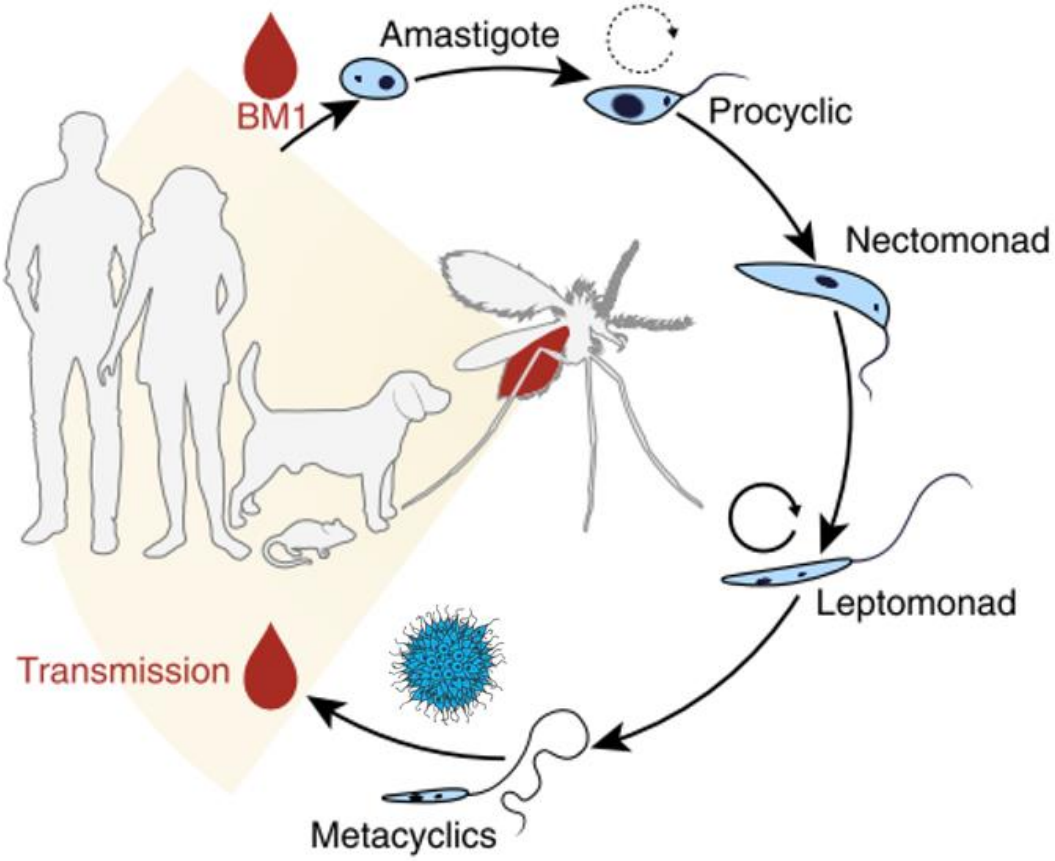

Figure 1.1. Schematic representation of the life cycle of *Leishmania* parasites (adopted from Serafim et al., 2018).

The dense blue parasite aggregate represents haptomonad parasite sphere.

1.1.3 Treatment Options for Leishmaniasis

Drugs used in the treatment of Leishmaniasis include pentavalent antimonials (such as sodium stibogluconate), amphotericin deoxycholate, liposomal amphotericin B, pentamidine, oral miltefosine, azoles-fluconazole and ketoconazole. Even though some are better tolerated, all of these drugs are toxic and have numerous side effects. Although cutaneous lesions caused by *L. major* and *L. Mexicana* self-resolve, for persistent and numerous lesions, treatment is recommended. Treatments include laser-therapy, thermotherapy, topical paromomycin and intralesional injections of antimonials. For mucocutaneous and visceral Leishmaniasis, systemic drug administration is required (Aronson et al., 2016; Mann et al., 2021).

1.2 Immune Protection and Evasion in Leishmaniasis

Below, interactions of *Leishmania* with the innate and adaptive immune cells are summarized. Innate immune system and adaptive immune system are intrinsically linked. Therefore, it is impossible to explain one without the other. For this reason, the interactions between the cells of the two categories were mentioned whenever it was necessary, but the general summary of both systems in the context of Leishmaniasis was explained categorically.

1.2.1 Dynamics of Interaction of *Leishmania* with the Innate Immune System

Upon regurgitation of parasites into the mammalian host, the first immune defense *Leishmania* parasites must deal with is the complement system. Metacyclic promastigotes express high levels of protein kinases important in the phosphorylation of C3, C5 and C9 proteins preventing activation of classical and alternative pathways of membrane attack complex (MAC) insertion. In addition, GP63 (an important *Leishmania* virulence factor) cleaves C3b to C3bi which serves

as an opsonin and prevent C5 convertase formation. Subsequent recognition of C3bi by CR3 and phagocytosis of the parasites results in inhibition of IL-12 production important in differentiation of naïve CD4+ T cells to Th1 cells (Brittingham et al., 1995; Hermoso et al., 1991; Marth & Kelsall, 1997).

Although *Leishmania spp.* have developed strategies to evade the complement-mediated lysis, they are no match against the complement system in a prolonged fight, and prefer to deal with the host immune responses intracellularly. Neutrophils are the first cells to reach sandfly bite site upon *Leishmania* infection (Müller et al., 2001). Neutrophils were shown to produce anti-microbial factors such as nitric oxide, neutrophil elastase, platelet activating factor and neutrophil extracellular traps against *Leishmania* promastigotes (Mélanie Charmoy et al., 2007; Guimarães-Costa et al., 2009; Flavia L. Ribeiro-Gomes et al., 2007). However, the role of neutrophils in *Leishmania* infection is not clear since neutrophil-deficient Genista mice were resistant to infection by virulent strains of *L. mexicana* and *L. major* (Melanie Charmoy et al., 2016; Hurrell et al., 2015). Furthermore, salivary components of the sandfly, delivered alongside the metacyclic parasites, protected the parasites from neutrophil-mediated killing (Chagas et al., 2014). In support of these findings, parasite-infected and apoptotic neutrophils acted as trojan horses delivering the parasites in an enclosed cargo which suppressed microbicidal activity of macrophages and activation of dendritic cells, subsequently leading to inhibition of naïve CD4+ T cell to Th1 differentiation as well as CD8+ T-cell priming (F. L. Ribeiro-Gomes et al., 2015; Flavia L. Ribeiro-Gomes et al., 2012; G. van Zandbergen et al., 2004).

Unlike neutrophils, natural killer (NK) cells are not the first responders to sandfly bite, but they play an important role in the early infection by producing IFNγ and inducing IL-12 production in dendritic cells in lymph nodes which drives the initial Th1 differentiation of naïve CD4+ T cells (Bajénoff et al., 2006; Scharton & Scott, 1993). Moreover, NK cells were shown to mediate direct cytotoxic activity against *Leishmania* and induce iNOS in infected macrophages (Lieke et al., 2011; Prajeeth et al., 2011).

A distinct subset of T lymphocytes, natural killer T (NKT) cells, is characterized by expressing an invariant TCR on their plasma membrane. Invariant TCRs of NKT cells recognize glycolipids presented by MHC-I-like molecule, CD1d, on antigen presenting cells, and respond quickly upon stimulation (Brossay et al., 1998; Krovi & Gapin, 2018). The prototypical NKT cell agonist was derived from the marine sponge *Agelas mauritianus* and found to be a glycosphingolipid capable of inducing antitumor and immunostimulatory effects, and was named as α-galactosylceramide (αGalCer) (Natori et al., 1994). It is known that NKT cells can produce large quantities of IFN-γ and IL-4 (Macho-Fernandez & Brigl, 2015; Michel et al., 2008; Moreira-Teixeira et al., 2011, 2012). Similar to NK cells, NKT cells play key roles during the early infection by inhibiting apoptotic death of infected macrophages through induction of HSP65, which was found to be a protective factor in *Toxoplasma gondii* and *Leishmania major* infections (H Hisaeda et al., 1997; Hajime Hisaeda & Himeno, 1997; Ishikawa et al., 2000). NKT cell stimulation also led to increased IFNγ production by lymphocytes upon CD1d recognition of *L. donovani* lipophosphoglycan (LPG) and glycoinositol phospholipids (GILPs) in intrahepatic lymph nodes (Amprey et al., 2004), and contributed to parasite clearance in BALB/c mice, but led to exacerbation of the disease in C57Bl/6 mice (Stanley et al., 2008). Later on, it was suggested that LPG and GILPs actually dampened the activation of NKT cells (Belo et al., 2017). This dampening was reversed through competition assays utilizing αGalCer (Amprey et al., 2004; Belo et al., 2017). *In vivo* studies found similar results where the parasites partially escaped NKT cell activation and antagonized their response to prototypical NKT cell ligand αGalCer (Mattner et al., 2006), suggesting a protective role for NKT cells in Leishmaniasis.

Another innate immune cell type, proinflammatory monocytes, seem to react to *Leishmania* infection quite differently when compared to macrophages. CCL2-dependent recruitment of inflammatory monocytes leads to subsequent killing of the parasites through ROS induction unlike macrophages which require IFNγ stimulation for efficient leishmanicidal activity. Also, a portion of these monocytes differentiate into dendritic cells and migrate to lymph nodes where they produce IL-

12 to induce Th1 differentiation of naïve T cells (Goncalves et al., 2011; Scott & Novais, 2016). Subsequent migration of Th1 cells to the infection site and stimulation of infected macrophages with IFNγ results in parasite clearance.

Leishmania parasites have evolved numerous strategies to evade and exploit macrophage responses. Upon recognition by TLR2 on the plasma membrane, *L. major* recruited suppressor proteins SOCS-1 and SOCS-3 to prevent the induction of TNFα, IL-12 and NO. Similarly, *L. donovani* prevented the ubiquitination of TRAF6 by activating de-ubiquitinating enzyme A20 which subsequently impaired TNFα and IL-12 release (de Veer et al., 2003; Srivastav et al., 2012). Similar to attenuation of TLR2 signaling, *Leishmania* glycolipid-induced TLR4 signaling was prevented through activation of SHP-1 in *L. donovani*, and through inhibition of neutrophil elastase in *L. major* infections (Das et al., 2012; Faria et al., 2011; Karmakar et al., 2011, 2012; Whitaker et al., 2008). In the early endosomes, *L. donovani* excluded vesicular proton-ATPase to delay acidification (Vinet et al., 2009) which allowed transformation of promastigotes to hydrolase-resistant amastigotes (Scianimanico et al., 1999). In addition, *L. donovani* caused F-actin accumulation and led to formation of physical barriers preventing early-stage inhibition of phagosome-late endosome interaction (Holm et al., 2001; Lodge & Descoteaux, 2005b). Recent publications suggest that even in acidified phagolysosomes, *L. donovani* amastigotes strictly controlled the microenvironment by preventing over-acidification and activation of lysosomal enzymes through upregulation of Rab5a (Verma et al., 2017). Similar to *L. donovani*, freshly phagocytosed *L. major* delayed phagolysosome maturation by preventing phagosome-endosome fusion (Desjardins & Descoteaux, 1997) and assembly of NADPH oxidase (Matheoud et al., 2013; Matte et al., 2016). Furthermore, *L. major* encoded arginase produced essential nutrients for its growth by diverting L-arginine to polyamine pathway. Also, activation of the polyamine pathway benefitted the parasites by consuming L-arginine and preventing host iNOS activity, ultimately reducing NO-mediated *Leishmania* killing in macrophages (Gaur et al., 2007; Reguera et al., 2009). Moreover, *Leishmania* parasites impaired IFN-γR signaling by SHP-1-mediated inhibition of JAK2, inhibition of STAT1 translocation

to nucleus, and disruption of lipid rafts by quenching membrane cholesterol (Blanchette et al., 1999, 2009; Forget et al., 2005; Sen et al., 2011). Additionally, *Leishmania* GP63 modified and degraded transcription factors NFκB and AP-1, downmodulating proinflammatory response (Cameron et al., 2004; Contreras et al., 2010; Gregory et al., 2008) in infected macrophages. Moreover, *Leishmania spp.* were reported to prevent antigen presentation on MHC-II molecules by antigen sequestration, increasing the fluidity of lipid rafts, and endocytosis-mediated degradation of MHC-II molecules (Chakraborty et al., 2005; De Souza Leao et al., 1995; Fruth et al., 1993; Kima et al., 1996; Prina et al., 1996). Activation of lymphocytes was further inhibited through downmodulation of co-stimulatory molecule B7-1 and impairment of CD40-CD40L signaling in infected antigen presenting cells (Awasthi et al., 2003; Mbow et al., 2001). Finally, it was shown that parasite LPG escaped to cytosol and induced non-canonical inflammasome activation. However, the role of inflammasome activation in *Leishmania* infection remains unclear as it can both limit parasite growth and cause dissemination and tissue destruction (Harrington & Gurung, 2020; Zamboni & Sacks, 2019).

Although there is numerous evidence regarding the exploitation of PRRs by *Leishmania spp.*, the role of cGAS-STING-TBK1 on *Leishmania* infection is left understudied. The only report focusing on the interaction of *L.* donovani with cGAS-STING-TBK1 pathway suggested deliberate activation and exploitation of this DNA-sensing pathway culminating in parasite persistence (Das et al., 2019). An overview of canonical activation of cGAS-STING-TBK1 pathway is summarized in Figure 1.2., and the role of this pathway in *Leishmaniasis* is discussed in Section 3.2.6.

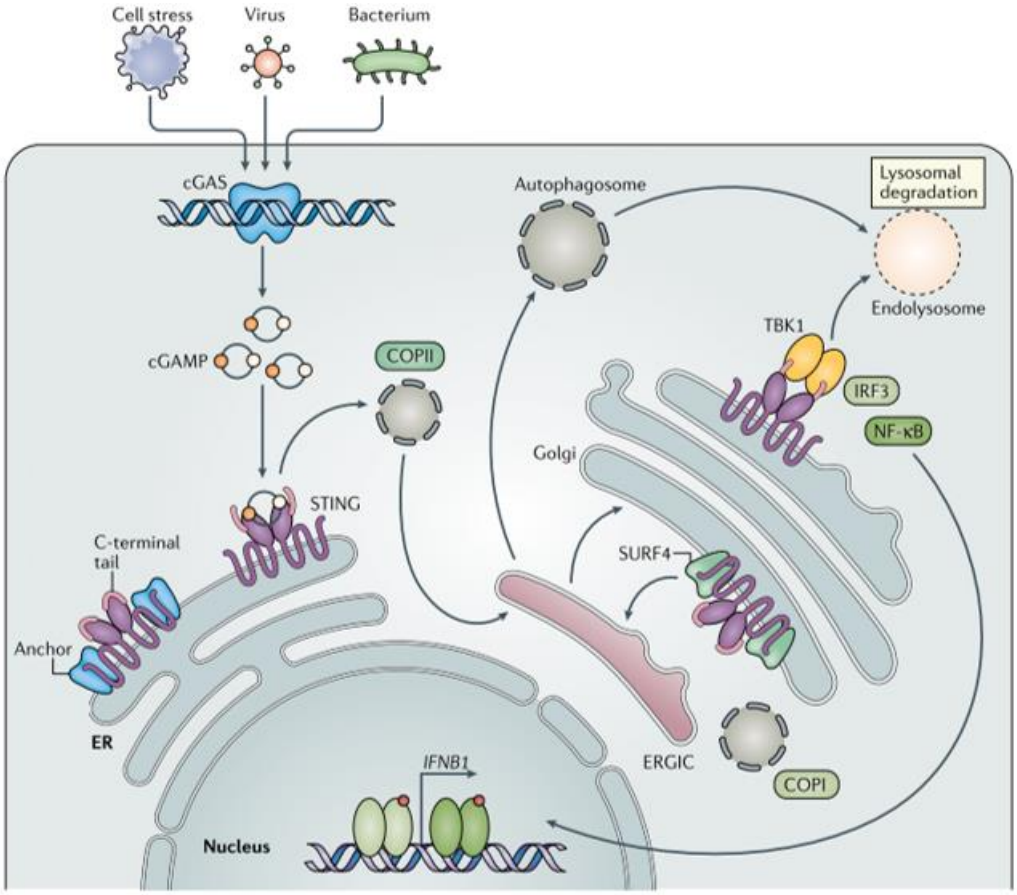

Figure 1.2. Overview of cGAS-STING-TBK1 pathway (adopted from Decout et al., 2021)

Pathogenic dsDNA in the cytoplasm binds to cGAS and catalyzes the production of cGAMP, which is a secondary messenger specifically recognized by STING. Activated STING promotes recruitment of TBK1 and subsequent promotion of phosphorylation of STING and TBK1 leading to recruitment of IRF3. Phosphorylated and dimerized IRF3 translocate to nucleus and induce the expression of type I IFNs and ISGs.

1.2.2 Dynamics of Interaction of *Leishmania* with the Adaptive Immune System

Early mouse models characterized resistant or susceptible strains based on dominant helper T cell response against *L. major* (Heinzel et al., 1989; Scott et al., 1988). The resistant mouse strain C57Bl/6 was able to overcome the infection and self-heal

unlike susceptible mouse strain BALB/c. Th1 subset provided resistance since related cytokines IFNγ and TNFα classically activated macrophages and worked synergistically to induce iNOS which is important for destruction of *L. major* amastigotes (Liew et al., 1997). On the contrary, Th2 cytokines were thought to have a role in inducing susceptibility since cytokines of this subset, IL4 and IL13, were associated with downregulation of Th1 response, alternative activation of macrophages, increasing arginase and polyamine synthesis (de Waal Malefyt et al., 1993; Doherty et al., 1993; Hesse et al., 2001), and subsequent inhibition of leishmanicidal activity of macrophages *in vivo* (Pascale Kropf et al., 2005). However, the outcome of the disease seems to be more complex than it was suggested by the initial mouse model studies because other *Leishmania* species, including a virulent *L. major* strain (Seidman), did not spontaneously heal despite Th1 polarization (Table 1.1).

Table 1.1 A list of mouse models of Leishmaniasis and dominant helper T cell responses against the parasite (adopted from Scott & Novais, 2016).

Leishmania spp.	Human disease	Mouse disease				Refs
		C57BL/6 mice		BALB/c mice		
		Type of disease	Dominant immune response	Type of disease	Dominant immune response	
Leishmania major	Self-healing or chronic cutaneous leishmaniasis usually caused by a single skin lesion	Self-healing	T_H1	Chronic	T_H2	5,6
Leishmania major Seidman strain	Chronic cutaneous leishmaniasis	Chronic	T_H1	Chronic	T_H2	138
Leishmania amazonensis	Self-healing or chronic cutaneous leishmaniasis usually caused by a single skin lesion, and diffuse cutaneous leishmaniasis	Chronic	T_H1 and T_H2	Chronic	T_H2	139–141
Leishmania mexicana	Healing or chronic cutaneous leishmaniasis usually caused by a single skin lesion, and diffuse cutaneous leishmaniasis	Chronic	T_H1 and T_H2	Chronic	T_H2	139,142, 143
Leishmania braziliensis	Healing or chronic cutaneous leishmaniasis usually caused by a single skin lesion, and mucosal leishmaniasis	Self-healing	T_H1	Self-healing	T_H1	76

T_H, T helper.

Furthermore, the extreme ends of the spectrum leads to severe disease in humans regardless of Th1 or Th2 dominance (Scott & Novais, 2016; Volpedo et al., 2021). While Th1 activation is indispensable against *Leishmania* parasites, a balanced Th1/Th2 response seems to be critical for the resolution of the disease (Figure 1.3.).

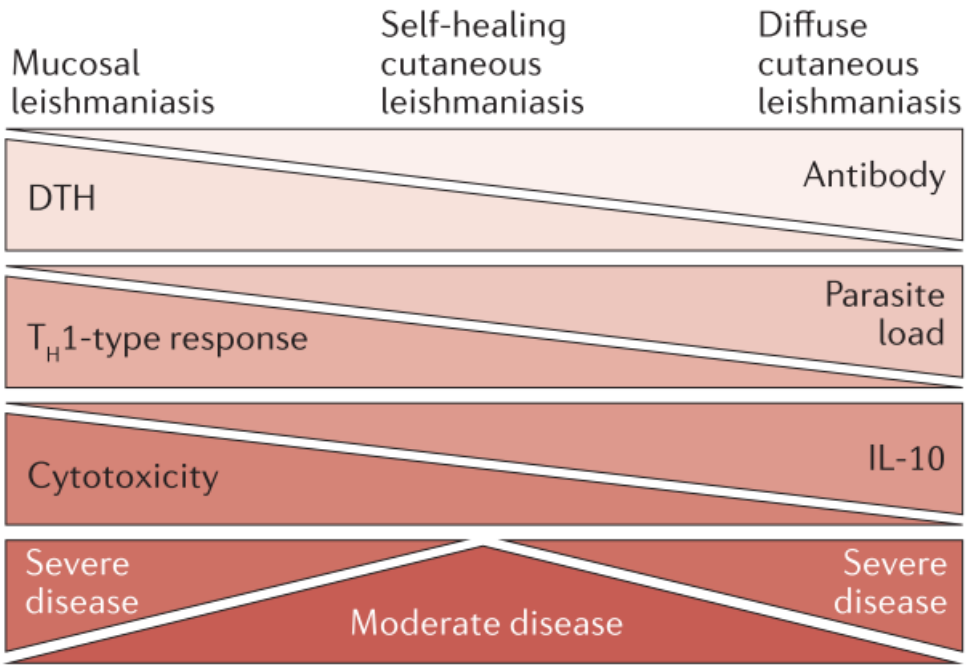

Figure 1.3. The spectrum of cutaneous Leishmaniasis depicting different phenotypes of the disease based on dominant immune response (adopted from Scott & Novais, 2016).

The role of CD8+ T cells in Leishmaniasis is not clear. While these cells can drive parasite metastasis in high-dose infection models, they secrete IFNγ resulting in enhanced IL12 production and Th1 polarization in the lymph nodes of C57Bl/6 mice in low-dose infection models (Belkaid, Von Stebut, et al., 2002; Uzonna et al., 2004). Furthermore, increased numbers of CD8+ T cells leads to enhanced tissue destruction and parasite persistence in mucocutaneous Leishmaniasis.

High antibody titers against *Leishmania* parasites were associated with diffuse form of the disease, a severe form of cutaneous Leishmaniasis associated with the absence of Th1 cytokines (Figure 1.3.). Immune complex formation can result in suppression of IL-12 and induction of IL-10 through low affinity FcγRs (Gallo et al., 2010;

Guilliams et al., 2014). IL-10 production through this route exacerbated cutaneous and mucocutaneous Leishmaniasis in mice infected with *L. amazonensis* and *L. Mexicana* (Buxbaum & Scott, 2005; Kima et al., 2000; Thomas & Buxbaum, 2008). These observations were not unique to mice, as delayed-type hypersensitivity (DTH) response in humans resulted in parasite elimination while immune complex-mediated disease exacerbation was associated with visceral Leishmaniasis (Basak et al., 1992; Haldar et al., 1983; Miles et al., 2005; Sundar et al., 1998) as well as local and diffuse cutaneous Leishmaniasis (as reviewed in Goncalves et al., 2020). In summary, FcγR mediated suppression of proinflammation seems to be deleterious for the host, and B cells do not seem to play a protective role in Leishmaniasis.

1.3 Aims of the Thesis

Leishmaniasis is a neglected tropical disease reported over 90 countries in Asia, Middle East, Africa, Central and South America. Currently, estimates of cutaneous Leishmaniasis ranges from 700,000 to 1.2 million cases per year (Centers for Disease Control and Prevention, 2020). The most important risk factors include poverty, malnutrition and immunocompromised state, affecting the poor people most severely (*World Health Organziation. Leishmaniasis.*, 2022). With the rising temperatures at the global scale, Leishmaniasis cases are expected to geographically spread and rise in number (González et al., 2010). Urgent development of drugs with lower toxicity compared to currently used ones is necessary. Furthermore, development of cost-efficient and protective vaccines against Leishmaniasis is required even if successful drugs with low side effects are innovated because the most severely affected portion of people by Leishmaniasis are not the target costumers of drug companies.

In the light of the previous studies conducted by our group (Ayanoğlu, PhD Thesis, 2019) and extensive exploitation of PRRs and intracellular signaling pathways by *Leishmania*, we aimed to investigate the role of cGAS-STING-TBK1 pathway on *L. major* infected THP1 cells. We utilized cGAS, STING or TBK1 KO THP1 cells, and chemical inhibition of TBK1 to further illuminate the role of this pathway. Also, we

aimed to investigate the possible mechanism of protection in the absence of cGAS-STING-TBK1 signaling through gene expression analysis.

In addition, we aimed to assess the protective effects of different *Leishmania* antigen compositions (lyophilized whole parasites, soluble *Leishmania* antigens and *Leishmania* exosomes) when used as vaccinations. Furthermore, we aimed to capitalize on early involvement of NKT cells in Leishmaniasis by combining the aforementioned antigen compositions with prototypical NKT cell adjuvant α-galactosylceramide.

CHAPTER 2

MATERIALS & METHODS

2.1 Materials

Table 2.1 List of THP-1 Dual™ Cell lines used in this thesis.

Cell line	**Company**	**Cat no**
THP1-Dual™ Cells	Invivogen, France	thpd-nfis
THP1-Dual™ KO-cGAS Cells	Invivogen, France	thpd-kocgas
THP1-Dual™ KO-STING Cells	Invivogen, France	thpd-kostg
THP1-Dual™ KO-TBK1 cells	Invivogen, France	thpd-kotbk

Table 2.2 List of materials and appliances utilized in this thesis.

Material/appliance	**Company**	**Cat no**
6-well tissue culture plates	Sarstedt, Germany	83.392
BD Vacutainer® SST™ II Advance	Becton, Dickinson, U.S.A.	367953
Corning® 96-well Solid Black Polystyrene Microplates	Corning, U.S.A.	3915
Corning® 96-well White Polystyrene Microplates	Corning, U.S.A.	3912
Filter-capped T25 cell culture flask	Sarstedt, Germany	
Filter-capped T75 cell culture flask	Sarstedt, Germany	83.3911.002
Flat-bottom 96-well tissue culture plates	Sarstedt, Germany	83.3924
FLoid™ Cell Imaging Station	Thermo Fisher Scientific, U.S.A	4471136
Immulon 1 B plates	Thermo Fisher Scientific, U.S.A	3355
Mr. Frosty™ Freezing Container	Thermo Fisher Scientific, U.S.A	5100-0001

Table 2.2 (continued) List of materials and appliances utilized in this thesis.

Plug-sealed T25 cell cultere flask	SPL life sciences, South Korea	
Plug-sealed T75 cell cultere flask	SPL life sciences, South Korea	SPL70175
Polycarbonate (PC) ultracentrifuge tubes	Hitachi, Japan	S308132A
Qubit® 3.0 Fluorometer	Invitrogen, U.S.A.	Q33216
Sodium Citrate tubes	Ayset, Turkey	70700

Table 2.3 List of reagents and kits utilized in this thesis.

Reagent/kits	**Company**	**Cat no**
Accutase® Cell Detachment Solution	Biolegend, U.S.A.	423201
Amlexanox	Invivogen, France	inh-amx
Blasticidin	Invivogen, France	ant-bl-1
Blue Loading Buffer Pack	New England Biolabs, U.S.A.	B7703S
BX-795 hydrochloride	Sigma Aldrich, Germany	SML0694
Chloroform	Sigma-Aldrich, Germany	288306
Dimethyl Sulfoxide (DMSO)	Merck, Germany	D8418
Dulbecco's Phosphate Buffered Saline	Biological Industries, Israel	02-023-1A
Ethanol, Absolute (200 Proof, Molecular Biology Grade	Fisher Scientific, U.S.A.	BP2818100
Fixation medium (medium A)	Thermo Fisher Scientific, U.S.A	GAS001S100
Goat Anti-Mouse IgG1-AP	Southern Biotech, U.S.A.	1071-04
Goat Anti-Mouse IgG2a-AP	Southern Biotech, U.S.A.	1081-04
Heat inactivated Fetal Bovine Serum	Biological Industries, Israel	04-127-1A
KRN7000 (α-Galactosyl Ceramide)	Avanti Polar Lipids, Inc., U.S.A.	867000
LEGENDplex™ MU Th Cytokine Panel (12-plex) w/ VP V03	Biolegend, U.S.A.	741044
LysoTracker™ Red DND-99	Thermo Fisher Scientific, U.S.A	L7528
Micro BCA™ Protein Assay Kit	Thermo Fisher Scientific, U.S.A	23235

Table 2.3 (continued) List of reagents and kits utilized in this thesis.

nCounter PanCancer Immune Profiling CS Kit (no MK)	NanoString Technologies, Inc., U.S.A.	XT-CSO-HIP1-12
NNN Modified Medium (Twin Pack)	HiMedia, India	M681
Normocin™ - Antimicrobial Reagent	Invivogen, France	ant-nr-1
PageRuler™ Prestained Protein Ladder, 10 to 180 kDa	Thermo Fisher Scientific, U.S.A.	26616
Phorbol 12-myrisate 13-acetate (PMA)	Invivogen, France	tlrl-pma
pHrodo™ Green Zymosan Bioparticles™ Conjugate for Phagocytosis	Thermo Fisher Scientific, U.S.A	P35365
Pierce™ Silver Stain Kit	Thermo Fisher Scientific, U.S.A.	24612
PNPP	VWR, U.S.A.	0405-100T
Qubit™ Assay Tubes	Thermo Fisher Scientific, U.S.A	Q32856
Qubit™ Protein Assay Kit	Thermo Fisher Scientific, U.S.A	Q33211
RiboExTM, total RNA isolation solution	Geneall Biotechnology CO., LTD, South Korea	301-001
RNA Clean & Concentrator™-25	Zymo Research, U.S.A.	R1018
RPMI 1640 Medium with L-glutamine and Phenol Red	Biological Industries, Israel	01-100-1A
SYTO™ 16 Green Fluorescent Nucleic Acid Stain	Thermo Fisher Scientific, U.S.A..	S7578
SYTOX™ Orange Nucleic Acid Stain	Thermo Fisher Scientific, U.S.A.	S11368
Trypsin EDTA Solution A (0.25%), EDTA (0.02%)	Biological Industries, Israel	03-050-1B
Water, Cell Culture Grade	Biological Industries, Israel	03-055-1A
XenoLight D-Luciferin	Perkin Elmer, U.S.A.	122799
ZAP-OGLOBIN II Lytic Reagent	Beckman Coulter, U.S.A.	NC0098316
Zeocin™	Invivogen, France	ant-zn-1

2.2 Methods

2.2.1 Maintenance of *Leishmania major* Cultures

2.2.1.1 Maintenance and Subculturing of Axenic Promastigote Cultures

Patient-isolate *Leishmania major* parasites were provided by Prof. Ahmet Özbilgin from Department of Molecular Parasitology, Celal Bayar University. The isolated parasites were subjected to *in vivo* passaging in BALB/c mice and transfected with an EGFP-Luc fusion protein-encoding plasmid which was inserted into 18S rRNA locus resulting in constitutive expression of fusion protein (Ayanoğlu, PhD Thesis, 2019).

When a fresh axenic promastigote culture was needed, frozen *Leishmania major* cryovials were thawed according to thawing procedure (explained in section 2.2.1.3). Later, they were kept in plug sealed T25 or T75 (SPL life sciences, South Korea) flasks in *Leishmania* growth medium (Table A.1., Appendix A). Initial inoculum was arranged to 5-7x10^6 parasites/ml depending on how quickly they were needed for the next experiment. Every time parasites reached their late-logarithmic phase (≈25x10^6 parasites/ml), they were sub-cultured by diluting culture media with fresh growth medium. Dilutions were done based on calculations explained in Section 2.2.1.2. Axenic promastigotes were passaged to a maximum of 12 passages (≈36 days) to keep them virulent. If volume of passaged culture was equal or lower than 10 ml, then a plug sealed T25 flask (SPL life sciences, South Korea) was used. If it was between 10-20 ml, then a plug sealed T75 flask (SPL life sciences, South Korea) was used. These flasks were placed in a vertical position in a 26°C incubator without CO2 or humidification.

2.2.1.2 Quantification of *Leishmania major* Cultures

When parasite cultures were needed to be quantified, culture flasks containing growing promastigote cultures were mixed using a serological pipette to homogenously disperse parasites. Then, 20 µl of culture medium was sampled and fixed with 20 µl of medium A (4% paraformaldehyde, Thermo Fisher Scientific, U.S.A) in a dropwise fashion in an eppendorf tube or a 15 ml falcon tube. After 10 minutes of incubation at room temperature, fixed parasites were diluted with DPBS (Biological Industries, Israel). The ratio of dilutions was arranged based on how concentrated parasite cultures were. If the sample was taken from a stationary phase promastigote culture, 160 µl of DPBS was used. This value was increased to 960 or 1960 µl if a parasite culture was first pelleted and resuspended in a small volume of medium of 1 to 5 ml in order to prevent overcrowding. After mixing with a pipette and thoroughly vortexing, samples were quantified using a Novocyte 2060R flow cytometer (ACEA Biosciences, U.S.A.) by running a small volume (such as 20 µl) of sample for quantification as shown in Figure 2.1.

To calculate number of parasites/ml of culture medium, number of events in an appropriate gate was multiplied by dilution factors of 10, 50 or 100 (based on the volume of DPBS used, respectively) and multiplication factor of 50. If total numbers of parasites in cultures were required, parasites/ml counts were multiplied by amounts of total volume (in terms of ml) in cultures or resuspended media.

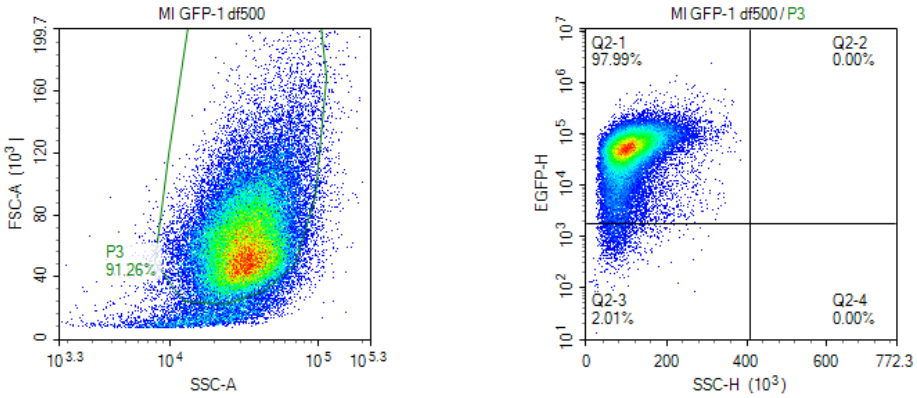

Gate	Count	% All	Mean X	Mean Y	CV X	CV Y
All	56,541	100.00 %	40,246	65,591	541.84 %	135.29 %
P3	51,598	91.26 %	35,383	66,209	41.43 %	39.24 %

Gate	Count	% P3	Mean X	Mean Y	CV X	CV Y
P3	51,598	100.00 %	111,171	54,209	38.64 %	76.43 %
Q2-1	50,561	97.99 %	111,718	55,301	38.35 %	74.39 %
Q2-2	0	0.00 %	0	0	0.00 %	0.00 %
Q2-3	1,037	2.01 %	84,487	967	47.15 %	43.87 %
Q2-4	0	0.00 %	0	0	0.00 %	0.00 %

Figure 2.1. An example image of quantification of *Leishmania* parasites using Novocyte 2060R flow cytometer (ACEA Biosciences, U.S.A.). P3 designates live parasite gate.

2.2.1.3 Cryopreservation and Thawing Procedures for *Leishmania major* Promastigotes

In order to increase the total number of cryopreserved axenic promastigote cultures, parasites were grown for 2 passages after thawing from a cryopreserved culture or after amastigote to promastigote transition following an in-vivo passage. It was important that parasites were not kept too long in axenic cultures to prevent loss of virulence. Once the parasites reached their late-logarithmic phase at the end of the second passage, they were pelleted and resuspended in pre-cooled RPMI 1640 medium without additives (Biological Industries, Israel). Next, the cells were divided into cryovials at a density of $24x10^6$ parasites/cryovial in 500 µl of RPMI 1640 medium without additives. Then, 500 µl of pre-cooled *Leishmania* freezing medium (Table A.2., Appendix A) was distributed to each cryovial. Once the distribution was complete, the cap of each cryovial was quickly sealed, and vials were mixed by inverting 4-5 times before placing them into an ice filled bucket. Afterwards, all vials were placed in a Mr. Frosty™ Freezing Container (Thermo Fisher Scientific, U.S.A)

which was filled with fresh isopropanol and subsequently placed at -80°C overnight. The next day, cryovials were transferred to a liquid nitrogen tank. A week later, as done with all cryopreserved cultures, one of the cryovials was thawed in order to assess the viability of the frozen cultures.

When a fresh culture was needed, a cryopreserved promastigote culture was thawed by placing the cryovial in a 15 ml falcon tube and placing the falcon tube into a water bath at 37°C. This was done to prevent a potential water bath contamination. Immediately after the frozen culture was liquefied, the cryovial was sterilized using 70% ethanol and brought into a cell culture hood. 1 ml of freshly defrosted culture was put into a 15 ml falcon tube filled with 9 ml 2% Regular RPMI medium (Table A.3., Appendix A) and mixed by inversion. This falcon was then centrifuged at 1500-2000 g for 10 minutes to pellet the parasites while supernatant was aspirated following the centrifugation. The pellet was resuspended using 1 ml of *Leishmania* growth medium (Table A.1., Appendix A) and transferred into a plug sealed T25 flask (SPL life sciences, South Korea) filled with 2 ml of growth medium to a total volume of 3 ml. Then, the flask was placed in a 26°C incubator and maintained as mentioned in section 2.2.1.1. The next day, the parasites were centrifuged and transferred into an equal volume of fresh growth medium (as before centrifugation) to help them recover quickly from the stress of cryopreservation.

2.2.1.4 Development of Stationary Phase *Leishmania Major* Cultures for Infection

A key trigger for the transition of procyclic promastigotes to metacyclic promastigotes is nutritional stress (D. L. Sacks & Perkins, 1984). Once parasite cultures reached their stationary phase, they were incubated at 26°C for an additional 2-6 days without any renewal or replenishment of their culture medium. Later, parasites were centrifuged at 1500-2000g and resuspended in 2% Regular RPMI medium for *in vitro* infection. For *in vivo* infection, the centrifugation step was followed by two DPBS washes followed by resuspension in DPBS.

2.2.2 Optimization of Biphasic Blood Agar Medium

Vacuumed sodium citrate tubes (Ayset, Turkey) with freshly drawn human blood were mixed by inversion and heat inactivated at 56°C for 30 minutes. These tubes were used to prevent blood coagulation. Later, one of the groups were subjected to three freeze and thaw cycles (-80 to 37°C) to hemolyze the red blood cells. NNN Modified Medium (HiMedia, India) was prepared according to the manufacturer's recommendations, and different concentrations of blood and hemolysis status were tested. Briefly, axenic promastigotes were seeded into flasks with NNN medium and counted every day with a hematocytometer to compare growth curves. At the end of fifth day, cultures were stained with SYTO™ 16 Green (Thermo Fisher Scientific, U.S.A.) and SYTOX™ Orange (Thermo Fisher Scientific, U.S.A.) nucleic acid stains to assess viability of the cultures.

2.2.3 Isolation and Quantification of SLA and Exosome Samples from *Leishmania Major*

2.2.3.1 Isolation of SLA and Exosome Samples

The first step in isolation of exosomes secreted from parasites was to remove bovine-originated exosomes in FBS which was necessary to prepare the Exosome-free culture medium (Table A.4., Appendix A). Required amount of FBS was distributed into swing-out ultra-centrifuge tubes and centrifuged at 100,000g overnight at +4°C. Supernatants were collected without disturbing the FBS-derived exosome pellet using 25 ml serological pipettes and stored at -20°C in 50 ml falcon tubes as exosome-free FBS.

Once the parasites were at their late-logarithmic phase, they were pelleted by centrifugation and resuspended in exosome collection medium (Table A.5., Appendix A) in the same parasite number to culture medium ratio (number/volume) previous to centrifugation, and distributed to filtered capped T75 flasks (Sarstedt,

Germany) to be incubated at 37°C and 5% CO_2 in a humidified incubator for 20-24 hours in a horizontal manner. Usually, one batch of exosome sample was isolated from 8 plug sealed T75. This number of parasites take a lot of time to proliferate. To reduce the time between exosome isolations, we prepared additional culture flasks (up to 4 plug sealed T75) whose purpose was to replenish the parasites used in the previous exosome isolations and make the next batch ready to be isolated in three days. Following overnight incubation in exosome collection medium which mimics the conditions inside a phagolysosome, parasites were centrifuged at 2000g for 10 minutes, and the supernatants were collected and transferred to polycarbonate (PC) ultracentrifuge tubes (Hitachi, Japan). Remaining parasite pellets were used for SLA preparation (explained in the next paragraph). These supernatants were centrifuged at 15,000g for 30 minutes at +4°C in an ultracentrifuge (Hitachi, Japan) to remove cellular debris and micro vesicles. Afterwards, supernatants were collected and put into 50 ml falcons temporarily. This step was important since the following filtration process took some time during which pellets formed in the 15,000g centrifugation step might have gotten destabilized and contaminated the supernatants. Then, the supernatants were transferred into a 50 ml syringe and filtered into 2 ultracentrifuge tubes, while the remaining was filtered into a fresh 50 ml falcon tube using 0.22 µm syringe filters (Jet-Biofill, China) to be stored at +4°C. Later, ultracentrifuge tubes that were filled with the filtered supernatants were centrifuged at 100,000g at +4°C for 1-1.5 hours. This step resulted in formation of exosome pellets and the supernatants were discarded. Without disturbing the exosome pellets, two ultracentrifuge tubes were filled by the remaining filtered supernatants, and 100,000g centrifugation followed by aspiration of exosome-free supernatants was repeated until the stored supernatants were used completely. Exosome pellets were resuspended in 1 ml of DPBS each. Following this, tubes were topped off with cold DPBS and centrifuged at 100,000g one final time to wash impurities off exosomes for 2 hours at +4°C. Finally, supernatants were aspirated, and exosome pellets were resuspended in 300-400 µl of DPBS to be stored at -20°C until use.

To prepare SLA (soluble *Leishmania* antigens), parasite pellets that were set aside during exosome isolations were washed two times with DPBS. Then, pellets were resuspended in small amounts of DPBS and distributed into eppendorf tubes. Afterwards, these tubes were cycled between ultra-low freezer (-80°C for 10-15 minutes) and a heat block (37°C for 2-3 minutes) 5 times. Finally, lysed samples were centrifuged at 5000g for 10 minutes, and supernatants were collected and stored in fresh eppendorf tubes at -20°C until use.

2.2.3.2 Quantification of SLA and Exosome Samples

SLA and exosome samples were quantified using the Qubit™ Protein Assay Kit (Thermo Fisher Scientific, U.S.A) or Micro BCA™ Protein Assay Kit (Thermo Fisher Scientific, U.S.A) according to manufacturers' directions.

Briefly, for Qubit protein assay kit, 3 µl from exosome samples and 3 µl from SLA samples (diluted with DPBS 1:1) were placed into provided Qubit™ Assay Tubes (Thermo Fisher Scientific, U.S.A) and the final volume was completed to 200 µl with master mix (detection dye + protein buffer). This was followed by vortexing the samples thoroughly and incubation at room temperature for 15 minutes in dark. Finally, protein content was quantified by selecting "protein" on the Qubit® 3.0 Fluorometer (Invitrogen, U.S.A). For BCA, a modified standard preparation was followed to minimize the amount of BSA spent since the original protocol wastes a significant amount of it. We needed 150 µl of standard samples as stated in the microplate protocol. Therefore, we prepared the minimum required amount plus some additional volume (such as 20 µl to account for pipette mistakes) as shown in Table 2.4. For this, we calculated starting from the least concentrated standard and prepared starting from the most concentrated standard.

Table 2.4 Guide for modified standard preparation of Micro BCA™ Protein Assay Kit (Thermo Fisher Scientific, U.S.A)

Concentration (µg/ml)	**Total required volume (µl)**	**Volume to be taken from next concentrated sample (µl)**	**Volume of DPBS to be added to reach the total required volume (µl)**
0.5	170	85	85
1	170 + 85	102	153
2.5	170 + 102	136	136
5	170 + 136	153	153
10	170 + 153	161.5	161.5
20	170 + 161.5	165.75	165.75
40	170 + 165.75	67.15	268.6
200	170 + 67.15	23.715	213.435

Working reagent was prepared according to the specified ratio of 25:24:1 (MA:MB:MC) and was protected from light. A 96-well flat bottom plate (Sarstedt, Germany) was placed on ice and 150 µl of standards and samples (usually diluted 1/50 with DPBS) were transferred into wells according to a plate design. Then 150 µl of working reagent was added on top of each standard and unknown sample as well as blanks. Wells were encouraged to mix by slowly tapping on the side of the plate which was then incubated at 37°C for 0.5-2 hours. Once the appropriate purple color developed, absorbance values were measured at 562 nm using a Multiskan™ GO Microplate Spectrophotometer (Thermo Fisher Scientific, U.S.A.), and the concentrations were calculated by constructing 4PL curves and fitting the unknown samples to this curve while taking the dilution factor of the unknown samples into account.

2.2.4 Cell Culture

2.2.4.1 Maintenance and Quantification of THP1-Dual™ Cell Cultures

THP1-Dual™ Cells (Invivogen, France), THP1-Dual™ KO-cGAS Cells (Invivogen, France), THP1-Dual™ KO-STING Cells (Invivogen, France) and THP1-Dual™ KO-TBK1 cells (Invivogen, France) were grown in 10% Regular RPMI medium (Table A.6., Appendix A) supplemented with 100 µg/ml Normocin (Invivogen, France), 10 µg/ml Blasticidin (Invivogen, France) and 100 µg/ml Zeocin™ (Invivogen, France). Selective antibiotics Blasticidin and Zeocin were added every other passage to keep selection pressure, whereas Normocin was always added to prevent mycoplasma contamination of culture media.

Briefly, when THP1-Dual cells needed subculturing, they were centrifuged at 300g for 5 minutes and resuspended in 1 ml of 10% Regular RPMI medium from which a 20 µl sample was withdrawn and diluted with 180 µl of DPBS. For cell counting, 20 µl of the diluted sample was acquired on a Novocyte 2060R flow cytometer (ACEA Biosciences, U.S.A.). The number of THP1-Dual cells in a viable gate (Figure 2.2.) was multiplied by 10 (dilution factor) and 50 (multiplication factor) to calculate the total number of cells resuspended in 1 ml of 10% Regular RPMI medium. Required volume of resuspended THP1-Dual cells was withdrawn and seeded into filter capped T25 or T75 (Sarstedt, Germany) flasks at a concentration of $5x10^5$ cells/ml in 10% Regular RPMI medium supplemented with 100 µg/ml Normocin (Invivogen, France), 10 µg/ml Blasticidin (Invivogen, France) and 100 µg/ml Zeocin™

(Invivogen, France). Every three days this protocol was repeated until the cells were passaged for a maximum of 20 times.

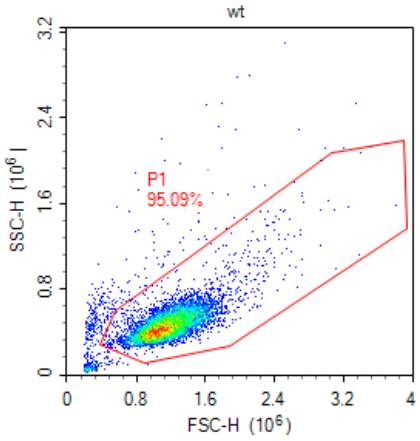

Gate	Count	% All	Mean X	Mean Y	CV X	CV Y
All	10,123	100.00 %	1,140,252	466,429	28.50 %	43.10 %
P1	9,626	95.09 %	1,172,605	461,907	23.61 %	29.51 %

Figure 2.2. An example image of THP1-Dual cells analyzed and quantified using Novocyte 2060R flow cytometer (ACEA Biosciences, U.S.A.). P1 designates the live cell gate.

2.2.4.2 Cryopreservation and Thawing Procedures for THP1-Dual™ Cell Cultures

Cryopreservation of THP1-Dual cells were done after 2-3 passages upon receiving the cell lines from the manufacturer in order to maximize the number of early-passage cryopreserved cells. Once cell cultures reached their stationary phase concentration of $2x10^6$ cells/ml, they were centrifuged at 300g for 5 minutes and resuspended in 100% FBS (Biological Industries, Israel) at a density of $10x10^6$ cells/ml. Resuspended cells were then distributed into cryovials as 0.5 ml each so that each cryovial had $5x10^6$ cells in total. Then, 0.5 ml of pre-cooled THP1-Dual freezing medium (Table A.7., Appendix A) was distributed into each cryovial. After closing the caps of each cryovial, they were mixed by inversion 4-5 times and placed into a Mr. Frosty™ Freezing Container (Thermo Fisher Scientific, U.S.A). The

container was placed into -80°C ultra-freezer overnight, and cryovials were transferred to liquid nitrogen tank the next day for long term preservation. THP1-Dual™ KO-TBK1 cells (Invivogen, France) had a slight modification to their freezing medium (Table A.8., Appendix A) which had a minor difference in its FBS to DMSO ratio.

In order to thaw frozen cultures, cryovials were retrieved from the liquid nitrogen tank and placed into a 37°C water bath. Immediately after thawing, vials were sterilized and taken into the cell culture hood. 1 ml of freshly thawed THP1-Dual cells were diluted with 9 ml of 2% Regular RPMI medium (Table A.3., Appendix A) to minimize toxic effects of DMSO. Cells were centrifuged at 300g for 5 minutes and resuspended in 5 ml of 10% Regular RPMI medium. Cultures were propagated in filter capped T25 cell culture flasks (Sarstedt, Germany) in a humidified 37°C incubator supplemented with 5% CO_2. Only after 1 to 2 passages were the selective antibiotics added.

2.2.5 *In vitro* Infection Experiments

2.2.5.1 PMA Induced Differentiation of THP-1-Dual™ Cell Line

THP1-Dual cell lines were differentiated into macrophage-like cells upon incubation with Phorbol 12-myrisate 13-acetate (PMA) (Invivogen, France) at varying concentrations. PMA induced differentiation is essential for a viable *in vitro* infection model as the ultimate host of *Leishmania* species is the macrophage. Different protocols regarding PMA induced differentiation are explained in Sections 2.2.5.2.1-2.2.5.2.4.

2.2.5.2 *In vitro* Infection Optimization

In vitro infection can potentially be influenced by many factors which includes macrophage-like state of THP1-Dual cells, infectivity of parasites, route of

internalization of *Leishmania* promastigotes, media in which infection took place and media of choice after initial infection took place. Considering the high number of variables, it was necessary to optimize our *in vitro* infection model for successful infection and consistency among experiments.

2.2.5.2.1 Effects of Various Stationary Phase Models on *in vitro* Infection

We first tested infectivity rates of parasite cultures which were induced to go thorough metacyclogenesis and apoptotic-like cell death. These states were induced by incubating late logarithmic phase parasite cultures in their naturally depleted media for an additional 3 or 6 days (D. L. Sacks & Perkins, 1984), reseeding the parasite cultures in FBS-free medium or DPBS, or treating them with low dose (200 μM) H_2O_2 (Basmaciyan et al., 2018). To test these various models, we followed a PMA induced differentiation protocol we had used before PMA concentration optimization explained in section 2.2.5.2.3. Briefly, THP1-Dual cells were differentiated into macrophage-like cells by incubating with PMA at a concentration of 5 ng/ml for 48 hours. After verifying the adherent state of these cells at 48th hour, cells were detached with trypsin (Biological Industries, Israel) for 8 minutes after one DPBS washing and diluted with 2% regular RPMI medium (Table A.3., Appendix A) at a ratio of 1/3 in a 15- or 50-ml falcon tube. Later, the cells were centrifuged at 300g for 5 minutes and re-seeded on a flat-bottom 96-well tissue culture plate (Sarstedt, Germany) at a density of 100,000 cells/well in 150 μl of 2% regular RPMI medium (Table A.3., Appendix A). Once the cells adhered to wells, parasite cultures were centrifuged at 2000g for 10 minutes and resuspended in 2% regular RPMI medium (Table A.3., Appendix A). After mixing, parasites were distributed to wells (in 50 μl) at a macrophage to parasite ratio of 1:10. Uninfected wells received 2% Regular RPMI medium. 24 hours later, infection percentages and MFI values were quantified using a Novocyte 2060R flow cytometer (ACEA Biosciences, U.S.A.) as explained in Section 2.2.5.4.

2.2.5.2.2 Determination of the Effect of Infection Time on *in vitro* Infection

Knowing which type of stationary phase model to use for *in vitro* infections, we tested whether co-incubating parasites with differentiated THP1-Dual cells for shorter or longer time frames changed infection rates. In one group, we tested a 6-hour infection period after which the wells were washed three times with DPBS to remove as much extracellular parasites as possible. After three washes with DPBS, cultures were replenished with 2% Regular RPMI medium. In another group, we tested a 24-hour infection period which we previously used. At 24th hour, readouts with Novocyte 2060R flow cytometer (ACEA Biosciences, U.S.A.) were recorded as explained in Section 2.2.5.4. Furthermore, pictures of infections were taken using a FLoid Cell Imaging Station (Thermo Fisher Scientific, U.S.A.) upon staining the wells with SYTO™ 16 Green (Thermo Fisher Scientific, U.S.A.).

2.2.5.2.3 Effects of Different PMA Concentrations on *in vitro* Infection

In another optimization experiment, we tested varying PMA concentrations for differentiation of THP1-Dual cells. Cells were differentiated with either overnight treatment of 5 or 10 ng/ml PMA, or 6h treatment of 20, 30, 40, 50, 75 or 100 ng/ml PMA and washed, detached with trypsin, re-seeded, and infected in 2% regular RPMI medium (Table A.3., Appendix A) for 6 hours with stationary phase *Leishmania Major* and washed with DPBS to remove extracellular parasites which was followed by replenishment with fresh culture medium. 24 h later, extent of infections was determined on a Novocyte 2060R flow cytometer (ACEA Biosciences, U.S.A.) based on eGFP expression as explained in Section 2.2.5.4.

2.2.5.2.4 Transition to 3-day *in vitro* Infection Model

2.2.5.2.4.1 Determination of the Effect of FBS Concentration on Infection Efficiency

THP-Dual WT cells were differentiated with 40 ng/ml PMA overnight and infected for 6 hours in 2% Regular RPMI (Table A.3., Appendix A). After the initial 24-hour period, medium was either replenished or changed to 10% Regular RPMI (Table A.6., Appendix A). Readouts were taken for 72 hours as explained in Section 2.2.5.4.

2.2.5.2.4.2 Effects of Opsonization and PMA Concentration/Exposure Time on Infection Efficiency

The following PMA-induced differentiation models were tested for a 3-day *in vitro* infection model: 5 ng/ml PMA for 48 hours, 30 ng/ml PMA overnight or 50 ng/ml PMA overnight. Differentiated THP1-Dual WT cells were infected with 3-day old stationary-phase parasites for 6 hours. 24 h after initiation of infection, 2% regular RPMI medium (Table A.3., Appendix A) was replaced by 10% regular RPMI medium (Table A.6., Appendix A). Samples were analyzed for parasite loads at three time points; 24, 48 and 72 h using Novocyte 2060R flow cytometer (ACEA Biosciences, U.S.A.) as explained in Section 2.2.5.4.

The above-mentioned protocol was also repeated with opsonized parasites to gain insight on the effect of opsonization on infection efficiency. For this, parasites were pelleted and resuspended as previously explained. Then, cells were opsonized in 1% (v/v) human serum (preparation is explained in Section 2.2.5.5) in 2% regular RPMI medium for 15 minutes at room temperature. Following the incubation, opsonized parasites were pelleted and resuspended once again to remove free serum components. Then, parasites were co-incubated with THP1-Dual cells for 2 hours (instead of 6 hours). The remainder of the protocol were followed exactly as explained in the previous paragraph.

2.2.5.3 Role of cGAS-STING-TBK1 Pathway on *in vitro* Infection Model

In the same set of experiments explained in section 2.2.5.2.4.2, the role of cGAS-STING-TBK1 pathway was investigated by using THP1-Dual™, THP1-Dual™ KO-cGAS, THP1-Dual™ KO-STING and THP1-Dual™ KO-TBK1 cell lines.

2.2.5.3.1 Assessment of Phagocytosis Rates of THP1-Dual Cell Lines

2.2.5.3.1.1 Phagocytosis Assessment Using Ph Sensitive Zymosan Bioparticles

THP1-Dual cells were differentiated into macrophage like cells with 5 ng/ml PMA for 48 hours and detached with cold DPBS to preserve cell surface receptors before re-seeding into a 96-well tissue culture plate at a density of 100,000 cells/well. Cells were allowed to acclimate 1-2 hours in 10% regular RPMI 1640 medium (Table A.6., Appendix A). Meanwhile, pHrodo™ Green Zymosan Bioparticles™ (Thermo Fisher Scientific, U.S.A) were suspended in 2 ml of 2% regular RPMI medium and sonicated at 100 amplitude (306 Watts) as 30 second on/30 seconds off for 10 minutes in an ice filled sonicator bath before thoroughly vortexing. The media on the cells were replaced with 2% Regular RPMI medium, and 25 µg pHrodo™ Green Zymosan Bioparticles™ were distributed to corresponding wells. 2 hours later, wells were washed with DPBS, detached, and analyzed using the FL-1 channel on a Novocyte 2060R flow cytometer (ACEA Biosciences, U.S.A.).

2.2.5.3.1.2 Phagocytosis Assessment using GFP Expressing *Escherichia coli*

THP1-Dual cells were differentiated into macrophage like state with 5 ng/ml PMA for 48 hours and detached with Accutase (Biolegend, U.S.A.) to preserve cell surface receptors before re-seeding into a 96-well tissue culture plate at a density of 100,000 cells/well. 1 hour prior to phagocytosis test, Amlexanox (Invivogen, France) treatment was performed as described in Section 2.2.5.8.1.

One day prior to phagocytosis test, *Escherichia coli* with a GFP expressing vector (provided by Sinem Ulusan) resistant to chloramphenicol was grown in LB broth supplemented with 25 µg/ml chloramphenicol. Before the phagocytosis test, *E. coli*-GFP was fixed using 4% paraformaldehyde solution (Thermo Fisher Scientific, U.S.A) at 1:1 volume ratio and opsonized with human serum as previously explained in Section 2.2.5.2.4. After washing and resuspension, fixed *E. coli*-GFP cells were co-incubated with THP1-Dual cells at a macrophage to bacteria ratio of 1:10. 1-2 hours later, cells were washed and detached to be analyzed using the FL-1 channel on a Novocyte 2060R flow cytometer (ACEA Biosciences, U.S.A.).

2.2.5.4 *In vitro* Infection Quantification

At designated time points of *in vitro* infection experiments, each well was washed 3 times with DPBS to remove free extracellular parasites which was followed by incubation with 50 µl trypsin-edta (0.25%-0.02%) (Biological Industries, Israel) for 8 minutes. Content of each well was pipetted and transferred into eppendorf tubes filled with cold 100 µl of 2% Regular RPMI medium and placed onto an ice-filled box. The infection percentage and MFI values were quantified using a Novocyte 2060R flow cytometer (ACEA Biosciences, U.S.A.) by acquiring 5000-10,000 events per well. Figure 2.3 demonstrates a representative readout and gating strategy for *in vitro* infection.

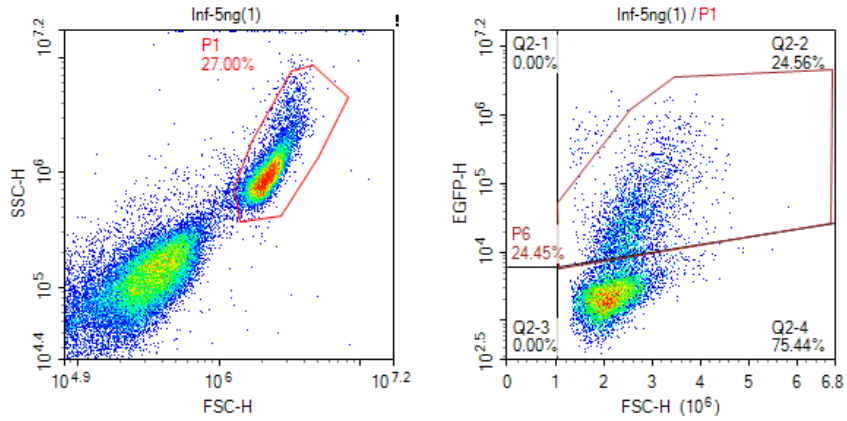

Gate	Count	Mean X	Mean Y
All	37,040	847,252	426,246
P1	10,000	2,277,239	1,116,164

Gate	Count	Mean X	Mean Y
P1	10,000	2,277,239	24,752
Q2-1	0	0	0
Q2-2	2,456	2,649,990	92,685
Q2-3	0	0	0
Q2-4	7,544	2,155,888	2,636
P6	2,445	2,665,259	79,947

Figure 2.3. Gating strategy and quantification of *in vitro* infection using Novocyte 2060R flow cytometer (ACEA Biosciences, U.S.A.). P1 depicts the live cell gate. Cells in the P6 gate define eGFP expressing parasite-infected cells.

2.2.5.5 Serum Isolation from Human Blood

Fresh human blood was drawn into BD Vacutainer® SST™ II Advance (Becton, Dickinson, U.S.A) tubes and left at room temperature undisturbed for 30 minutes to allow the blood to clot. Serum collection tube was placed into a 50 ml falcon tube to remove the clot by spinning the tube at 2000g for 10 minutes with an appropriate counterweight inside the centrifuge. Afterwards, the supernatant, which corresponds to serum, was collected with a Pasteur pipette immediately and distributed into PCR tubes in small volumes. Aliquoted sera were stored at -20°C for weeks to months, and each aliquot was only thawed once and discarded without freezing again because serum is sensitive to freeze-thaw cycles.

2.2.5.6 Staining for Visual Representation of *in vitro* Infection

In order to evaluate the success of the 3-day *in vitro* infection model, we developed an enhanced staining protocol to amplify the weak eGFP signal of *Leishmania major* amastigotes for optimal imaging on a FLoid Cell Imaging Station (Thermo Fisher Scientific, U.S.A.). For this, the infection protocol was carried out as described in Section 2.2.5.2.4 with 5 and 50 ng/ml PMA. After 48-96 hours post infection, wells were washed with DPBS three times and stained with SYTO™ 16 Green Fluorescent Nucleic Acid Stain (Thermo Fisher Scientific, U.S.A) at a final concentration of 0.4 µM for 30 minutes in 2% Regular RPMI medium (Table A.3., Appendix A). Afterwards, wells were inspected under the FLoid Cell Imaging Station (Thermo Fisher Scientific, U.S.A.) using the green channel and images were captured to demonstrate amastigote proliferation within cells.

2.2.5.7 Assessment of Lysosomal Acidity Levels of THP1-Dual Cell Lines

Relative lysosomal acidity levels of THP1-Dual cells were compared qualitatively and quantitatively using the LysoTracker™ Red DND-99 (Thermo Fisher Scientific, U.S.A) staining. THP1-Dual cells were treated with 5 ng/ml PMA for 48 hours. As described in Section 2.2.5.2.1, they were detached with trypsin and re-seeded into a 96-well clear bottom tissue culture treated plate (Sarstedt, Germany) and a 96-well opaque white plate (Corning, U.S.A) at a density of 100,000 cells/well in 10% regular RPMI medium supplemented with LysoTracker™ Red DND-99 (Thermo Fisher Scientific, U.S.A) at three different concentrations of 25, 50 and 75 nM. After 60 minutes of incubation in a humidified incubator with 5% CO_2 at 37°C, the plates were centrifuged at 250g for 5 minutes using a plate rotor to minimize the loss of cells during media replacement following centrifugation. The fluorescent signals of groups on the clear bottom plate were observed under FLoid Cell Imaging Station (Thermo Fisher Scientific, U.S.A.) whereas fluorescent signals of groups on the opaque plate was quantified using a multi-mode plate reader (Molecular Devices,

U.S.A.) with a fluorescent detection mode at excitation and emission wavelengths of 577/590 nm for 90 minutes.

2.2.5.8 Determination of the Effect of cGAS-STING-TBK1 Pathway Inhibition on Infection Efficiency

2.2.5.8.1 Dose Optimization of TBK1 Inhibitors BX-795 And Amlexanox for *in vitro* Infection Experiments

THP1-Dual cells were differentiated with 30 ng/ml PMA as described previously in Section 2.2.5.2.4. Wells were washed once with DPBS, and media was replaced with 2% Regular RPMI medium. 6 hours pre-infection, BX-795 hydrochloride (Sigma Aldrich, Germany) was added to corresponding wells at final concentrations of 10, 100, 1000 and 10,000 nM. 1 hour pre-infection, Amlexanox (Invivogen, France) was added to corresponding wells at final concentrations of 1, 4, 16 and 64 µg/ml. *In vitro* infection was carried out at a macrophage to parasite ratio of 1:10. Infection percentage and MFI values corresponding to parasite loads were quantified at 24 hours post-infection as described in Section 2.2.5.4.

2.2.5.8.2 Effect of TBK1 Inhibition on Infection Efficiency in A 3-Day *in vitro* Infection Model

THP1-Dual cells were differentiated with 30 ng/ml PMA as described previously in Section 2.2.5.2.4. Wells were washed once with DPBS, and medium was replaced with 2% Regular RPMI medium. 1 hour prior to infection, 64 µg/ml Amlexanox (Invivogen, France) was added to corresponding groups, and the drug additions were repeated every 24-hour. In one group, Amlexanox was added 24-hour late (after the initial 24-hour period) to observe the effect of receiving the drug later. Infection percentages and MFI values were quantified every 24 hours as described in Section 2.2.5.4.

2.2.6 RNA Isolation and Quantification for Nanostring Analysis

2.2.6.1 Preparation of Infected THP1-Dual Cell Lines for RNA Isolation

THP1-Dual cell lines were differentiated by incubating in media with 30 ng/ml PMA overnight in 6-well plates at a density of $2.7x10^6$ cells/well in 1.5-2 ml of 10% regular RPMI medium. 2 hours before infection, 64 μg/ml Amlexanox (Invivogen, France) or 40 μM Chloroquine (Sigma Aldrich, Germany) treatments were carried out in 2% Regular RPMI medium. Later, parasites were added to corresponding wells at a 1:10 (macrophage:parasite) ratio and spun down at 250g using a plate rotor. After 6 hours of infection period, each well was washed 3 times with DPBS, and media was replenished. 48 hours later, supernatant of each well was aspirated and 1 ml of RiboEx™ (Geneall Biotechnology CO., LTD, South Korea) was distributed to each well. After thoroughly pipetting each well to collect cellular material, technical duplicates were pooled into 15 ml falcon tubes, and stored at -80°C for 2 weeks.

2.2.6.2 Isolation of RNA from Collected Samples

Isolation of total RNA was achieved using a combination protocol of RiboEx™ (Geneall Biotechnology CO., LTD, South Korea) and RNA Clean & Concentrator™-25 (Zymo Research, U.S.A.). Briefly, samples dissolved in RiboEx™ were thawed and mixed with 0.2 ml of chloroform (Sigma-Aldrich, Germany) per 1 ml of RiboEx, followed by vigorous mixing. Following incubation at room temperature for 2 minutes, samples were centrifuged at 12,000 g for 15 minutes at +4°C in a microcentrifuge. Aqueous phases were transferred into RNase free eppendorf tubes and mixed with 1 volume of absolute ethanol (Fisher Scientific, U.S.A.) and mixed. Then, RNA clean-up protocol of RNA Clean & Concentrator™-25 kit was exactly followed. During the isolation procedure, working area was kept RNA-safe using RNase Away reagent. Obtained RNA samples were kept on ice to be used immediately for Nanostring procedure.

2.2.6.3 Gene Expression Analysis Using Nanostring Pancancer Immune Profiling Panel

Following quantification of RNA samples and assessment of their purity (A_{260}/A_{280} and A_{260}/A_{230}) using NanoDrop™ Spectrophotometer (Thermo Fisher Scientific, U.S.A), 50 ng of RNA sample for each group was processed with nCounter PanCancer Immune Profiling CS Kit (no MK) (NanoString Technologies, Inc., U.S.A.) according to the manufacturer's instructions by Deniz Kahraman in Kansil Laboratory. Obtained raw data was analyzed using nSolver Analysis software (v4, NanoString Technologies, Inc., U.S.A.) and nCounter® Advanced Analysis Software (v2, NanoString Technologies, Inc., U.S.A.).

2.2.7 Zymographic Assessment of GP63 Activity of SLA and Exosomes Isolated from *Leishmania major*

Separating gels supplemented with gelatin (Table B.1., Appendix B) and stacking gels (Table B.2., Appendix B) were freshly prepared and casted into 1.0 mm thick gel plates of Mini-PROTEAN II electrophoresis cell system (Biorad, Germany).

Exosome, SLA and mock-exosome samples were mixed with 3X SDS sample buffer without a reducing agent (New England Biolabs, U.S.A.) and placed on ice until loaded into the wells of the gels. Plates were placed on a vertical PAGE system, and the tank was filled with 1X Running Buffer (Table C.2., Appendix C). Around 20-25 μg of exosome and SLA samples or 800,000 lyophilized parasites were loaded to corresponding wells and PageRuler™ Prestained Protein Ladder (Thermo Fisher Scientific, U.S.A.) was loaded to one of the wells. Gels were run at 150 V for 1 to 2 hours until clear band separation was achieved. Afterwards, the gels were carefully taken out of the cell system for removal of stacking gel portions while separating gel portions were transferred to a clean box filled with washing buffer (Table B.3., Appendix B). Gels were washed for 30 minutes, and the wash buffer was replenished for washing the gels for another 30 minutes in order to remove remaining SDS from

the gels. This was followed by incubation of the gels in incubation buffer (Table B.4., Appendix B) for 10 minutes at 37°C. After refreshing the incubation buffer, gels were incubated for 20-24 hours at 37°C for gelatinase reaction to take place. The gels, then, were incubated with staining solution (Table B.5., Appendix B) for 30 minutes at room temperature followed by thoroughly rinsing them with distilled H_2O. Finally, gels were incubated in destaining solution (Table B.6., Appendix B), until enzymatic activity appeared as white bands against a dark blue background (1-3 hours). It was important to stop the destaining process by replacing the destaining solution with distilled H_2O once the desired contrast was achieved.

The gels were visualized using a ChemiDoc™ Gel Imaging System (Biorad, U.S.A.) by carefully placing them on top of a transparent plastic sheet and keeping them wet at all times.

When zymographic activity experiments were to be repeated, it was crucial to add fresh $ZnCl_2$ to incubation buffer because as $ZnCl_2$ dissolves in a water-based buffer with neutral pH, insoluble Zn(OH)Cl tend to form which prevents cofactor binding, resulting in failure of enzymatic activity.

2.2.8 Silver Staining of *Leishmania major* SLA and Exosome-specific Proteins in SDS-PAGE Gels

Pierce™ Silver Stain Kit (Thermo Fisher Scientific, U.S.A.) was used to observe the protein profile of exosome and SLA samples. Instructions on the user manual was followed with a minor change: using distilled water instead of recommended ultrapure water.

2.2.9 In vivo Immunization Experiments

2.2.9.1 Maintenance of BALB/c Mice

6-10 weeks old adult female BALB/c mice were used for *in vivo* experiments. They were maintained at Animal Facility of Molecular Biology and Genetics Department at Bilkent University (Ankara, Turkey). Animals were kept in filtered cages which were connected to an equipment providing filtered fresh air. Light/dark cycles were 12 hours each and temperature was set at 22°C ± 2. Animals were fed *ad libitum* and provided sterilized water. All animal protocols carried out in this thesis were approved by the animal ethical committee of Bilkent University.

2.2.9.2 Preparation of Lyophilized Vaccine Formulations

Composition and antigen/adjuvant content of formulations used in in vivo immunization studies are shown in Table 2.5.

Table 2.5 Composition of vaccine formulations used in immunization studies. All formulations were lyophilized and then resuspended except for the unvaccinated group.

Vaccination group	**Antigen type**	**Antigen dose/mouse**	**Adjuvant dose/mouse**
PBS	None	None	None
SLA	SLA	30 μg	None
SLA + α-GalCer	SLA	30 μg	0.06 μg
Parasites	Whole parasite	$5x10^6$	None
Parasites + α-GalCer	Whole parasite	$5x10^6$	0.06 μg
Exo	Exosome	30 μg	None
Exo + α-GalCer	Exosome	30 μg	0.06 μg

2.2.9.2.1 Preparation of α-GalCer and Lyophilization Procedure

α-GalCer was stored as concentrated stock solution (5 mg/ml) at -20°C in DMSO. Before lyophilization of vaccine formulations, it was thoroughly vortexed for 2-3 minutes, sonicated on iced water for 5 minutes and vortexed again before diluting it 1/25 with DPBS. 0.2 mg/ml intermediate stock was further diluted 1/4 using the same procedure to obtain a final α-GalCer solution (0.05 mg/ml) from which 0.06 µg/mouse of α-GalCer was distributed to corresponding formulation tubes after sonicating for 2-3 minutes and thoroughly vortexing.

Vaccine formulations were prepared according to Table 2.5. and were distributed to cryovials in a cell culture hood. Cryovial caps were stored to be used later. Each formulation was prepared for two injections to account for day 0 and day 14 injections. A large amount of parafilm was sterilized with 70% EtOH, dried and layered on top of each cryovial such that the opening parts of cryovials were protected by 4-5 layers of stretched parafilm. A tweezer with a thin edge was used to pierce the parafilm 8-10 times to form little pores. Then, cryovials were snap frozen in liquid nitrogen and kept in it for 5-10 minutes. Later, they were transferred into glass holders of a Virtis freeze-dryer (SP Scientific, U.S.A.). After sealing the glass holders with appropriate plastic pieces, they were put into liquid nitrogen to cool their temperature while keeping the plastic sealer outside, untouched. Previously established vacuum was released and glass cups containing the cryovials were placed on specified locations on the Virtis freeze-dryer (SP Scientific, U.S.A.). While the vacuum was being reestablished to 20 µBar and temperature was dropping down to -56.9°C, glass cups were kept cool by dipping them in a bucket full of liquid nitrogen while carefully avoiding contact with plastic sealers. Vaccine formulations were left overnight and retrieved in lyophilized form the next day. Cryovial caps were closed tightly and parafilmed to be stored at +4°C to only be resuspended on day 0 and 14 of vaccination schedule.

2.2.9.2.2 Resuspension of Lyophilized Vaccine Formulations

The lyophilized vaccine formulations were dissolved in 10% of their "before-lyophilization" volume with cell culture grade water (Biological Industries, Israel) by extensively vortexing for 30 seconds every 3-5 minutes for 25 minutes to achieve a milky texture. Then, an equal volume of DPBS was added to each cryovial and vortexed gently for 3 seconds only once. This was followed by incubation at room temperature for 10-15 minutes. Finally, formulations were filled with DPBS to their final injection volume for each group and immediately transferred to an ice filled box until injected.

2.2.9.3 Viability Test for Lyophilized Parasites

One sample of lyophilized parasites was resuspended as explained in the Section 2.2.9.2.2 and seeded into *Leishmania* growth medium (Table A.1., Appendix A) to be compared with control groups of logarithmic phase promastigotes and stationary phase promastigotes. Numbers of parasites in cultures were counted using a hematocytometer, and MFI values were analyzed using a Novocyte 2060R flow cytometer (ACEA Biosciences, U.S.A.) for 12 days. Aside from daily counting, whole parasite cultures in T25 flasks (SPL life sciences, South Korea) were observed daily for verification of viable parasites using the FLoid Cell Imaging Station (Thermo Fisher Scientific, U.S.A.).

2.2.9.4 Vaccination and Challenge Procedures

The vaccine formulations were prepared as explained in Section 2.2.9.2 and injected subcutaneously to female BALB/c mice (5 mice/group, 7 mice for unvaccinated group) on Day 0 and 14. After the primary and secondary injections, blood samples were collected on Day 13 and 27 for serum isolation and IgG ELISA procedures (explained in Sections 2.2.9.4.1 and 2.2.9.4.2). On day 29, animals were challenged

with live stationary phase promastigotes by injection of $10x10^6$ parasites/mouse in 50 µl into their left footpad using a 1 ml syringe with a 26G needle (Ayset, Turkey). Footpad sizes and parasite loads were quantified using a digital caliper and IVIS Lumina III (Perkin Elmer, U.S.A.) in vivo imager at regular intervals. These procedures are explained in detail in Sections 2.2.9.4.3 and 2.2.9.4.4, respectively. 31 days after challenge, spleens and lymph nodes were collected upon sacrificing the animals for splenocyte pulsing and detection of parasite metastasis to lymph nodes (explained in sections 2.2.9.4.6 and 2.2.9.4.5. Figure 2.4 summarizes the schedule used for vaccination, blood-collection, challenge and follow-up.

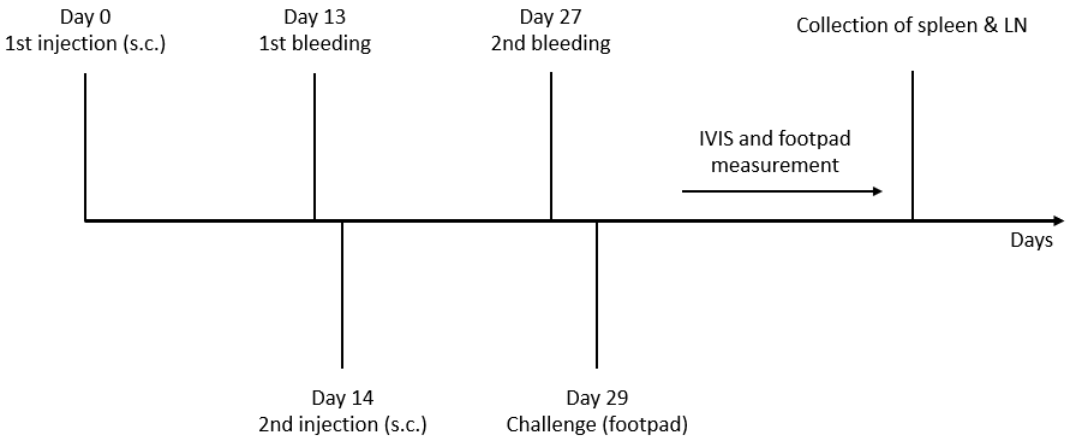

Figure 2.4. Outline of vaccination and challenge procedures.

2.2.9.4.1 Blood Collection and Sera Isolation

On Day 13 and 27, blood samples of the animals were collected via tail bleeding. Briefly, animals were subjected to a heat lamp for 5 minutes for dilation of tail veins. This step simplifies and speeds up the blood collection process. Then, each mouse was placed into a strainer, exposing their tails. After sterilizing the tails with %70 ethanol, sterile razors were used to slightly cut the tail veins open. 100-200 µL of blood was collected to sterile glass tubes. The bleeding was stopped by applying pressure to the tail cuts with a tissue paper. Collected blood in glass tubes were

allowed to coagulate for 2 hours at 37°C in a slanted position. In this state, usually sera were separated from the rest of the blood, but the separation was not clear cut. Therefore, sera were collected into eppendorf tubes and centrifuged at 8000g for 5 minutes to remove red blood cells and clots completely. Finally, clear sera were collected and put into a 96-well plate to be stored at -20°C.

2.2.9.4.2 Determination of Humoral Immune Response Induced by Vaccine Formulations by ELISA

Collected sera were utilized for quantification of SLA specific IgG1 and IgG2a levels by ELISA. 50 µL of SLA (10 µg/ml) in Coating Buffer (Appendix B, Table B.7.) was distributed to each well of Immulon 1 B Plates (Thermo Fisher Scientific, U.S.A.), and incubated at +4°C overnight following a 15-minute RT incubation. Then, plates were warmed to room temperature for 30-45 minutes before flicking the supernatants and filling each well with Blocking Buffer (Appendix B, Table B.8.). After incubating the plates in Blocking Buffer for 2 hours, plates were flicked and soaked in ELISA wash buffer (Appendix B, Table B.9.) for 5 times at 5-minute intervals (each time plates were flicked). Then, they were soaked in dH_2O for 3 times and flicked each time. Following drying of wells with tapping on a towel surface, 100 µL of PBS diluted sera (1:200) were added to top rows of the plates while the remaining wells were filled with 50 µL PBS. Sera in the top rows were diluted serially down the bottom of the plates using a multichannel pipette, and the final 50 µL remaining in tips of the multichannel pipette were discarded after mixing the last wells thoroughly. This procedure resulted in 8 serial dilutions ranging from 1:200 to 1:25,600. Overnight incubation at +4°C, washing and drying procedures were repeated. Goat anti-mouse IgG1-AP or IgG2a-AP (Southern Biotech, U.S.A.) solutions were diluted 1:2000, distributed to wells at 50 µL and incubated at RT for 2 hours. Plates were then washed and dried as described previously. Finally, 50 µL of PNPP substrate solution (Appendix B, Tab B.10.) were added to wells. The absorbance values were recorded at 405 nm using a Multiskan™ GO Microplate

Spectrophotometer (Thermo Fisher Scientific, U.S.A.) at regular intervals until the saturation points were reached.

Antibody titers were calculated using GraphPad Prism software (v8.0.1, U.S.A.) by determining a background level of mean ODs + 1.5 times standard deviation of all unvaccinated readings. Then, this determined cut-off value was fit into four parametric logistic regression curves (dilutions vs. OD readings) created for each mouse of vaccinated groups, and calculated dilution values were recorded as antibody titers.

2.2.9.4.3 Measurement of Footpad Lesions

On the day of the challenge, heights and depths of the footpads of mice were measured by a digital caliper as baseline levels of footpad size. Following challenge, measurements were taken weekly to follow the development of lesions until the mice were sacrificed. Recorded heights and depths were multiplied for each mouse, and the results were reported as lesion area (height x depth).

2.2.9.4.4 Quantification of Parasite Loads in Footpad Lesions

To estimate the parasite loads of each mouse, luciferase reporting system of transgenic *L. major* parasites were utilized. Firstly, 15 mg/ml D-luciferin (Perkin Elmer, U.S.A.) was prepared by diluting necessary amount of D-luciferin in DPBS and filter-sterilization (0.22 µm). This solution was put on an ice-filled box until use. Secondly, FOV24 lens attachment of IVIS Lumina III (Perkin Elmer, U.S.A.) was installed and the device was initialized to adjust the camera temperature to -90°C and base temperature to 37°C on which the mice would lay. Thirdly, the mice were anesthetized using Isoflurane Vaporizer (VetEquip, U.S.A.) in groups of five, and injected with 50 µl of 15 mg/ml D-luciferin solution (0.75 mg/mouse) intraperitoneally right before being transferred to the cabinet of IVIS Lumina III which was supplied with isoflurane. Finally, luminescence protocol was initiated to

capture 40 images in 20 minutes with 30 seconds of exposure times. Region of interests were placed on the footpads, and enzymatic activity curves of total flux for each mouse were constructed using GraphPad Prism 8 (v8.0.1, U.S.A.). Highest peak point values of total flux for each mouse were used as estimated parasite loads in constructed graphs.

2.2.9.4.5 Quantification of Parasite Metastasis

To quantify parasite metastasis, popliteal lymph nodes on the side of the challenged footpad were collected and placed into wells of a 96-well black opaque plate (Corning, U.S.A.) filled with 100 µl 2% Regular RPMI medium. As controls, 3 popliteal lymph nodes from the unchallenged footpad side from unvaccinated group were also collected. D-luciferin solution dissolved in cell culture grade water was added to the wells of the 96-well black plate to end up with a final concentration of 150 µg/ml of D-luciferin. This addition was done with a multichannel pipette in a quick fashion to ensure simultaneity for each sample. The plate was placed into the cabinet of IVIS Lumina III with detached FOV24 lens, and the location of the stage was adjusted to ensure the field of view contained the entirety of the plate. Each well with a lymph node was assigned a region of interest, and the recordings were collected as described in Section 2.2.9.4.4. Highest peak point values of total flux for each lymph node were used as estimated parasite loads in constructed graphs.

2.2.9.4.6 Isolation of Splenocytes and Pulsing Experiments

Animals were sacrificed and incisions were introduced to skin and peritoneum to open the intraperitoneal cavity. After removal, each spleen was placed into one well of 6-well plates (Sarstedt, Germany) filled with 2% Regular RPMI medium (Appendix A, Table A.3.). Plates were kept on ice until all the spleens were removed. Later, spleens were mashed using the back of sterile syringe plungers in a cell culture hood. Using Pasteur pipettes, splenocytes in media were collected and transferred to

15 ml falcons filled with 2% Regular RPMI medium while connective tissues of the spleens were left in the plates. These cells were washed 2 times at 300g for 5-10 minutes. After each wash, cells were resuspended, and any remaining lipid aggregates and connective tissues were removed. Then, the pellets were resuspended in 2 ml of 10% Regular RPMI medium (Appendix A, Table A.6.). Cell counts were quantified by Accuri C6 Flow Cytometer (Becton, Dickinson, U.S.A.) after 20 µL of each sample were diluted to 10 ml with isotonic solution and adding ZAP-OGLOBIN II Lytic Reagent (Beckman Coulter, U.S.A.) for the lysis of erythrocytes. Acquired cell numbers on splenocyte gate were multiplied by 100 x 500 to obtain total cell number for each sample. Splenocytes were diluted and distributed to U-bottom 96-well plates in duplicate as 10^6 cells/well in 100 µl and rested for 2 hours in a 37°C, 5% CO_2 supplemented and humidified incubator. Then, 100 µl of 100 µg/ml SLA solution in 10% Regular RPMI was distributed to each well of stimulation groups. Control groups, on the other hand, received only media. After 48 hours of incubation, plates were centrifuged at 300g for 5 minutes to collect and transfer the supernatants into fresh plates which were then stored at -20°C until use.

2.2.9.5 Cytometric Bead Array of Supernatants Collected from Pulsed Splenocytes

Supernatants of pulsed splenocytes were used for the detection of Th1, Th2, Th9, Th17 and Th22 cytokines using the LEGENDplex™ MU Th Cytokine Panel (12-plex) w/ VP V03 (Biolegend, U.S.A.).

In preparation for the assay, Novocyte 2060R flow cytometer (ACEA Biosciences, U.S.A.) was set up according to the instructions of the kit manufacturer to obtain the clearest results. For the preparation of reagents, pre-mixed beads were sonicated in an ice-cold, distilled water-filled sonicator bath and vortexed for 1 minutes to completely resuspend the beads. Also, 20X wash buffer was brought to room temperature, and 475 ml of dH_2O was added to reach 1X working concentration. Finally, standards were prepared by reconstituting lyophilized standard cocktail in

250 µl Assay Buffer. Following a 10-minute incubation at RT, this solution was transferred to an eppendorf tube to be used as top standard. 75 µl of Assay Buffer was added to 6 different tubes. Serial 1:4 dilutions were done by transferring 25 µl of higher-concentration cocktail to a fresh tube filled with 75 µl of Assay Buffer. The final (eight tube) tube was left untouched to be used as 0 pg/ml standard.

Every reagent and supernatant were left to warm up in room temperature. Provided V-bottom plate was filled with 25 µl Assay Buffer and 25 µl standard or sample supernatant. Beads were vortexed once again for 30 seconds, and 25 µl of bead suspension was added to each well. Then, the plate was sealed with a plate sealer to prevent accidental mixing up of wells and covered with aluminum foil. The plate was put onto a plate shaker for 2 hours. Every 40 minutes, wells were mixed with a multichannel pipette to prevent bead settling at the bottom. Following the incubation, the plate was centrifuged at 250g for 5 minutes using a swinging bucket rotor and immediately flicked into the sink to remove supernatants. Then, wells were washed with 200 µl of 1X wash buffer for 1 minute before centrifugation step was repeated. 25 µl of Detection Antibodies were added to each well and the plate was incubated for 1-1.5 hour as described previously. Once the incubation finished, 25 µl of SA-PE was added to wells without any washing step, and 30 minutes of incubation was done as described previously. After repeating centrifugation and washing steps, 150 µl of 1X Wash buffer was used as final resuspension medium. Finally, samples were transferred to eppendorf tubes to be analyzed using Novocyte 2060R flow cytometer (ACEA Biosciences, U.S.A.) according to the instructions of the kit's manufacturer. Following analysis was done using LEGENDplex™ data analysis software (Biolegend, U.S.A.) according to the instructions of the software developers.

2.2.10 Statistical Analyses

Graphpad Prism (v8.0.1.) was used for construction of the graphs and statistical analysis. For *in vitro* assays, one-way ANOVA followed by Dunnett's multiple comparison test or unpaired t-test were used. For *in vivo* assays, Kruskal-Wallis

followed by Dunn’s multiple comparison test or Mann-Whitney test were used. Data were demonstrated as means ± SD. The test used and p-values of each comparison is noted in the legend section of each figure.

CHAPTER 3

RESULTS & DISCUSSION

3.1 Growth of *L. major* on Human Blood Supplemented NNN Media

To prevent the loss of virulence of *Leishmania* cultures, the number of passages in an axenic promastigote culture should not exceed 10-15. Therefore, it is important to passage axenic promastigote cultures *in vivo* to enhance their virulence before frozen stocks are all used up. Biphasic blood agar medium induces transformation of amastigotes to promastigotes once they are isolated from mice and humans (Maurya et al., 2010; Titus et al., 1985). Previously, our blood agar preparation protocol included the use of rabbit blood. In the absence of rabbit blood, we had to use human blood to replace it. However, human blood did not support the growth of *Leishmania major* to the same extent at the recommended concentration of 10% (v/v). Therefore, an optimized protocol was necessary.

3-days post inoculation of *L. major* to NNN modified medium (HiMedia, India) supplemented with 10% (v/v) blood, 30% (v/v) blood or 30% (v/v) hemolyzed blood, morphology of *L. major* was observed under microscope for deformities (Figure 3.1 top panel). No deformities were found except for apoptotic-like parasites at similar frequencies found in standard growth medium (data not shown). Cultures were left for an additional 2 days without any refreshment of media to induce nutritional stress. At the end of the fifth day, whole cultures were stained with SYTO™ 16 Green and SYTOX™ Orange (Thermo Fisher Scientific, U.S.A.) and observed under fluorescence microscope to qualitatively assess cell death (Figure 3.1 bottom side). All cultures were considered healthy based on observations that both SYTOX™ Orange signal and rosette formation (indicators of stress) were low.

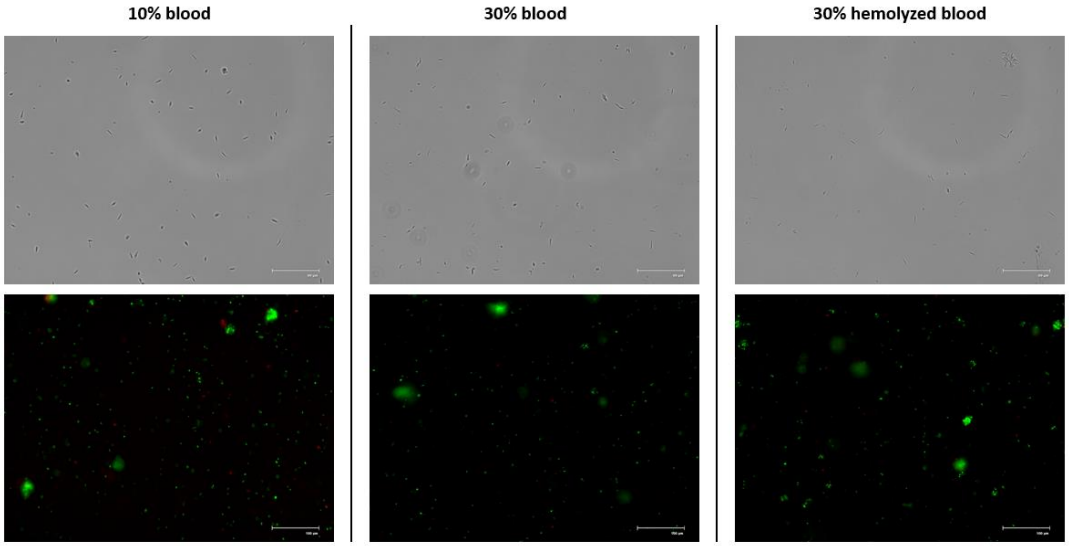

Figure 3.1. Morphologic and viability analysis of *L. major* parasites in NNN media. Parasites were transferred onto slides and observed under white light (top panel) using FLoid Cell Imaging Station (Thermo Fisher Scientific, U.S.A.) for morphological deformities. Whole *L. major* cultures in T25 flasks were stained with 0.4 μM SYTO™ 16 Green and 1 μM SYTOX™ Orange (bottom panel) and observed with green/red channels of FLoid Cell Imaging Station (bottom panel).

To assess the growth of *L. major* quantitatively, cultures were counted with a hematocytometer for 5 days (Figure 3.2a). NNN modified medium supplemented with 30% (v/v) blood supported the growth and survival of *L. major* better than the two other medium compositions throughout the 5-day period. At the end of the 5th day, this group had 1.36- and 2.44-fold higher levels of parasites/ml compared to media counterparts supplemented with 30% (v/v) hemolyzed blood and 10% (v/v) blood, respectively (Figure 3.2b). A following passage on the same medium confirmed that this effect was not transient (Figure 3.2c). Therefore, we chose to use 30% human blood for amastigote to promastigote transformation.

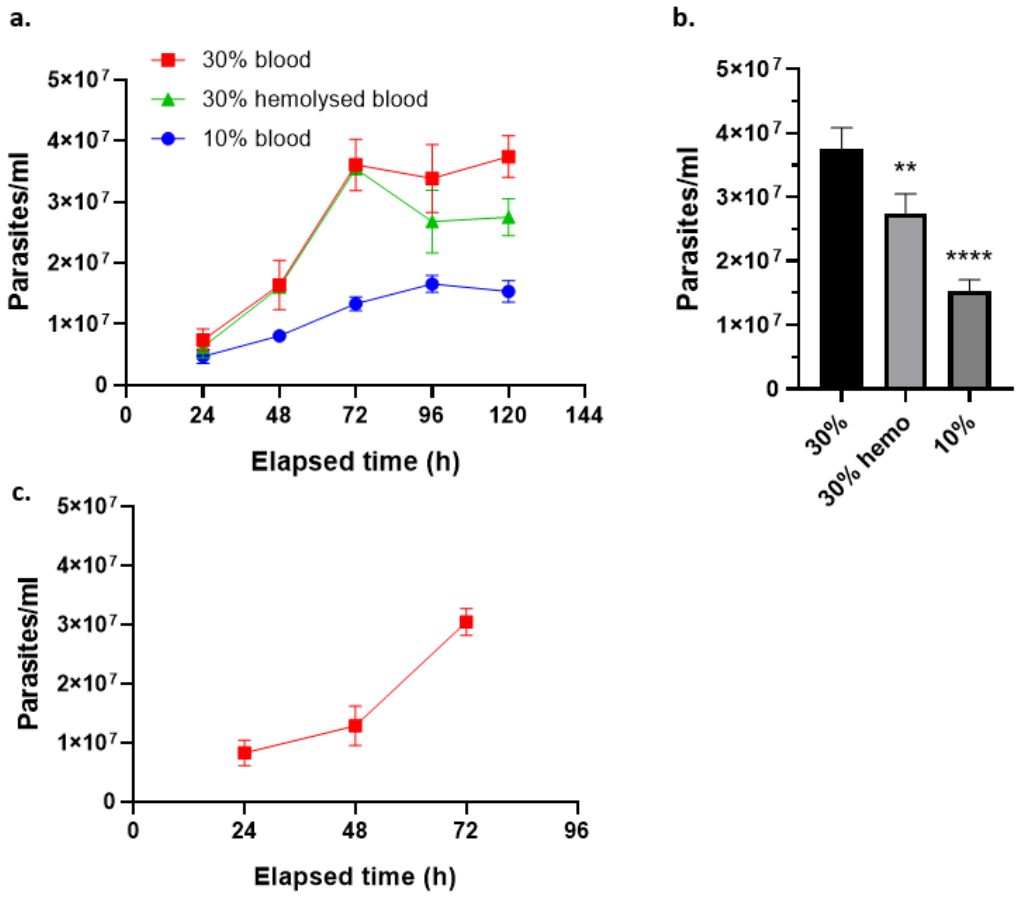

Figure 3.2. Quantitative assessment of proliferation and viability of *L. major* parasites in NNN media.

a. Comparison of *L. major* growth and endurance in NNN media prepared with 10% blood, 30% blood and 30% hemolyzed blood. **b.** Parasite concentration 120h after the initiation of culture. **c.** Growth curve of passaged parasites (sampled from 30% blood group) showing the effect was not transient. Groups were statistically analyzed by ordinary one-way ANOVA followed by Dunnet's multiple comparison test (**: p=0.0014, ****: p<0.0001).

3.2 *In vitro* Infection Optimization Experiments

3.2.1 Optimization of Stationary Phase Infective Parasite Preparation Method for *in vitro* Infection Experiments

Presence of *L. major* parasites that have gone through metacyclogenesis or apoptotic-like cell death is important for successful infection of macrophages. Metacyclic parasites readily counteract offensive strategies of macrophages and neutrophils, whereas apoptotic-like parasites contribute to successful infection by suppressing inflammatory cytokines and inducing anti-inflammatory cytokines (Crauwels et al., 2015; Ger Van Zandbergen et al., 2006), resulting in the survival of the population rather than individual parasites. Transformation of procyclic promastigotes to metacyclic promastigotes have been shown to be induced by nutrient deprivation both *in vitro* and *in vivo* (D. L. Sacks & Perkins, 1984). Furthermore, procyclic to metacyclic transformation has been linked to autophagy machinery of *L. major* (Besteiro et al., 2006), which further supports the notion that the initial induction of transformation is nutrient deprivation. Similarly, apoptotic-like parasites gradually increase in frequency as parasites are left in stationary-phase cultures (Ger Van Zandbergen et al., 2006).

Therefore, we aimed to investigate *in vitro* infection rates under conditions of increased metacyclogenesis and apoptotic-like cell death. We used three methods to achieve these states. The first method was to transfer late-logarithmic phase promastigotes to FBS-free medium to increase nutritional stress for 24 hours prior to infection. The second method aimed to increase apoptotic-like leishmania in late logarithmic phase promastigotes by treating with low dose H_2O_2 (200 μM) for 24 hours before infection (Basmaciyan et al., 2018). The final method, previously used by our group, was to leave stationary phase promastigotes in their culture for an additional 3 to 6 days without refreshment or addition of fresh medium. These parasites, then, were used to infect PMA differentiated THP1 cells. As demonstrated in Figure 3.3, lowest parasite loads at the end of 24-hour infection period were

observed in positive control groups; Stat(6d) and Stat(3d). No FBS, H_2O_2 (200 μM) and procyclic promastigotes had 2-, 2.7- and 1.96- fold higher levels of parasite loads, respectively.

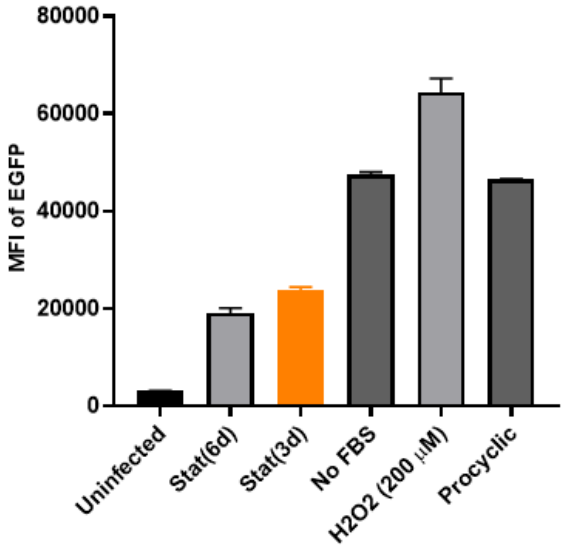

Figure 3.3. Parasite loads of THP1 cells infected with various stationary phase models.

PMA-differentiated (5 ng/ml) THP1 cells were incubated with eGFP-expressing *L. major* at a MOI of 1:10 (macrophage:parasite) for 24 hours. At the end of 24 hours, MFI values were quantified using a flow cytometer. The graph was constructed from only one experiment; hence, statistical tests were not performed.

However, these high levels did not translate well to a 3-day infection model as parasites of these groups proliferated significantly lower in THP1 cells compared to the positive control groups (Figure 3.4). Low infection potential of procyclic *Leishmania* promastigotes has already been reported (Ueno et al., 2009) which supports our findings. This suggests that the initial high infection rates of these groups are false positive events resulting from fresh parasites expressing higher eGFP signals unlike our positive control groups which lost a noticeable amount of eGFP expression due to being under nutrient deprived conditions for an extended period (Figure 3.5). Since our test groups did not work as well in 3-day infection model as expected, we used our previous model to induce metacyclogenesis for

further experiments. This choice simplified *in vitro* infection protocol and provided reproducible data since freshly produced eGFP signal following infection indicated amastigote proliferation.

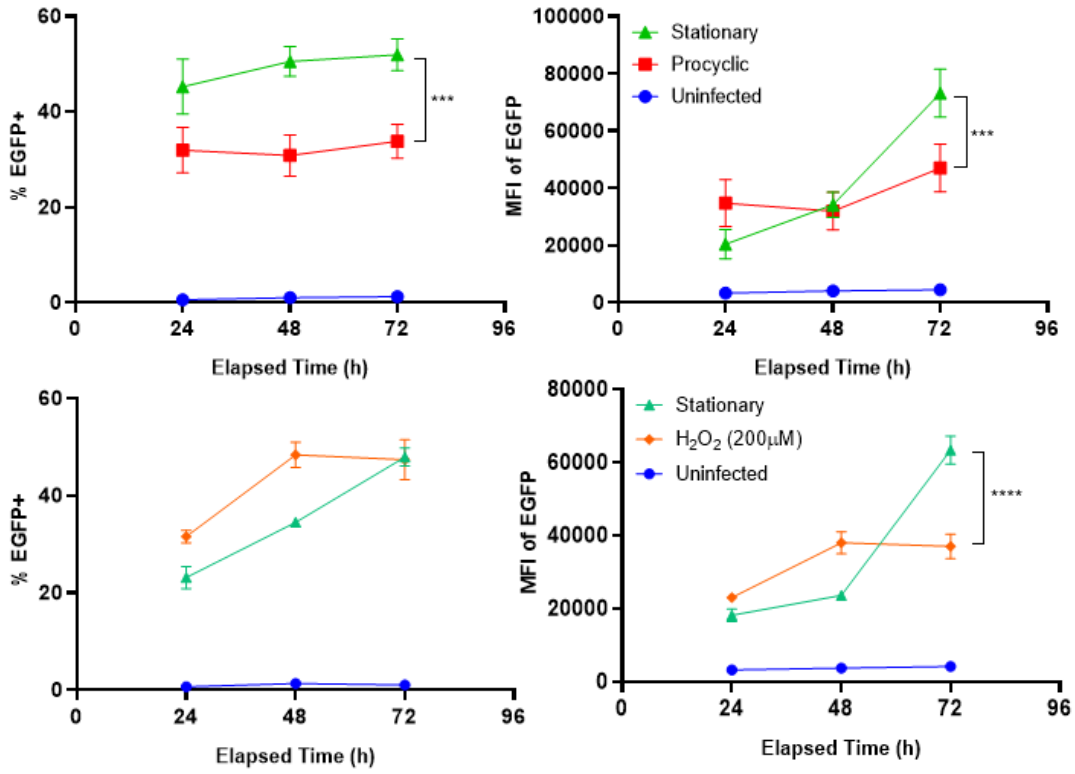

Figure 3.4. Infection percentages and parasite loads of THP1 cells infected with various stationary phase models in a 3-day infection model.

PMA-differentiated (5 ng/ml) THP1 cells were infected with EGFP-expressing *L. major* at a MOI of 1:10 (parasite:macrophage) for 24 hours followed by DPBS washes. At the end of 72 hours, MFI values were quantified using a flow cytometer. Top panel represent infection levels of procyclic and stationary phase parasites, while bottom panel represent infection levels in stationary and H_2O_2 (200 μM)-treated parasites. The graphs were constructed from three (for top panel) and two (for bottom panel) biological replicates. Final time point infection levels of infected groups were statistically compared to each other using unpaired t-test (from left to right ***: p=0.0003, ***: p=0.0006, ****: p<0.0001).

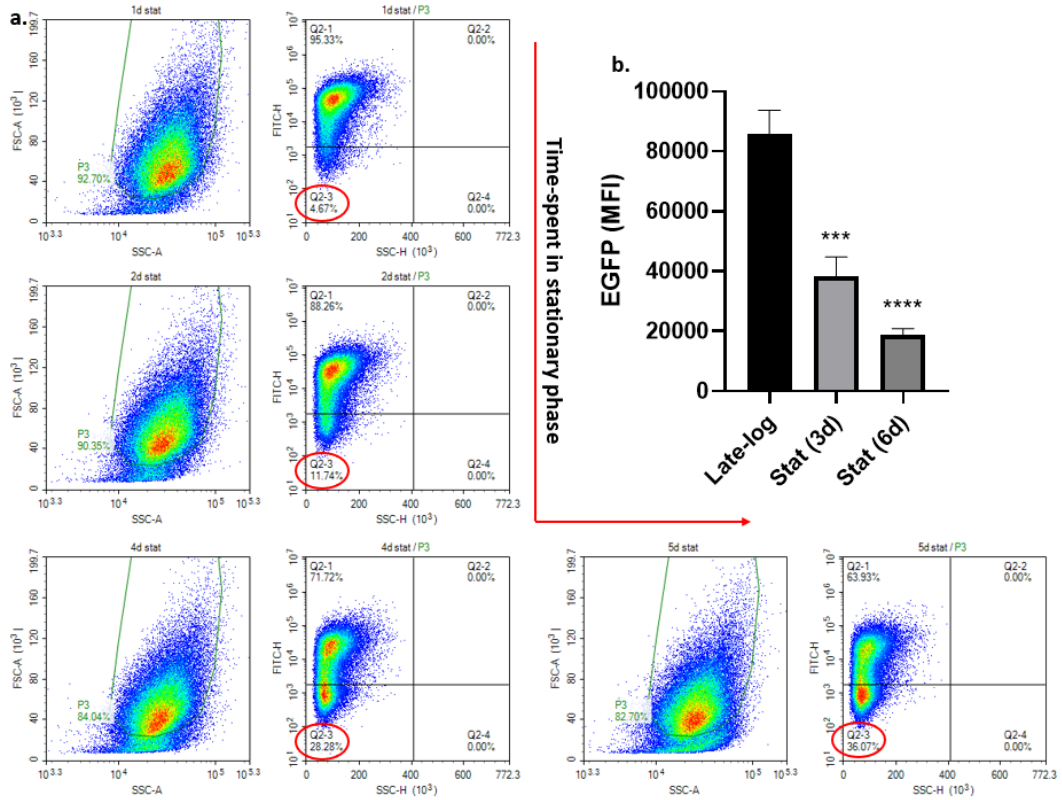

Figure 3.5. Gradual decrease of EGFP signal of transgenic *L. major* parasites during incubation period in stationary phase cultures.

a. Representative density plots of EGFP signal diminishing as the age of stationary phase increases. Four time points for density plots are shown in the direction of the red arrow (day 1, 2, 4 and 5). **b.** Bar graph of MFI (EGFP) values taken from 3 independent stationary phase cultures followed for 6 days starting from late-logarithmic phase. Stationary phase MFI values were statistically compared to late-logarithmic phase MFI values using ordinary one-way ANOVA followed by Dunnett's multiple comparison test (***: p=0.0001, ****: p<0.0001).

3.2.2 Optimization of Parasite Inoculation Duration on Efficiency of *in vitro* infection

Infection of macrophages by *Leishmania spp.* has been reported to take as short as 30 minutes (Peters et al., 2009). Previously, we performed *in vitro* infection of THP1

cells for 24 hours. However, this resulted in uninternalized parasites stuck to the cell membrane of macrophages which in turn resulted in false positive events complicating evaluation of infection rate based on the eGFP signal. Therefore, we tested a 6-hour inoculation period followed by three DPBS washes to reduce false positive events. As seen in Figure 3.6., 6-hour infection group had noticeably lower infection percentage and parasite load. However, this difference was not statistically significant. Furthermore, as shown in Figure 3.7., additional 3 DPBS washes performed at 6-hour post-infection resulted in clear images devoid of thousands of extracellular promastigotes. Therefore, we chose to continue with the 6-hour inoculation followed by 3 DPBS washes in further experiments.

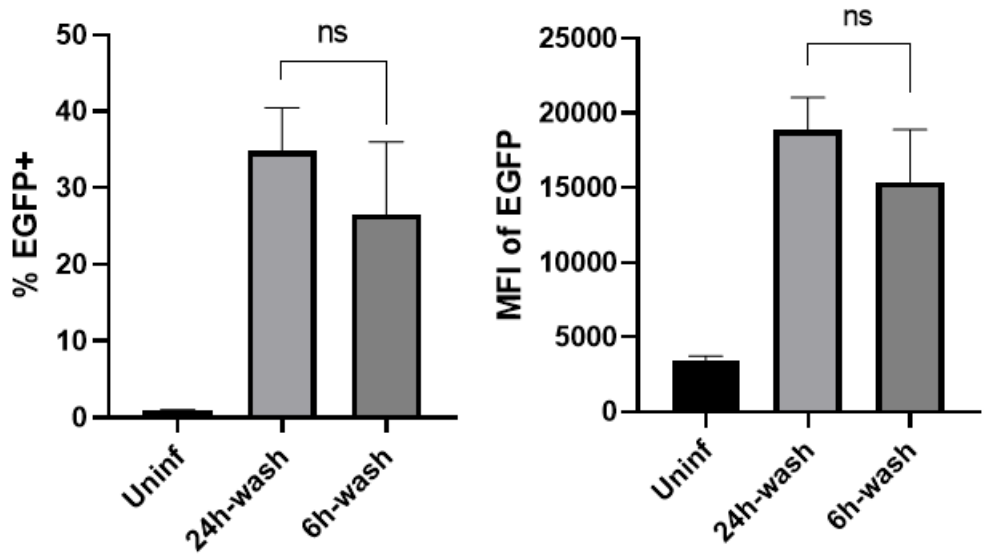

Figure 3.6. Effect of an additional DPBS wash at 6-hour post-infection on false positive events.

PMA-differentiated (40 ng/ml overnight) THP1 cells were infected with EGFP expressing *L. major* parasites at a 1:10 (macrophage:parasite) ratio. The wells were washed 3 times either at 24-hour post-infection alone or at both 6- and 24-hour post-infection. At the end of 24th hour, infection percentages and parasite loads were quantified using a flow cytometer. The graphs were constructed using two independent experiments. The infected groups were compared to each other using unpaired t test (ns: not significant).

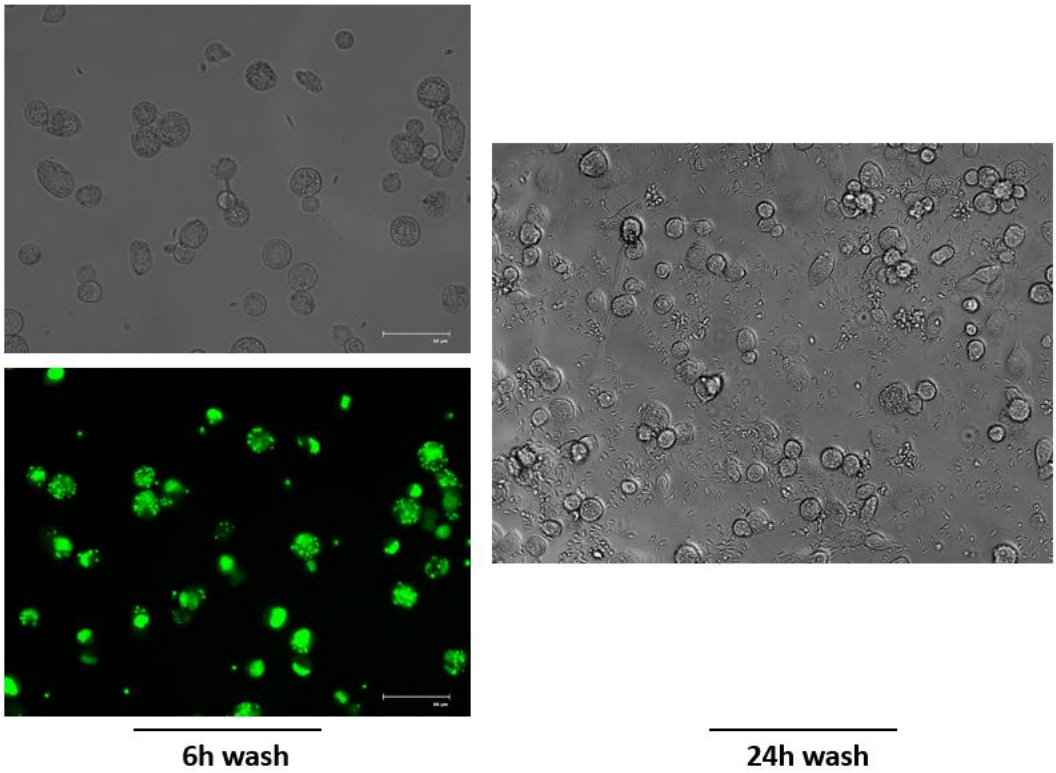

Figure 3.7. White light and fluorescent images of infection at 24th hour.

PMA-differentiated (5 ng/ml) THP1 cells were infected with eGFP expressing *L. major* parasites at a a MOI of 1:10 (macrophage:parasite). The wells were either washed at 6 hours or left unwashed. The images were taken prior to the 24th hour wash and depict the reduction in extracellular parasites in washed group. The green signal of amastigotes inside THP1 cells were enhanced by staining with 0.4 μM SYTO™ 16 Green (Thermo Fisher Scientific, U.S.A.).

3.2.3 Effect of PMA Concentration on PMA-differentiated THP1 macrophage model of *in vitro* Leishmania Infection

Our previous trials using THP1 differentiation with low dose (5 ng/ml for 48 hours) and moderate doses (30-50 ng/ml overnight) of PMA, promoted adherent macrophage-like phenotype and enabled *L. major* infection (Figure 3.8), although

high-PMA differentiated THP1 cells showed more extensive macrophage-like extensions.

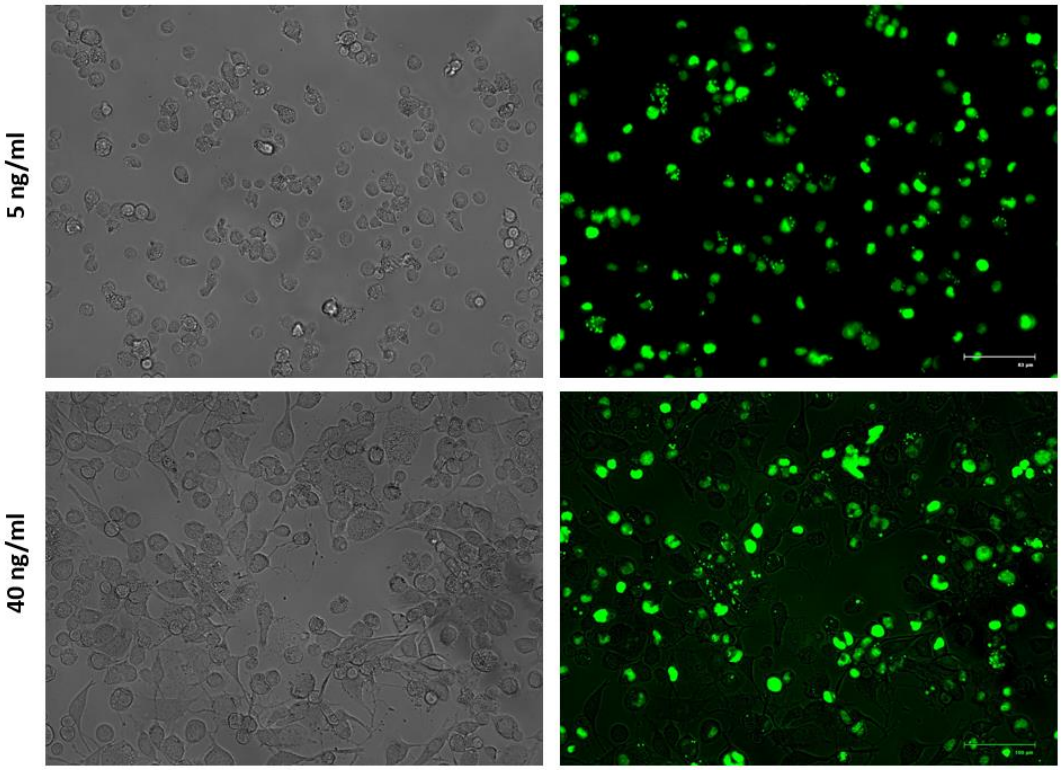

Figure 3.8. Morphology of and infection rates of THP1 cells differentiated with low and high dose of PMA.

PMA-differentiated THP1 cells were infected with EGFP expressing *L. major* parasites at a MOI of 1:10 (macrophage:parasite). Morphology of THP1 cells were observed using white light of FLoid Cell Imaging Station (Thermo Fisher Scientific, U.S.A.). The green signal of amastigotes inside THP1 cells were enhanced by staining with 0.4 μM SYTO™ 16 Green (Thermo Fisher Scientific, U.S.A.).

As infection percentages and parasite loads varied noticeably from one experiment to another, we wanted to optimize PMA concentration for differentiation of THP1 cells for subsequent use in *in vitro* infection trials. To achieve this, we chose to use manufacturer's differentiation protocol (as explained in Section 2.2.5.2.3.) rather than our previous protocols. As demonstrated in Figure 3.9., moderate

concentrations of PMA-induced differentiation resulted in highest infection percentages and parasite loads in wild type THP1 cells.

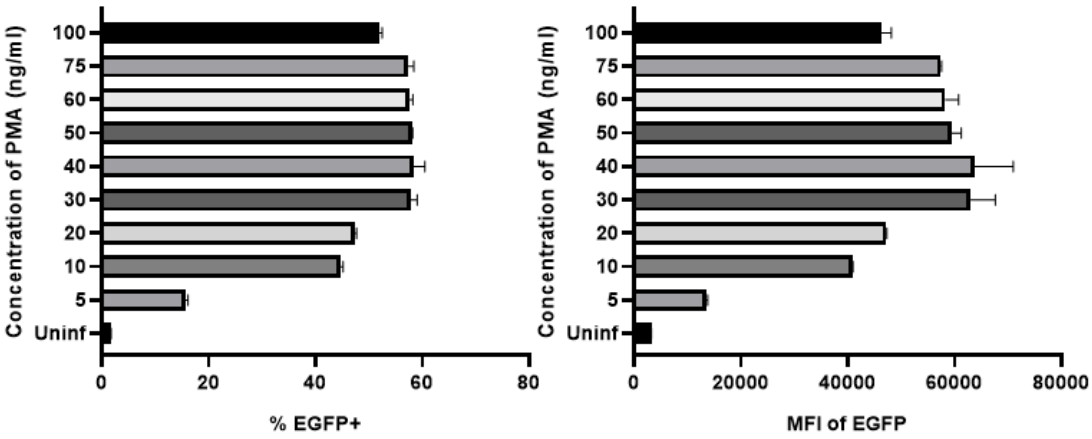

Figure 3.9. Infection percentages and parasite loads of THP1 cells differentiated with increasing doses of PMA.

THP1 cells were incubated with 5 and 10 ng/ml PMA overnight. For higher concentrations, incubation period was limited to 6 hours. PMA-differentiated THP1 cells were infected with eGFP expressing *L. major* parasites at a 1:10 MOI of (macrophage:parasite). At the end of 24 hours, infection percentages and parasite loads were quantified using a flow cytometer. The graphs were constructed using data from only one experiment; hence, statistical tests were not performed.

Furthermore, this level of macrophage-like phenotype activation was not exclusive to moderate concentrations of PMA but could be achieved with lower levels of PMA-induced differentiation with longer differentiation time as suggested by our previous trials (Figure 3.10.; first four independent experiments compared to 5 ng/ml PMA group from Figure 3.9.). In conclusion, it became apparent that a moderate level of activation, rather than a specific concentration of PMA, is essential for a successful *in vitro* infection as both low levels of activation (induced by low dose PMA and short differentiation time) and high levels of activation (induced by high dose PMA) resulted in lower infection percentages and lower parasite loads. Therefore, we chose

to use differentiation conditions as summarized in Table 3.1. in our subsequent experiments.

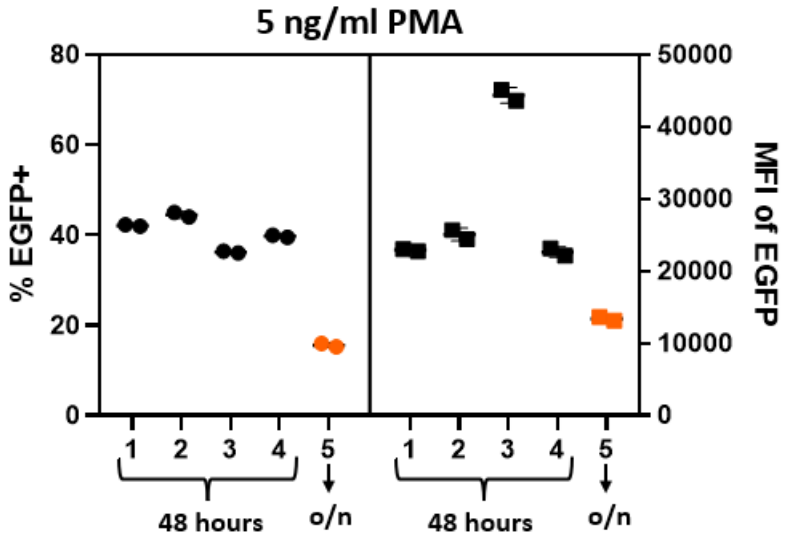

Figure 3.10. Infection percentages and parasite loads of THP1 cells differentiated with 5 ng/ml PMA.

THP1 cells were either differentiated with 5 ng/ml PMA for 48 hours (first four independent experiments) or overnight (fifth experiment; formatted in orange color), before infection. At the end of 24 hours, infection percentages and parasite loads were quantified using a flow cytometer.

Table 3.1 Selected PMA differentiation conditions for successful *in vitro* infections.

Concentration of PMA	**Differentiation Time Period**
5 ng/ml	48 hours
30 ng/ml	Overnight
50 ng/ml	Overnight

3.2.4 Transition to 3-day *in vitro* Infection Model

3.2.4.1 Determination of the Effect of FBS Concentration on Infection Efficiency

Our previous trials (data not shown) had shown us that 2% Regular RPMI medium (Table A.3., Appendix A) improved *in vitro* infection levels by the end of 24 hours. Therefore, we tested whether this limited serum supplementation could be of benefit for amastigote proliferation in a prolonged *in vitro* infection model, possibly by lowering the defenses of THP1 cells. Figure 3.11. illustrates that the progression of infection in 2% Regular RPMI medium lagged compared to infection in 10% Regular RPMI medium (Table A.6., Appendix A) following the first 24-hour period. By the end of 72-hour infection period, an increase of 1.2- and 2.2-fold had occurred in infection percentage and parasite load, respectively, in the group that was kept in 10% Regular RPMI medium. In conclusion, FBS-rich medium (10% Regular RPMI medium) was more suitable for aggressive proliferation of amastigotes inside THP1 macrophages compared to FBS-poor medium (2% Regular RPMI medium) following the initial 24-hour period.

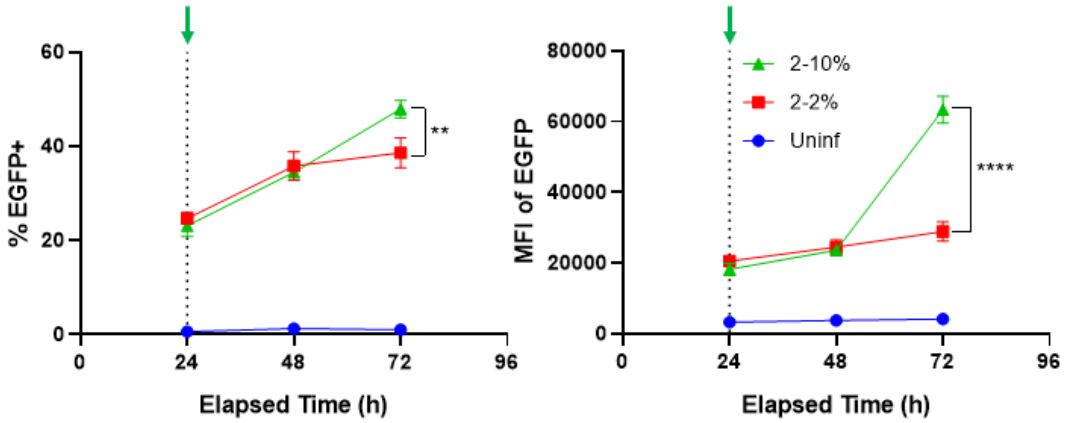

Figure 3.11. Progression of *L. major* infection in differentiated THP1 cells in media supplemented with different concentrations of FBS.

Figure 3.11. (continued) Progression of *L. major* infection in differentiated THP1 cells in media supplemented with different concentrations of FBS.

Differentiated (40 ng/ml) THP1 cells were infected with eGFP expressing *L. major* parasites at a MOI of 1:10 (macrophage:parasite). Every 24-hours, infection percentages and parasite loads were quantified using a flow cytometer. The graphs were constructed based on two biological replicates. Green arrow shows the time point at which 2% FBS medium was exchanged to 10% FBS medium. Final time point infection levels of infected groups were statistically compared to each other using unpaired t-test (**: $p=0.0024$, ****: $p<0.0001$).

3.2.4.2 Effect of Opsonization and PMA Concentration/Exposure Time on Infection Efficiency

Our previous trials led us to the hypothesis that the level of PMA induced activation of THP1 cells is a crucial determining factor for *in vitro* infection. Therefore, we observed how different PMA levels affected 3-day *in vitro* infection model. Figure 3.12. depicts that infection percentages varied meagerly between groups at the end of 72 hours. However, THP1 cells differentiated with 5 ng/ml PMA had 2.5- and 2.1-fold increase in parasite load compared to those differentiated with 30 and 50 ng/ml PMA, respectively. It is clearly illustrated that differentiation of THP1 cells by incubation with 5 ng/ml PMA for 48 hours resulted in the most striking amastigote proliferation. However, using higher PMA concentrations for differentiation proved useful in terms of equalizing initial phagocytosis rates between THP1 WT, cGAS- and TBK1-KO cells as explained in Section 3.2.6. In conclusion, all of the three protocols of differentiation resulted in successful 3-day *in vitro* infections based on proliferation of *L. major* in amastigote form. Therefore, we utilized all three differentiation methods in further experiments.

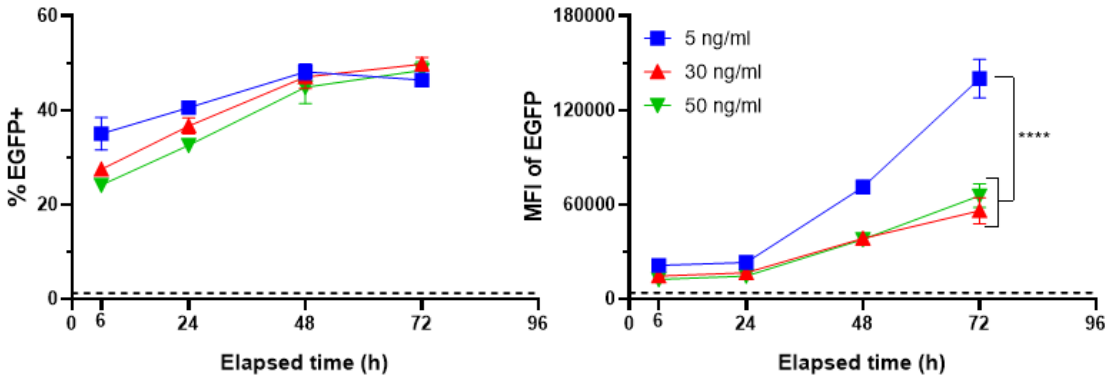

Figure 3.12. Progression of *L. major* infection in THP1 cells differentiated with different PMA concentrations.

Differentiated THP1 cells were infected with eGFP expressing *L. major* parasites at a MOI of 1:10 (macrophage:parasite). At designated time points, infection percentages and parasite loads were quantified using a flow cytometer. The graphs were constructed based on two biological replicates. Dotted lines represent average of all uninfected groups at all time points. Final time point infection levels of infected groups were statistically compared to each other using ordinary one-way ANOVA followed by Dunnett's multiple comparison test (****: $p<0.0001$).

In the same experimental procedure, we tested whether opsonization of *L. major* with human serum facilitated the 3-day *in vitro* infection levels since opsonin mediated phagocytosis is a key mechanism of entry into macrophages utilized by *Leishmania spp.* (Ueno & Wilson, 2012). 2-hour infection analysis suggested that opsonization increased levels of phagocytosis of *L. major* in all three of the PMA differentiation groups (1.8, 1.7 and 1.6-fold for infection percentages & 2.1, 1.8 and 1.6-fold for parasite loads) (Figure 3.13., top panel). At the end of the 6 hours, non-opsonized infection groups had similar levels of phagocytosis compared to opsonized infection (Figure 3.13., middle panel). At the end of the 3-day infection period, there were no significant differences between opsonized and non-opsonized *L. major* infection percentages and parasite loads (Figure 3.13., bottom panel). In conclusion, our observations suggested that although opsonization greatly increased initial phagocytosis rate, it did not change the course of the infection, final infection

percentages and parasite loads significantly. Therefore, we did not opsonize *L. major* in the future experiments for simplicity.

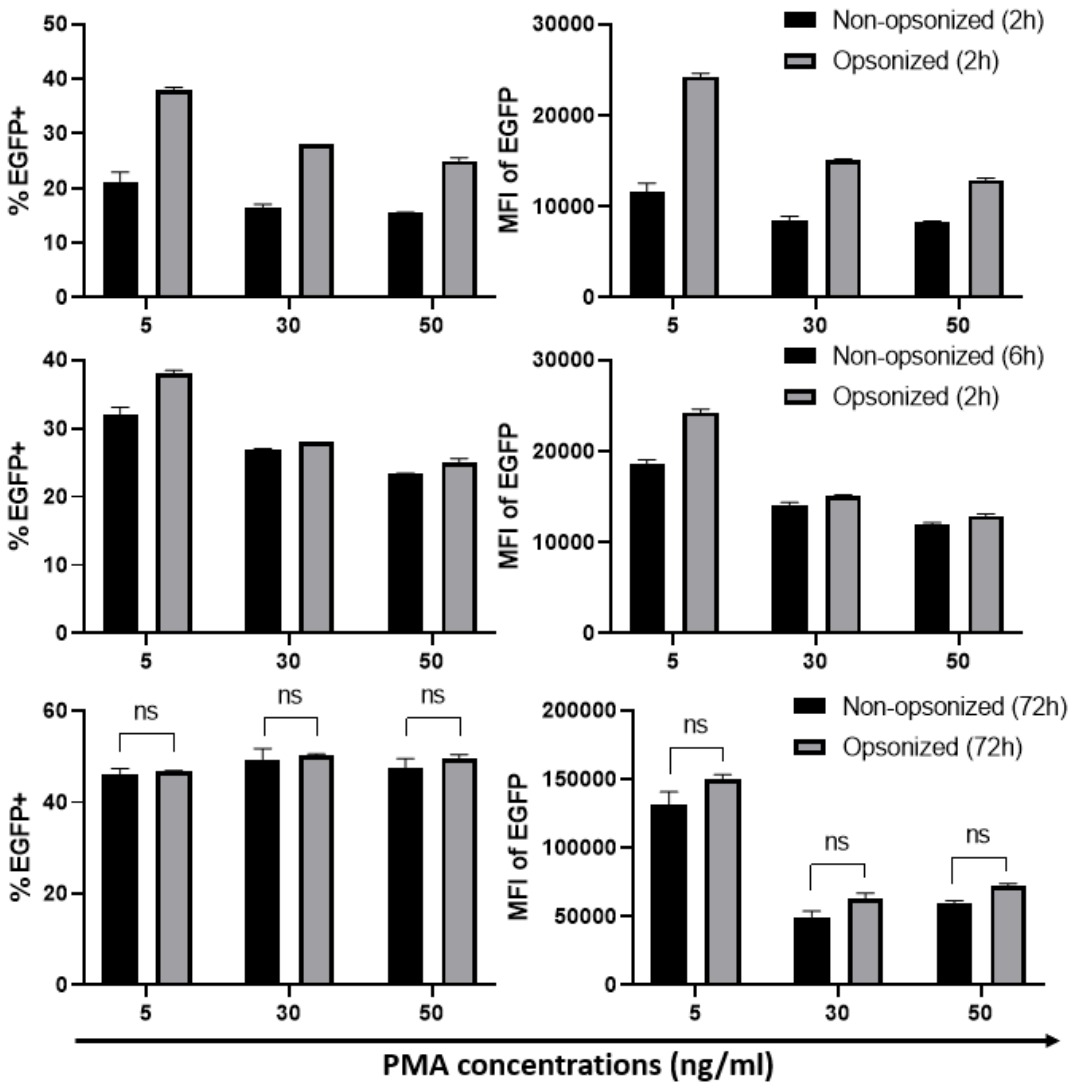

Figure 3.13. Analysis of opsonization in the context of THP1 infection.

Differentiated THP1 cells were infected with EGFP expressing *L. major* parasites at a MOI of 1:10 (macrophage:parasite). At designated time points, infection percentages and parasite loads were quantified using a flow cytometer. The graphs were constructed based on one experiment. Non-opsonized and opsonized groups were statistically compared to each other using multiple t tests followed by correction using Holm-Sidak method (alpha=0.05, ns: not significant).

3.2.5 Phagocytic Capacities of cGAS, STING and TBK1-KO Cells

Our previous data have suggested differences in phagocytosis capacity in THP1-Dual WT cells and KO-cell lines as measured at the end of 24-hour infection period (Figure 3.14.). While cGAS-KO cells had a slightly lower phagocytosis rate compared to WT cells, STING-KO cells showed almost no phagocytosis of *Leishmania major* promastigotes. We could not, however, include TBK1-KO cell line as it was purchased from the manufacturer at a later point in time. These lower levels prompted us to explore phagocytic capacity of KO-cells using GFP expressing *E. coli* and pHrodo™ Green Zymosan Bioparticles™.

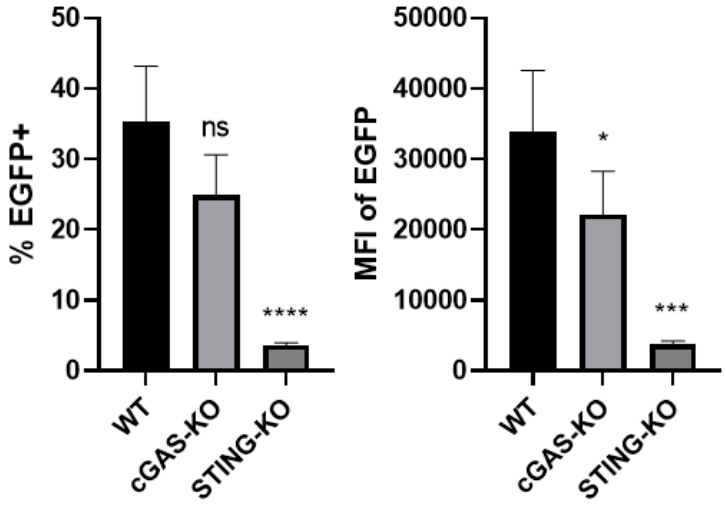

Figure 3.14. Comparison of phagocytic capacity of THP1 cell lines.

Differentiated THP1 cells were infected with EGFP expressing *L. major* parasites at a MOI of 1:10 (macrophage:parasite). At 24 hours post-infection, infection percentages and parasite loads were quantified using a flow cytometer. The graphs were constructed based on two independent experiments. Groups were statistically compared to WT using one-way ANOVA followed by Dunnett's multiple comparison test (ns: not significant, *: p=0.045, ***: p=0.0001, ****: p<0.0001).

3.2.5.1 Phagocytosis Assessment Using GFP Expressing *Escherichia coli*

Escherichia coli is a gram-negative bacterium previously reported to be phagocytosed by a variety of receptors including class A scavenger receptors (Peiser et al., 2000; van der Laan et al., 1999), CR3 (Agramonte-Hevia et al., 2002), mannose receptors (Felipe et al., 1991; Pacheco-Soares et al., 1992) and TREM2 (Gawish et al., 2015) not to mention cooperative and synergistic effects of TLRs on phagocytosis (Fu & Harrison, 2021).

We tested whether lower phagocytosis rates of *Leishmania major* (Figure 3.14.) seen in KO THP1-Dual cell lines, could be reproduced for *E. coli*. We observed lower phagocytosis rates and phagocytosis loads for cGAS-, STING- and TBK1-KO cell lines (0.74-, 0.56- and 0.79-fold for phagocytic rates; 0.65-, 0.67- and 0.76- fold for phagocytic load). Our results suggested that there was a tendency of lower phagocytic capacity in KO-cells.

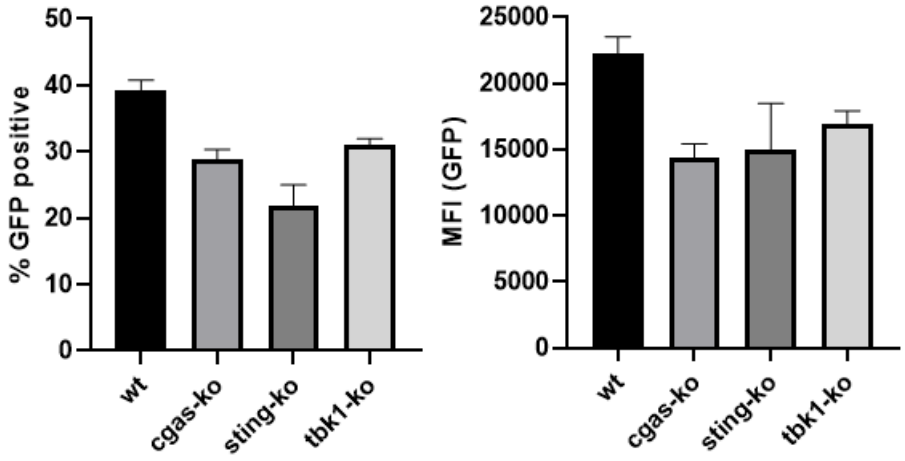

Figure 3.15. Assessment of phagocytosis of GFP expressing *E. coli* in THP1 cells.

PMA differentiated (5 ng/ml) THP1 cells were incubated with fixed and opsonized *E. coli*-GFP (provided by Sinem Ulusan) at 1:10 ratio (macrophage:bacteria). 1.5 hours later, % GFP positive events and MFI (GFP) were analyzed using a flow cytometer following an extensive wash with DPBS. The graphs were constructed from only one experiment; hence, statistical analysis was not performed.

3.2.5.2 Phagocytosis Assessment Using pH Sensitive Zymosan Bioparticles

Receptors that are implicated in the phagocytosis of *Leishmania spp.* are CR3 (complement receptor type 3), CR1 (complement receptor type 1), MR (mannose receptor), FnRs (fibronectin receptors), FcγRs (Fc gamma receptors) and DC-SIGN (dendritic cell-specific intercellular adhesion molecule-3-grabbing nonintegrin). The sub-species together with the life cycle stage of *Leishmania* parasites (procyclic, metacyclic and amastigote forms) are factors influencing the route of entry whose roles vary greatly in terms of parasite persistence (Ueno & Wilson, 2012). On the other hand, zymosan is a *Saccharomyces cerevisiae* cell wall component made up of β(1,3)(1,6) glucans and mannose. It is recognized and phagocytosed by mannose-fucose receptors (Sung et al., 1983; Taylor et al., 1990), lectin binding site of the α chain of CR3 (Ross et al., 1987) and β-glucan receptors (Czop & Kay, 1991; Goldman, 1988). Both *Leishmania spp.* and zymosan particles share the characteristic of recognition by multiple phagocytic receptors some of which are used in the phagocytosis of both.

In an attempt to further verify that phagocytosis rates were lower in the KO but not the WT cell lines, we tested the phagocytosis capacity of THP1-Dual cells using the pHrodo™ Green Zymosan Bioparticles™. These bioparticles only fluoresce once they are in acidified phagosomes which essentially shows true phagocytic events and prevents false positive ones. Similar to our previous *Leishmania* phagocytosis data (Figure 3.14.), pHrodo™ Green Zymosan Bioparticles™ assay illustrated significantly lower phagocytosis percentages and phagocytosis loads in cGAS-KO cells (0.72- and 0.48-fold), STING-KO cells (0.21- and 0.08-fold) and TBK1-KO cells (0.61- and 0.2-fold) compared to WT cells (Figure 3.16.). In summary, we observed reduced phagocytic events and phagocytic loads for *Leishmania major*, zymosan and *E. coli* in cGAS-KO, STING-KO and TBK1-KO cell lines. These observations suggest that there is a general phagocytosis downregulation in KO-cells since a variety of receptor complexes are used in the internalization of *Leishmania spp.*, zymosan and *E. coli*. This creates a problem for 3-day *in vitro* infection model

because comparison of late time point infection levels may be heavily influenced by initial parasite loads, i.e., phagocytic events. A potential solution to this problem is explained in Section 3.2.6.

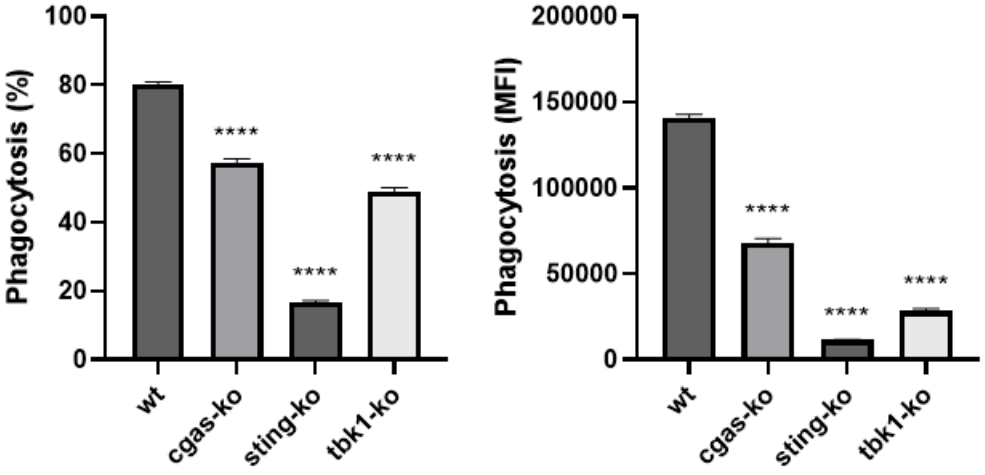

Figure 3.16. Assessment of phagocytosis in THP1 cells using pHrodo™ Green Zymosan Bioparticles™.

PMA differentiated (5 ng/ml) THP1 cells were incubated with pHrodo Green Zymosan Bioparticles according to the manufacturer's instructions. 2 hours later, phagocytic capacity of THP1 cells were analyzed using a flow cytometer. The graphs are representative figures of two independent experiments. The groups were statistically compared to WT cells using one-way ANOVA followed by Dunnett's multiple comparison test (****: $p<0.0001$).

3.2.6 Role of cGAS-STING-TBK1 Pathway on *in vitro* Infection Model

cGAS-STING-TBK1 pathway has been reported numerous times to be exploited by non-viral pathogens to favor their persistence. To start with, Nandakumar et al. (2019) reported gram (+) pathogenic bacteria *Listeria monocytogenes* activated cGAS-STING-TBK1 which then targeted MVB12b to sort DNA into extracellular vesicles to be delivered to bystander cells. These extracellular vesicles, in turn, inhibited T-cell proliferation and primed them for apoptosis, ultimately, favoring bacteria survival. Similarly, Scumpia et al. (2017) reported the activation of cGAS

and STING proteins by another gram (+) bacteria *Staphylococcus aureus* to induce an antiviral type-I IFN response which favored bacterial persistence whereas TLR signaling protected the host in a cutaneous infection model. Another study shows detrimental effects of cGAS-induced type-I IFNs in gram (-) bacteria *Neisseria gonorrhea* infection (Andrade et al., 2016).

The role of cGAS-STING-TBK1 pathway in infections caused by protozoan parasites is more controversial. Majumdar et al. (2015) reported the exploitation of cGAS-STING-TBK1-IRF3 pathway by *Toxoplasma gondii* to promote its replication both *in vitro* and *in vivo*. Interestingly, they argued that the effects were observed even in the absence of type-I IFNs. However, in IRF3-KO cells, stimulation with type-I IFNs still promoted replication of *Toxoplasma gondii*, suggesting the presence of shared but unknown regulators downstream of both IRF3 and IFNARs mediating this effect. In contrast, another study found protective effects of cGAS, STING and type-I IFNs in *Toxoplasma gondii* infection (P. Wang et al., 2019). On another note, low levels of type-I IFNs induced through TLR7 and RIG-I like receptors protected against protozoan parasite *Plasmodium yoleii* (Wu et al., 2014; Yu et al., 2016) and *Plasmodium berghei* (Liehl et al., 2014). In contrast, high levels of type-I IFNs resulted in severe pathology and death while TBK1, IRF3, IRF7 or type-I IFN receptor KO mice were resistant to cerebral malaria (Sharma et al., 2011). The relationship of *Plasmodium spp.* and cGAS-STING-TBK1 pathway seems to be complex and the outcome of the disease is heavily dependent on which DNA-sensing pathway is activated through DNA/RNA delivered by *Plasmodium* extracellular vesicles (Sisquella et al., 2017; Y. Sun & Cheng, 2020). Furthermore, a closer relative to *Leishmania spp.*, *Trypanosoma cruzi*, has been reported to induce PARP1-cGAS-NFkB to exacerbate chronic inflammation and disease severity through oxidized DNA delivered by extracellular vesicles (Choudhuri & Garg, 2020).

Currently, the only report focusing on cGAS-STING-TBK1 pathway in *Leishmania* infection was published by Das et al. (2019). The researchers argued that production of type-I IFNs through cGAS-STING-TBK1 pathway downmodulated type-II IFN (IFNγ) receptors and p-STAT1, critical for parasite control, and promoted

Leishmania donovani survival in RAW264.7 macrophages. Interestingly, the researchers showed kDNA binding to cGAS through immunoprecipitation assays, as well as IFNβ production in RAW264.7 and BMDMs upon stimulation with DNA isolated from *Leishmania donovani*. This, in turn, results in downregulation of MHC-II surface receptor and upregulation of IL-10 and host MRP1 (multi drug resistant associated protein 1), both playing a critical role in delivery of parasite DNA to cytosol increasing cGAS-STING signaling and enhancing drug resistance of the parasites. Furthermore, they showed increased infection in RAW264.7 cells treated with DNA of *L. donovani* and resistance to infection in cGAS-KO cells. However, the researchers never showed type-I IFN production in infected cells. Correspondingly, our group previously showed type-I IFN induction in kDNA stimulated THP1 cells and increased *L. major* infection levels in both THP1 cells and mouse BMDMs treated with kDNA (Ayanoğlu, PhD Thesis, 2019). However, type-I IFNs were not induced in *L. major* infected WT THP1 reporter cells (Figure 3.17.) which, interestingly, is not included in report published by Das et al. (2019). This suggests that the exploitation of cGAS-STING-TBK1 pathway may be independent of type-I IFNs similar to the aforementioned report regarding *Toxoplasma gondii* infection (Majumdar et al., 2015).

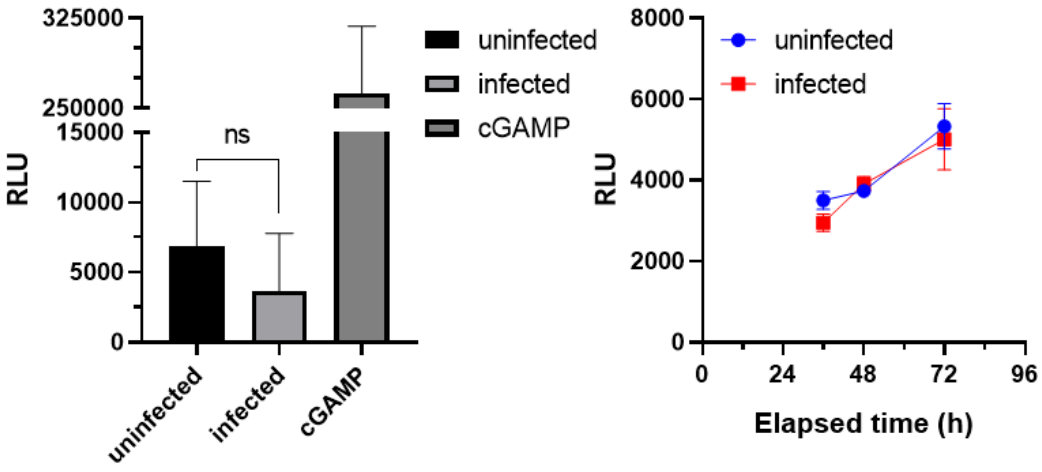

Figure 3.17. Assessment of IRF induction in *L. major* infected WT THP1 cells as an indicator of Type I IFN signaling.

THP1-Dual cell line is genetically engineered to express a secreted luciferase reporter gene that enables study of IRF/type I interferon signaling pathway, which can be triggered by multiple pathways one of which is through cGAS-STING-TBK1 pathway. PMA differentiated (5 ng/ml) THP1 cells were infected with eGFP expressing *L. major* parasites at a MOI of 1:10 (macrophage:parasite) or treated with cGAMP as positive control. At 24, 36, 48 and 72 hours, supernatants were collected, centrifuged to remove cells, and luciferase activities were detected according to the manufacturer's instructions using a multiplate reader. On the bar graph, the 24-hour readouts of luciferase activity of two independent experiments are shown. On the line graph, luciferase activity throughout 3-day infection period is shown. The line graph is constructed as representative figure of two independent experiments. The groups were statistically compared to each other using two-way ANOVA followed by Tukey's multiple comparison test (ns: not significant).

In our experiments, we observed *L. major* infection and proliferation in the absence of cGAS, STING or TBK1 proteins in differentiated THP-1 cells (with 5 ng/ml PMA) using 3-day *in vitro* infection model. As illustrated in Figure 3.18., infection rate and load of WT cells increased considerably while KO-cells resisted the infection throughout the 3-day infection period.

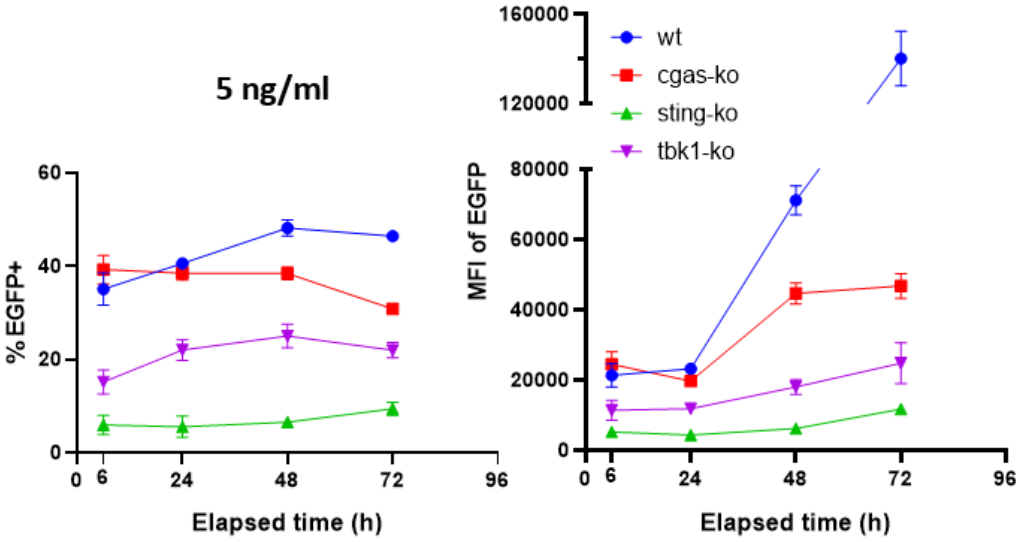

Figure 3.18. Progression of *L. major* infection in THP1 cell lines.

Differentiated (5 ng/ml) THP1 cells were infected with eGFP expressing *L. major* parasites at a MOI of 1:10 (macrophage:parasite). At designated time points, infection percentages and parasite loads were quantified using a flow cytometer. The graphs were constructed based on two biological replicates. Statistical analyses are shown in Figures 3.19. and 3.21.

However, phagocytic capacities (rates and loads) of KO-cells were significantly lower than WT cells (Figure 3.19. left panel) in the first 24 hour. Therefore, lower levels of infection rates at the end of *in vitro* infection in KO-cells could be attributed to fewer infecting *L. major* at the beginning.

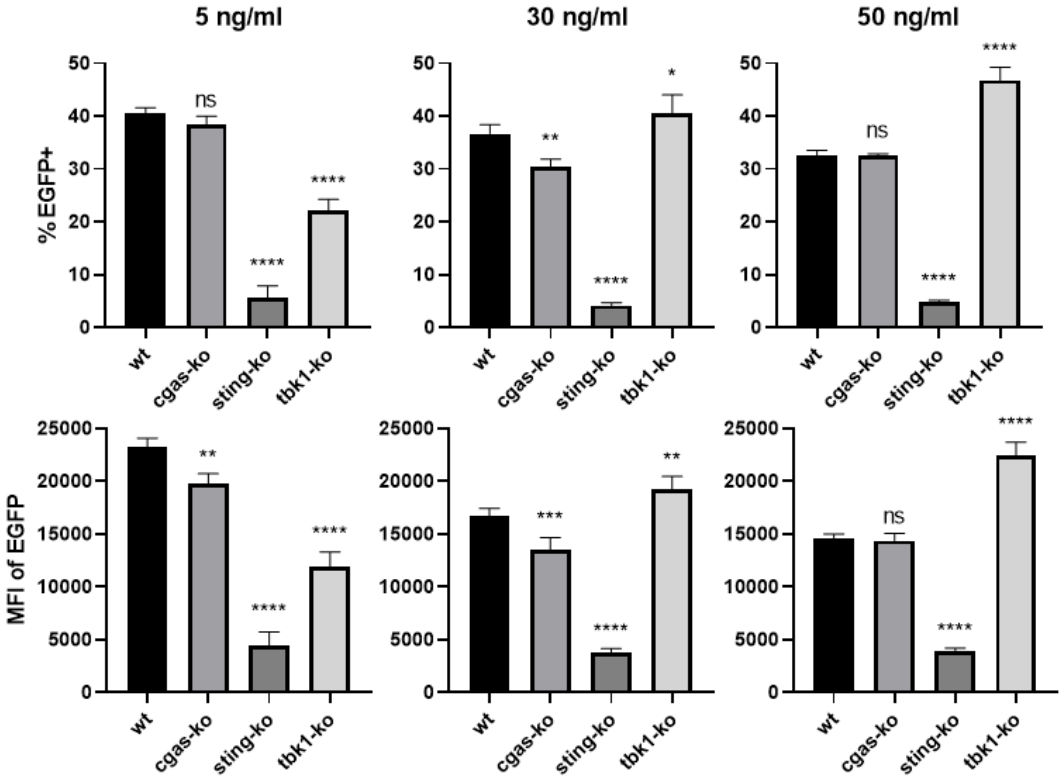

Figure 3.19. Comparison of 24-hour phagocytic capacities of THP1 cell lines differentiated at different PMA concentrations.

Differentiated THP1 cells were infected with EGFP expressing *L. major* parasites at a MOI of 1:10 (macrophage:parasite). At designated time points, infection percentages and parasite loads were quantified using a flow cytometer. The graphs were constructed based on two biological replicates. Each cell line in each PMA group were statistically compared to WT cells using ordinary one-way ANOVA followed by Dunnett's multiple comparison test (for top panel; ns: not significant, *: p=0.0465, **: p=0.0026, ****: p<0.0001, for bottom panel from left to right; ns: not significant, **: p=0.0026, **: p=0.0055, ***: p=0.001, ****: p<0.0001).

To overcome this problem, we differentiated THP-1 cells with higher PMA concentrations (30 and 50 ng/ml) to possibly increase phagocytic receptors and capacity of KO-cells. As expected, this method yielded comparable initial phagocytic capacities of WT, cGAS- and TBK1-KO cells (Figure 3.19. middle and right panels). Moreover, the phagocytic capacity of TBK1-KO cells exceeded that of WT cells at higher PMA concentrations. However, none of the conditions could increase the phagocytic capacity of STING-KO cells. Even when phagocytosis rates of WT, cGAS- and TBK1-KO cells were comparable, we still observed higher levels of proliferation of *L. major* in WT cells while KO-cells hindered parasite proliferation throughout the experiments (Figures 3.20. and 3.21.).

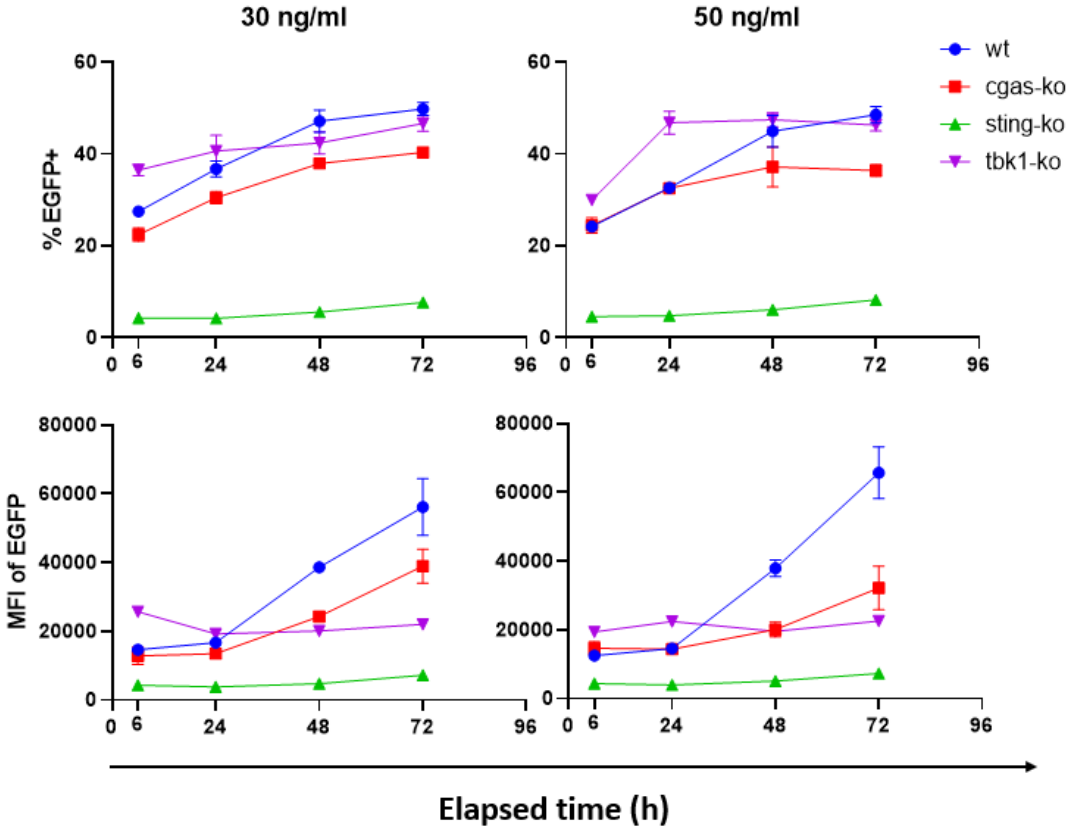

Figure 3.20. Progression of *L. major* infection in THP1 cell lines differentiated at higher PMA concentrations.

Differentiated (30 and 50 ng/ml) THP1 cells were infected with eGFP expressing *L. major* parasites at a MOI of 1:10 (macrophage:parasite). At designated time points, infection percentages and parasite loads were quantified using a flow cytometer. The graphs were constructed based on two biological replicates. Statistical analysis is shown in Figure 3.21.

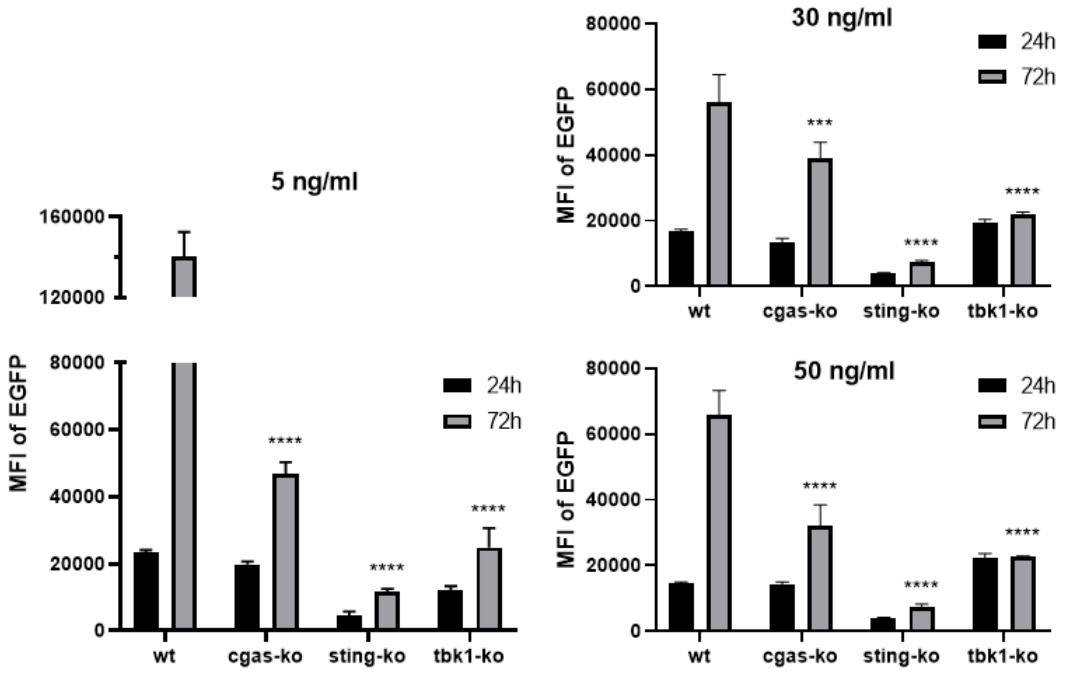

Figure 3.21. Summary of progression of *L. major* infection depicted in Figures 3.18. and 3.20.

Differentiated THP1 cells were infected with eGFP expressing *L. major* parasites at a MOI of 1:10 (macrophage:parasite). At designated time points, infection percentages and parasite loads were quantified using a flow cytometer. The graphs were constructed based on two biological replicates. **72-hour** values of each cell line in each PMA group were statistically compared to WT cells using ordinary one-way ANOVA followed by Dunnett's multiple comparison test (***: p=0.0008, ****: p<0.0001).

3.2.7 Staining for Imaging of *in vitro* Infection

Although flow cytometric eGFP detection is very sensitive, we wanted to verify that the detected signal was not due to extracellular parasites by staining the amastigotes in infected cells. Differentiated WT THP1 cells, (both lower and higher concentrations of PMA stimulation), showed high infection percentages and parasite loads upon staining with SYTO™ 16 Green (Thermo Fisher Scientific, U.S.A.).

(Figure 3.22.). The results verified presence of intracellular amastigotes in macrophages and were consistent with flow cytometric data since THP1 cells differentiated with low PMA concentration harbored visibly more parasites.

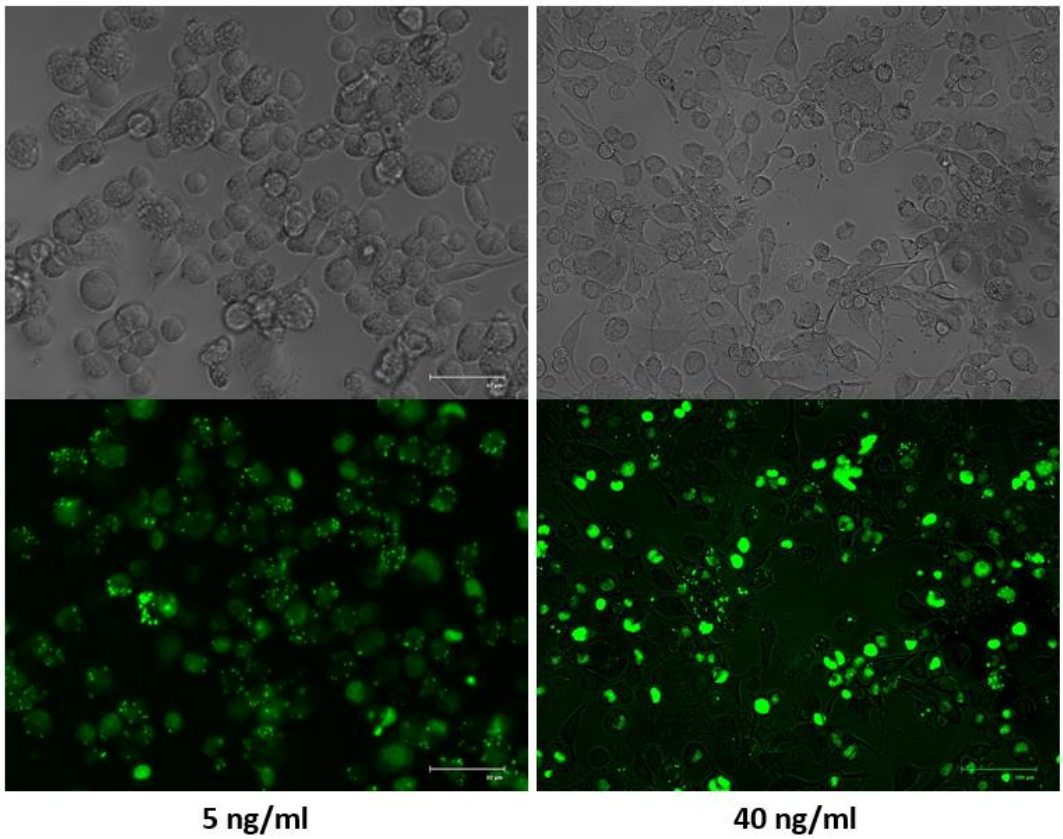

Figure 3.22. White light and fluorescence microscopy images of *L.* major infection of WT THP1 cells differentiated at low and high concentrations of PMA.

PMA-differentiated THP1 cells were infected with eGFP expressing *L. major* parasites at a MOI of 1:10 (macrophage:parasite). The wells were washed at 6 hours post-infection. The green signal of amastigotes inside THP1 cells are enhanced by staining with 0.4 μM SYTO™ 16 Green (Thermo Fisher Scientific, U.S.A.) 72-hour post-infection.

3.2.8 Assessment of Lysosomal Acidity Levels of THP1 Cells

Although *Leishmania spp.* have adapted to survive in the harsh environment of phagolysosomes, there are numerous evidence that the parasites delay the endosome

maturation process and modify the compartments they reside in. *L. donovani* excludes vesicular proton-ATPase to delay acidification upon phagocytosis (Vinet et al., 2009) which allows transformation of promastigotes to hydrolase-resistant amastigotes which can continue replicating under acidic and hydrolase-rich conditions (Scianimanico et al., 1999). Recent publications suggest that even in acidified parasitophorous vacuoles, the environment is strictly controlled by preventing over-acidification and activation of lysosomal enzymes; hence, creating modified early endosomes by upregulating Rab5a for *L. donovani* amastigotes to reside in (Verma et al., 2017). Similarly, freshly phagocytosed *L. major* delay phagolysosome maturation by preventing phagosome-endosome fusion (Desjardins & Descoteaux, 1997) as well as assembly of NADPH oxidase (Matheoud et al., 2013; Matte et al., 2016).

Knowing that the resistance of cGAS-, STING- and TBK1-KO cells to *L. major* infection were independent of type-I IFNs (Figure 3.17.), we tested whether these cells have inherently lower lysosomal pH levels that can combat manipulation of pH of phagolysosomes (4.5-5.5) by *L. major* (Pal et al., 2017). Although we have observed significantly more acidic lysosomes in TBK1-KO cells, we could not observe similar results in cGAS- and STING-KO cells (Figure 3.23. and 3.24.). Rather than pH levels of lysosomes, the fusion dynamics of early endosomes and lysosomes could be more important as *Leishmania* is known to delay this interaction as mentioned in the previous paragraph. In future studies, we plan to investigate this aspect of the observed results.

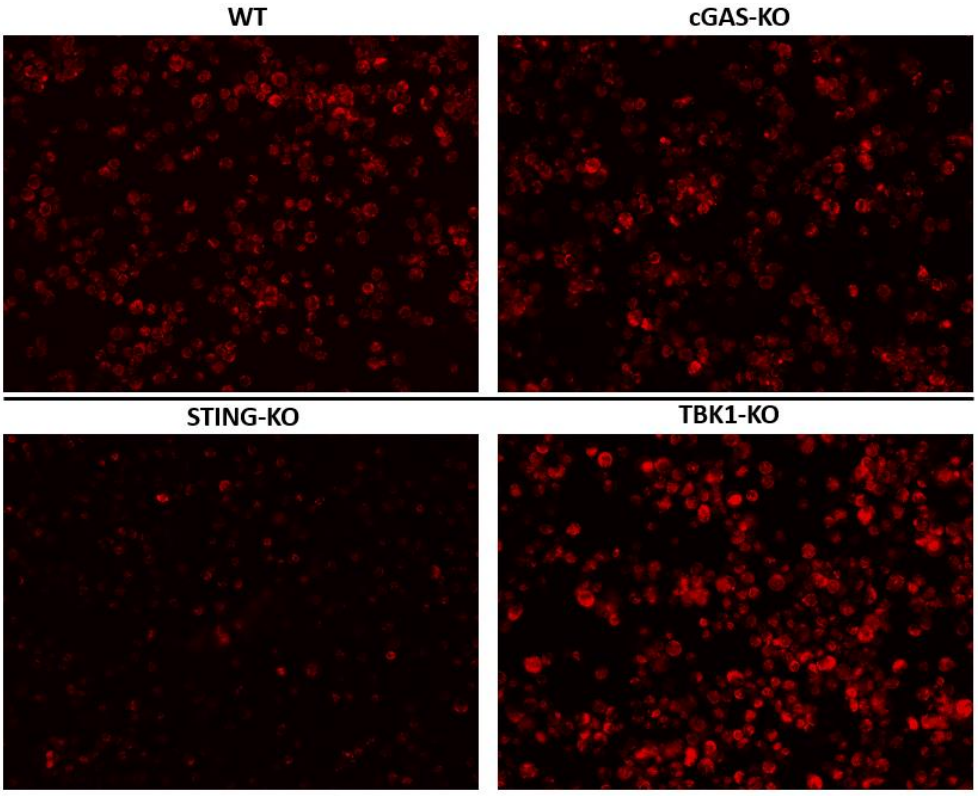

Figure 3.23. Representative images of lysosomal acidity levels of THP1 cell lines.

Differentiated THP1 cells on clear plates were washed and incubated in 10% Regular RPMI containing 50 nM LysoTracker™ Red DND-99 (Thermo Fisher Scientific, U.S.A) for 1 hour at 37°C. After replacement of media, images of cells were captured using the red channel on FLoid Cell Imaging Station (Thermo Fisher Scientific, U.S.A.).

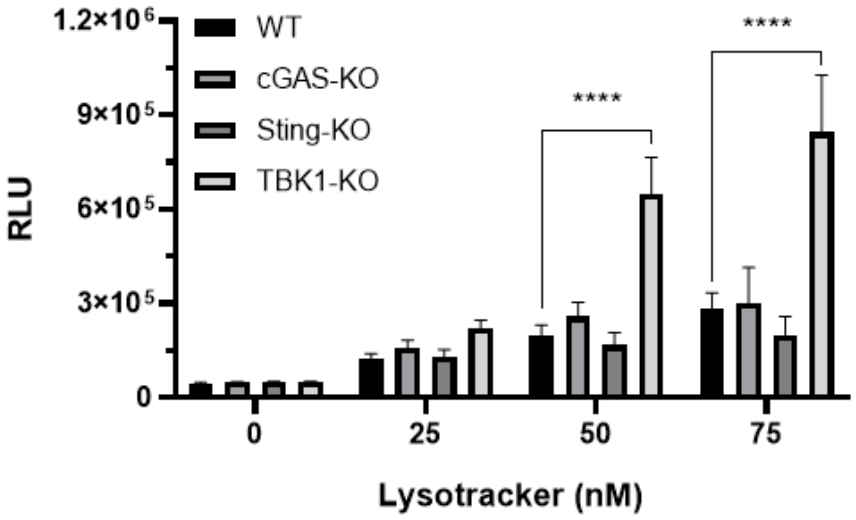

Figure 3.24. Quantitative assessment of lysosomal acidity levels of THP1 cells.

Differentiated THP1 cells on white opaque plates were washed and incubated in 10% Regular RPMI containing LysoTracker™ Red DND-99 (Thermo Fisher Scientific, U.S.A) for 1 hour at 37°C. After replacement of media, fluorescent signal was quantified using a multi-mode plate reader (Molecular Devices, U.S.A.) with a fluorescence detection mode at excitation and emission wavelengths of 577/590 nm.

3.2.9 Determination of the Effect of cGAS-STING-TBK1 Pathway Inhibition on Infection Efficiency

3.2.9.1 Dose Optimization of TBK1 Inhibitors BX-795 and Amlexanox for *in vitro* Infection Experiments

To further prove that the observed resistances of KO THP1 cells is a result of the blockage of cGAS-STING-TBK1 pathway, we treated WT THP1 cells with two TBK1 inhibitors; Amlexanox and BX-795, at increasing concentrations prior to a 24-hour *L. major* infection. The results showed that Amlexanox treatment diminished the percentage and parasite load of infected cells significantly, while BX-795 treatment was only capable of reducing parasite loads in a dose dependent

manner (Figure 3.25.). The effect of Amleaxanox was much more striking compared to BX-795. Amlexanox competes for ATP-binding to TBK1, whereas BX-795 blocks the phosphorylation of TBK1. Considering the fact that Amlexanox treatment, also, reduced parasite loads cGAS-KO (Figure D.1., Appendix D) and TBK1-KO (Yılmaz, PhD thesis, 2020) cells, we hypothesize that the effectiveness of Amlexanox may be partly related to the ability of Amlexanox to induce disassembly of actin stress fibers (Landriscina et al., 2000). This hypothesis is rooted in numerous reports suggesting key roles of accumulation of F-actin in the phagocytosis of *Leishmania spp.* (Courret et al., 2002; Roy et al., 2014), formation of physical barriers preventing early-stage inhibition of phagosome-late endosome interaction (Lodge & Descoteaux, 2005b), and dynamic modulation of F-actin to exploit the cytoskeleton of host cells (Lodge & Descoteaux, 2005a).

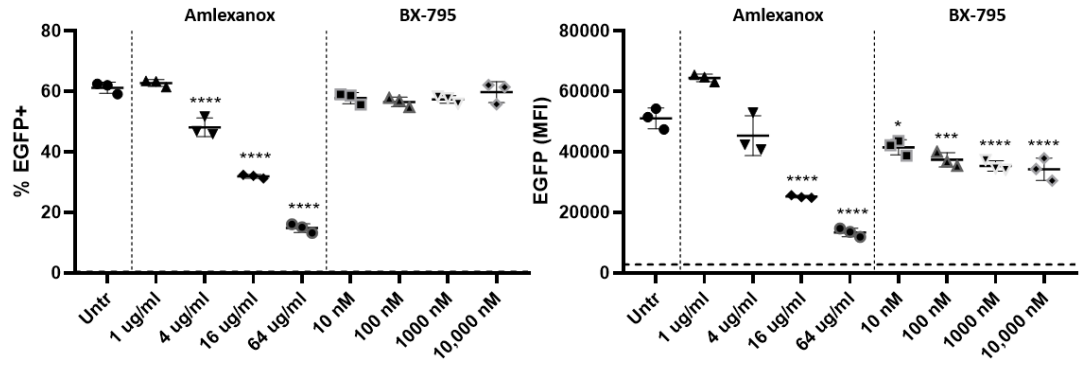

Figure 3.25. Effect of increasing doses of TBK1 inhibitors on *L. major* infection.

Differentiated (50 ng/ml) WT THP1 cells were pre-treated with increasing doses of Amlexanox for 1 hours and BX-795 for 6 hours. Without removing the inhibitors, eGFP expressing *L. major* parasites were co-incubated with THP1 cells for 24 hours. Following 3 DPBS washes, infection percentages and parasite loads were quantified using a flow cytometer. The graphs were constructed based on one experiment. Treatment groups were statistically compared to untreated group using one-way ANOVA followed by Bonferroni's multiple comparison test (*: p=0.0121, ***: p=0.0003, ****: p<0.0001).

3.2.9.2 Effect of TBK1 Inhibition on Infection Efficiency in a 3-day *in vitro* Infection Model

Although the findings on TBK1 inhibitors proved promising, the initial 24-hour infection predominantly represent phagocytosis rates rather than proliferation in the amastigote form. Therefore, we tested Amlexanox in our 3-day *in vitro* infection model. Amlexanox treatment starting from the beginning of the experiment inhibited both infection rate and proliferation of *L. major* parasites (Figure 3.26.). Since the parasite load at the end of 3-day infection period can be influenced by initial infection levels, we added Amlexanox 24-hours later in another group. The results suggested that even when the initial phagocytosis rates are the same with untreated cells, there was still significant resistance to *L. major* infection. We think that low levels of eGFP signals in late-Amlexanox group is not due to inhibition of infection of uninfected cells, but rather due to inhibiton of proliferation of amastigotes. The rationale behind this is that the increase in infection percentage between 24 and 72 hours in untreated cells is around 1.32-fold while the increase in MFI is around 4.63-fold which suggest that the majority of fresh signal being detected is due to proliferation of amastigotes in already infected cells, which is significantly inhibited in late-amlexanox group.

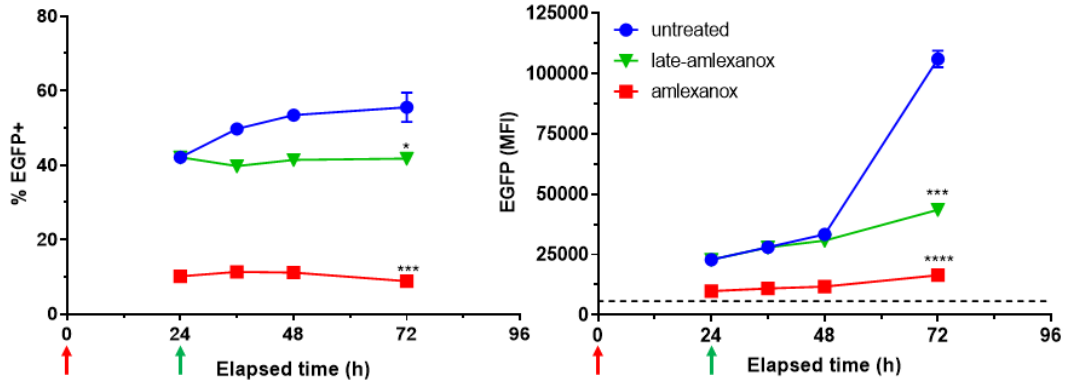

Figure 3.26. Inhibition of *L. major* infection od WT THP1 cells using 3-day infection model.

Differentiated (5 ng/ml) THP1 cells were infected with eGFP expressing *L. major* parasites at a MOI of 1:10 (macrophage:parasite) ratio. At designated time points, infection percentages and parasite loads were quantified using a flow cytometer. The red and green arrows show Amlexanox addition to amlexanox and late-amlexanox groups, respectively. The graphs were constructed based on one experiment. The readouts taken at the last time points were statistically compared to untreated group using ordinary one-way ANOVA followed by Bonferroni's multiple comparison test (from left to right; *: p=0.0182, ***: p=0.0005, ***: p=0.0002, ****: p<0.0001).

3.2.10 Gene Expression Analysis Using Nanostring Pancancer Immune Profiling Panel

In order to understand the intrinsic resistance of KO-cell lines and Amlexanox-treated WT-cells to *L. major* infection better, we compared the gene expression of these groups to THP1-WT cells. Below, the differential gene expressions of *L. major* infected cGAS-KO, TBK1-KO and Amlexanox-treated WT cells are discussed. Since *L. major* infection did not take place in STING-KO cells due to very low phagocytosis levels (Figure 3.16. and 3.21.), and global downregulation of transcription in these cells (suggested by global significance score analysis, Figure 3.27.) coupled with the fact that STING-KO cells were susceptible to cell death upon

PMA induction, we suspected dysregulation of cellular functions in STING-KO cells and did not include them in the discussion.

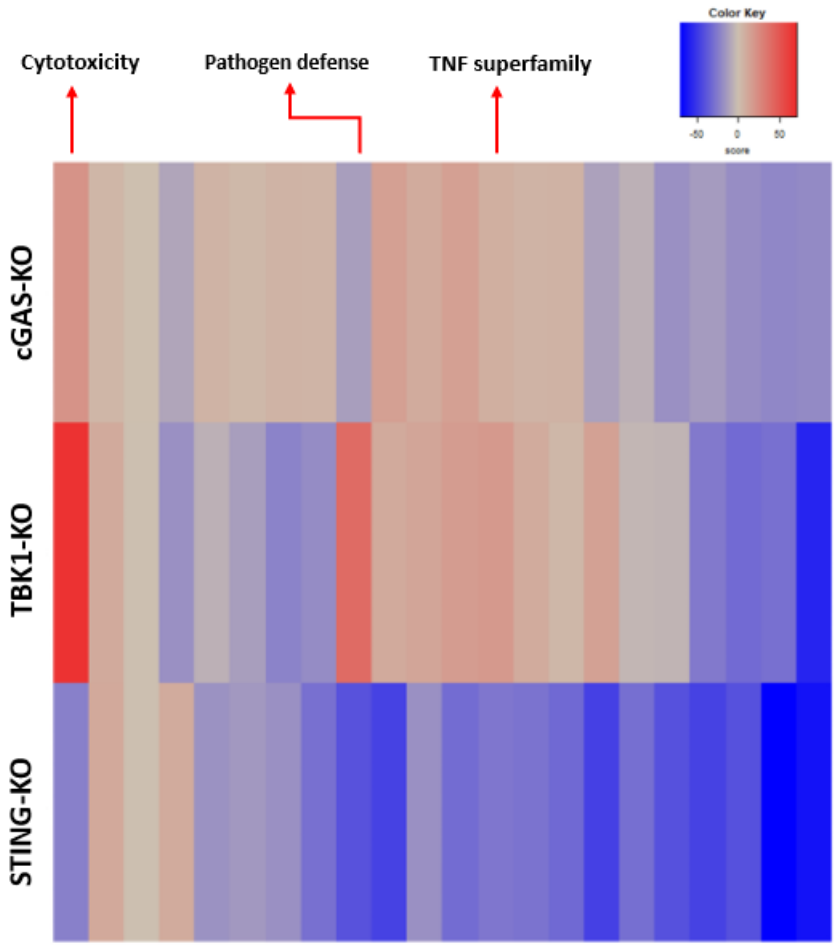

Figure 3.27. Global significance score analysis of *L. major* infected THP1-KO cells in comparison to THP1-WT cells.

The preparation of *L. major* infected THP1 cells, RNA isolation and Nanostring procedure using nCounter PanCancer Immune Profiling CS Kit (no MK) (NanoString Technologies, Inc., U.S.A.) is explained in detail in Section 2.2.6. Obtained raw data was analyzed using nSolver Analysis software (v4, NanoString Technologies, Inc., U.S.A.) and nCounter® Advanced Analysis Software (v2, NanoString Technologies, Inc., U.S.A.). The results of differential expression testing were summarized at the gene set level. Relevant gene sets are marked with red arrows.

It is known that IFNγ and TNFα classically activate macrophages and work synergistically to induce iNOS expression which is important for destruction of *L. major* amastigotes (Liew et al., 1997). Unfortunately, the nCounter PanCancer Immune Profiling CS Kit (no MK) (NanoString Technologies, Inc., U.S.A.) used in this experiment, did not include iNOS in its gene set. Nevertheless, expression of TNF superfamily was upregulated in cGAS- and TBK1-KO cells compared to WT cells (Figure 3.27.). One member of this superfamily, TNFSF15 increased ROS, RNS and autophagy through NFκB pathway, ultimately clearing intracellular bacteria, in monocyte derived macrophages (R. Sun et al., 2021). Since these anti-microbial mediators are, also, considered as resistance factors against *L. major* infection, it is possible that increased transcription of TNFSF15 in cGAS- and TBK1-KO cells (Figure 3.28.) could have played a role in resistance to *L. major* infection. Furthermore, we observed decreased transcription of NFKBIA (inhibits NFκB-Rel complexes and inflammatory response) in both cell lines, and increased NFKB1 (NFκB subunit 1) mRNA levels in TBK1-KO cells, in contrast to cGAS-KO cells which may be one of many reasons of higher parasite loads in cGAS-KO cells in comparison to TBK1-KO cells. Although less relevant to our *in vitro* infection model, expression of another member of TNF superfamily, TNFSF14, was increased in both cGAS- and TBK1-KO cells (Figure 3.28.), and it was implicated in *in vivo* protection against *L. major* and *L. donovani* (Stanley et al., 2011; Xu et al., 2007). Furthermore, TLR4 expression was higher in TBK1-KO cells, which was found in significantly higher levels in patients with self-healing lesions (Tolouei et al., 2013). In the context of M1/M2 polarization, the differential expression analysis suggested decreased levels of M2-like macrophage related mRNAs such as FN1 (Jablonski et al., 2015), ALCAM (Lécuyer et al., 2017) and ITGA5 (Becker et al., 2012) in cGAS- and TBK1-KO cells. Van Raemdonck et al. (2020) characterized M1-like macrophages with elevated levels of CCR7 expression and CCL21 responsiveness in monocyte-derived macrophages. Similar results were found in another report (Xuan et al., 2015). Correspondingly, we observed increased levels of CCL21 in TBK1-KO cells, and increased levels of CCR7 in both cGAS-KO and

TBK1-KO cells suggesting polarization of these cells towards a classically activated M1-like phenotype. In contrast, higher levels of parasite loads in cGAS-KO cells could be related to increased expression of AXL (a member of receptor tyrosine kinase subfamily) whose expression was associated with retaining M2-like phenotype in dermis resident macrophages in C57Bl/6 mice, indicated by high expression of arginase and low expression of iNOS (Chaves et al., 2020). However, higher expression of AXL was not accompanied by any significant changes in arginase levels in cGAS-KO cells, underlying the necessity to validate the mRNA levels with qPCR, and perform further tests at the translational level.

The directed global significance score, also, suggested increased expression of gene sets categorized under "cytotoxicity" in cGAS- and TBK1-KO cells compared to WT cells (Figure 3.27.). One key gene in this data set was granulysin (GNLY). Dotiwala et al. (2016) reported that granzyme B and granulysin worked together to kill intracellular parasites *T. gondii*, *T. cruzi* and *L. major*. The mechanism of action involved recognition and lysis of cholesterol-poor microbial membranes by granulysin (Barman et al., 2006) and concurrent generation of portals through which granzyme B entered these intracellular parasites. Subsequently, granzyme B caused oxidative damage to parasites' DNA and simultaneously cleaved proteins responsible for detoxification, ultimately destroying amastigotes. In our experiment, we observed increased levels of granulysin (Figure 3.28.) in cGAS- and TBK1-KO cells, and non-significant changes in granzyme B mRNA levels, suggesting that observed resistance to *L. major* could be related to higher levels of anti-microbial protein granulysin in KO cells.

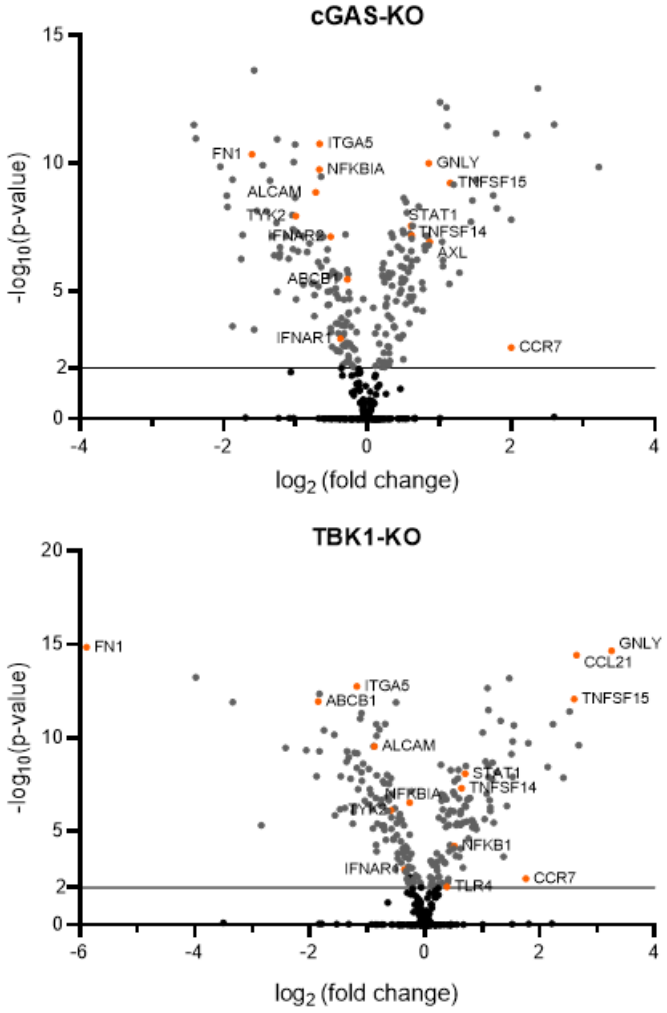

Figure 3.28. Volcano plots depicting selected differentially expressed genes in L.major infected cGAS- and TBK1-KO cells in comparison to WT cells.

The preparation of *L. major* infected THP1 cells, RNA isolation and Nanostring procedure using nCounter PanCancer Immune Profiling CS Kit (no MK) (NanoString Technologies, Inc., U.S.A.) is detailly explained in Section 2.2.6. Obtained raw data was analyzed using nSolver Analysis software (v4, NanoString Technologies, Inc., U.S.A.) and nCounter® Advanced Analysis Software (v2, NanoString Technologies, Inc., U.S.A.). The Log_2(fold change) and $-log_{10}$(p-values) were processed with Graphpad Prism (v8.0.1.) to construct volcano plots. The horizontal black line represents the threshold above which $p<0.01$.

In addition, key mRNAs in Type I and II IFN signaling pathways were significantly different in cGAS- and TBK1-KO cells compared to WT cells (Figure 3.28.). IFN-γR signaling involves kinases JAK1/JAK2 and STAT1 homodimers while IFNAR signaling involves TYK2, JAK1, STAT1/STAT2 heterodimers as well as STAT1 homodimers (Platanias, 2005). Das et al. (2019) reported that recognition of *Leishmania donovani* DNA through cGAS, in WT THP1 and RAW264.7 cells resulted in downregulation of IFNGR1 mRNA (ligand-binding α-chain of IFNγ receptor) and upregulation of IFNAR and IFNβ which was associated with increased levels of MRP-1 (multi drug resistance associated protein 1, belonging to MDR subfamily) and IL10 secretion, which was not observed in cGAS-KO cells. In support of this, Shaw et al., (2006) argued that TYK2 (tyrosine kinase downstream of IFNAR) mediated both pro- and anti-inflammatory cytokine responses with an emphasis on upregulation of IL-10 signaling. Furthermore, the absence of TYK2 was associated with control of *L. major in vivo* (Schleicher et al., 2004). Additional reports detailed suppression of anti-parasitic immunity by type I IFN signaling (Khouri et al., 2009; Kumar et al., 2020; Van Bockstal et al., 2020). In our experiment, we observed downregulation of IFNAR1 and TYK2 transcription in cGAS- and TBK1-KO cells, and downregulation of IFNAR2 expression only in cGAS-KO cells. In contrast, IFNGR1 transcription was not significantly altered compared to WT cells. Additionally, there was increased levels of STAT1 expression in both cGAS- and TBK1-KO cells. Interestingly, transcription of ABCB1 (a member of MDR/TAP subfamily) was reduced in cGAS- and TBK1-KO cells, which is in line with decreased MRP-1 levels in cGAS-KO cells in the report published by Das et al. (2019). In conclusion, there was decreased levels of mRNAs related to type I IFN signaling and increased/unchanged levels of mRNAs related to type II IFN (IFNγ) signaling in cGAS- and TBK1-KO cells which could be related to observed infection resistance of these cells since type-II IFN signaling is known in protection against *L. major.*

Amlexanox-treated WT cells had similarities with cGAS- and TBK1-KO cells, predominantly in downregulated mRNAs such as NFKBIA, FN1, ITGA5, ALCAM,

IFNAR1, IFNAR2 and TYK2. However, it was apparent that Amlexanox treatment of WT cells led to global downregulation of mRNA expression (Figure 3.29.). In support of this, mRNAs upregulated in cGAS- and TBK1-KO cells (TNF superfamily, CCR7/CCL21, GNLY etc.) were not upregulated in Amlexanox-treated WT cells. Therefore, we think that the anti-parasitic effect of Amlexanox may be unique, and possibly related to inhibition of exploitation of cytoskeleton by *L. major* as previously discussed in Section 3.2.9.1. Investigation of other TBK1 inhibitors with fewer off-targets and knockdown experiments on IRF3 may enlighten whether *L. major* exploits canonical cGAS-STING-TBK1 pathway or utilize non-canonical pathways in which these proteins take part, in order to increase its survival and replication.

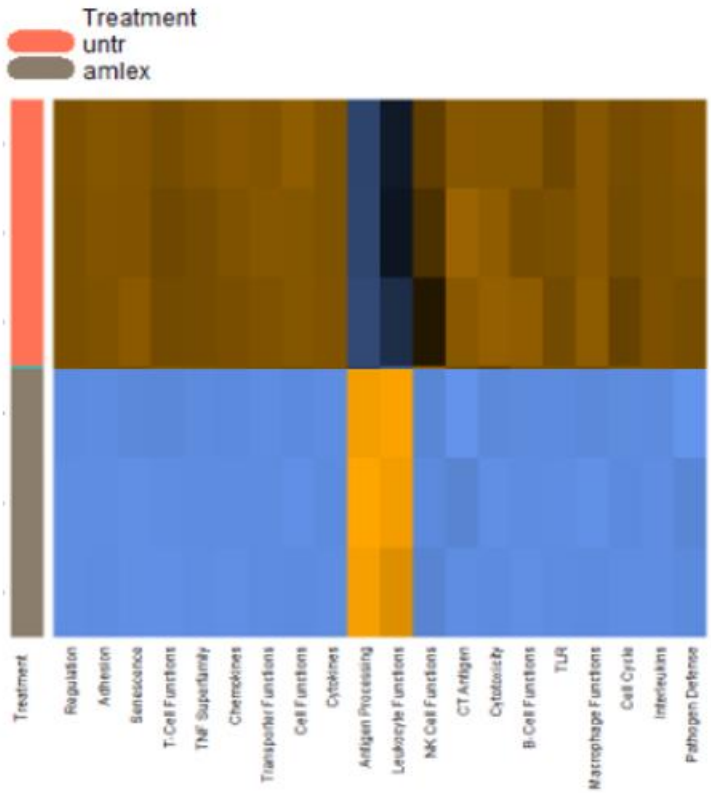

Figure 3.29. Pathway score analysis of Amlexanox treatment on transcription of predetermined gene sets.

The preparation of *L. major* infected THP1 cells, RNA isolation and Nanostring procedure using nCounter PanCancer Immune Profiling CS Kit (no MK) (NanoString Technologies, Inc., U.S.A.) is detailly explained in Section 2.2.6. Obtained raw data was analyzed using nSolver Analysis software (v4, NanoString Technologies, Inc., U.S.A.) and nCounter® Advanced Analysis Software (v2, NanoString Technologies, Inc., U.S.A.).

3.2.11 In vivo Immunization Experiments

For immunization experiments, exosomes, SLA and lyophilized parasites were prepared from *L. major* as antigen sources as explained in Sections 2.2.3. and 2.2.9.2.1. These antigen sources, then, were either combined with α-GalCer (KRN7000) or not, which is a synthetic NKT cell ligand recognized through CD1d

receptor (Brossay et al., 1998). NKT cells can release high levels of IFN-γ, IL-4, 10, 13 and 17 upon induction with α-GalCer (Macho-Fernandez & Brigl, 2015; Michel et al., 2008; Moreira-Teixeira et al., 2011, 2012). Therefore, these cells can modify cytokine milieu following immunization, which in turn may generate a proper immune response against *Leishmania* parasites.

3.2.11.1 Assessment of Purity and GP63 Activity of *L. major* Antigens Used in Vaccination Experiments

3.2.11.1.1 Assessment of Purity of Exosome Samples Using Silver Staining

Exosome isolation by differential centrifugation is susceptible to contamination by bovine proteins due to FBS used in exosome isolation medium. We tested the level of contamination and *Leishmania* specific protein profile by silver-stained polyacrylamide gels loaded with exosome samples and SLA samples as positive control. As a negative control, exosome isolation protocol was done in the absence of *L. major* and this group was named as "mock". Overlapping protein profile in mock and exosome samples pointed to high-level FBS-related contamination in exosome samples (Figure 3.30. lanes 1-4 and 7-8). SLA samples can be regarded as devoid of contamination since it was easier to pellet the parasites and perform washing steps to remove medium components as explained in Section 2.2.3.1. When the protein bands of SLA, exosome and mock samples were compared, most *Leishmania* and bovine proteins were found to have similar molecular weights, resulting in an overlapping protein profile, an observation which is also supported by zymography results (Figure 3.31. lanes 2-7) as explained in the following section.

Our group previously performed mass spectrometry analysis of isolated exosomes and found GP63 as one of the most abundant proteins in isolated exosomes (Ayanoğlu, PhD thesis, 2019). Alongside exosomes (Hassani et al., 2014), GP63 is found in soluble form in the cytosol and as GPI anchored in the membrane and organelles (Hsiao et al., 2008; Isnard et al., 2012). Although bovine related protein

contamination was unavoidable without further purification steps, we tested the presence of GP63 in our exosome, SLA and lyophilized parasite samples as an indicator of successful isolation using zymography.

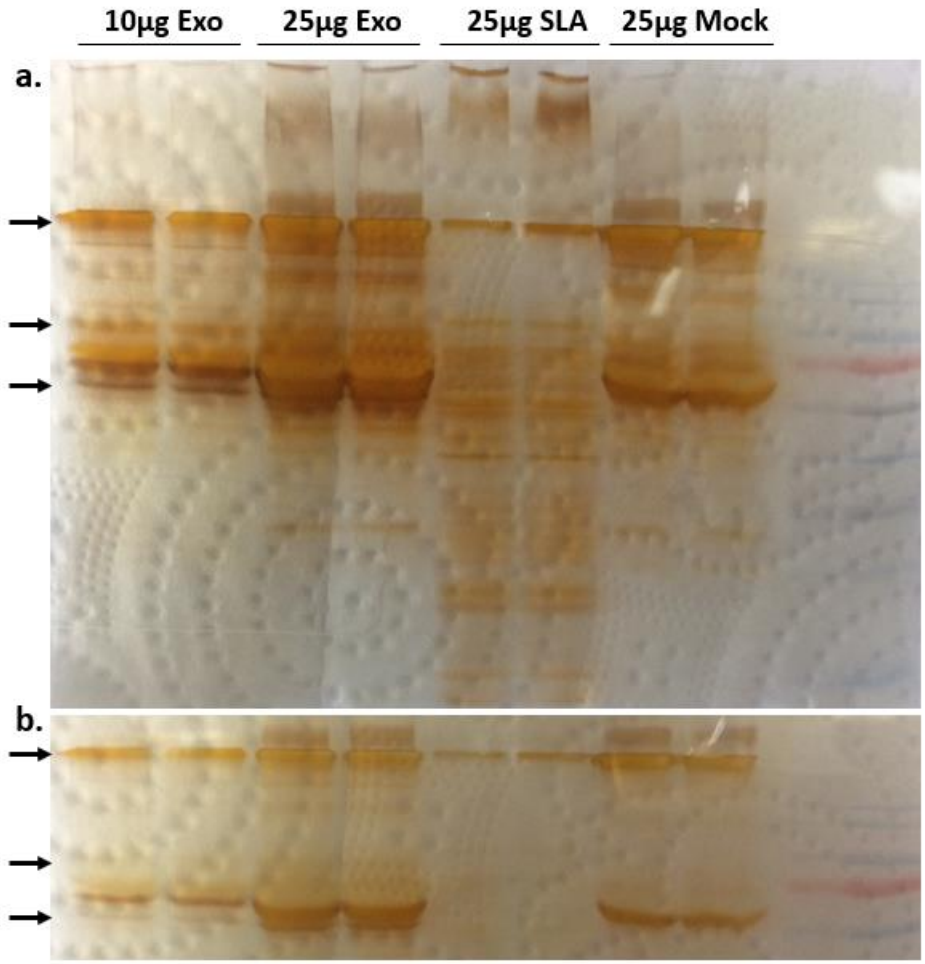

Figure 3.30. Silver staining of polyacrylamide gel loaded with exosome, SLA and mock samples.

Isolation of exosome and SLA samples were performed as described in Section 2.2.3.1. Silver staining was performed according to the instructions of the manufacturer. Exosome samples are examples (lanes 1-2 and 3-4) of two independent isolations. Black arrows show bands that are either also present in the positive control (SLA) sample, or bands which are not present in the mock sample. **a.** Protein profiles of exosome, SLA and mock samples are shown in PAGE. **b.** Image of the same gel shown in **(a)**, with a shorter staining duration to better identify distinct protein bands. As a negative control, exosome isolation protocol was done in the absence of *L. major* and this group was named as "mock".

3.2.11.1.2 Assessment of GP63 Activity of Lyophilized Parasites, SLA and Exosomes using Zymography

GP63 is a key protein expressed by *Leishmania spp.* It has been implicated in numerous reports to subvert the immune response of the host. Gomez et al. (2009) reported GP63 mediated activation of protein tyrosine phosphatase (PTP) SHP-1, which results in downmodulation of JAK/STAT and MAPK signaling, preventing inflammatory response and microbicidal activity of macrophages. Furthermore, GP63 modifies PTPs, PTP1B and TCPTP through proteolytic cleavage and contributes to immunosuppression and disease progression *in vivo*. Matte et al. (2016) reported that *L. major* evades LC3 associated phagocytosis through GP63-mediated downmodulation of VAMP8, essentially preventing assembly of NADPH oxidase and LC3 recruitment to phagosomes. Furthermore, GP63 has been implicated in evasion from complement-mediated lysis (Chaudhuri & Chang, 1988; Joshi et al., 1998, 2002) and neutrophil extracellular traps (Gabriel et al., 2010), protection against antimicrobial peptide-induced cell death (Kulkarni et al., 2006), inhibition of mTORC1 resulting in aggravation of cutaneous Leishmaniasis (Jaramillo et al., 2011), and modification and degradation of transcription factors NFκB and AP-1, downmodulating proinflammatory response (Cameron et al., 2004; Contreras et al., 2010; Gregory et al., 2008) of infected macrophages.

Since GP63 has gelatinase activity (Cuervo et al., 2006; Raymond et al., 2012), we tested the presence of this protein in exosome, SLA and lyophilized parasite samples through assessment of its protein degrading activity. Comparison of mock, exosome and SLA samples indicated the presence of multiple proteins with gelatinase activity, all of which were of similar molecular weights (Figure 3.31. top panel; between 70 and 55 kDA). It is highly likely that bovine originated MMP-2 (63 kDa), which also has gelatinase activity, overlapped with GP63 activity in exosome and SLA samples (lanes 5-6 and 7-8, respectively). In another PAGE experiment, better separation was achieved. Distinct bands, which were absent in mock but visible in exosome and lyophilized parasite samples were identified (Figure 3.31. bottom panel lanes 2-3 and

8-9). Of note, bovine MMP-2 and GP63 are very similar in terms of molecular weights and GPI-anchored GP63 may still be overlapping with the upper band despite the separation. In conclusion, our results suggested the presence of *Leishmania* specific protein GP63 in isolated exosome, SLA and lyophilized parasite samples; however, bovine related contamination was clearly high in exosome samples. Also, gelatinase activity of lyophilized parasites was barely detectable as the amount of sample added to wells were extremely low (800,000 parasites/well). Further purifications of isolated exosome samples should be considered in future experiments to truly assess the potency of exosomes as vaccine candidates.

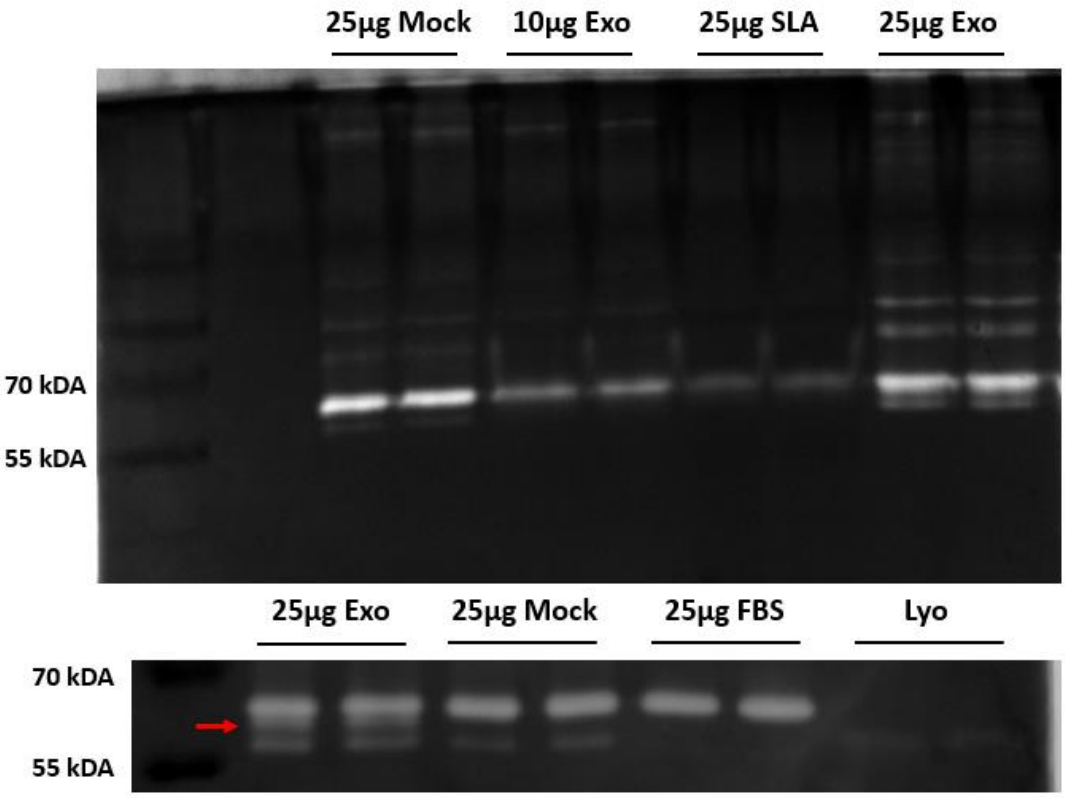

Figure 3.31. Gelatinase activity of exosome, SLA, lyophilized parasites and mock samples.

Isolation of exosome and SLA samples were done according to the protocol explained in Section 2.2.3.1. Gelatinase activity assay was done as explained in Section 2.2.7.

Figure 3.31. (continued) Gelatinase activity of exosome, SLA, lyophilized parasites and mock samples.

Exosome samples are examples (lanes 5-6 and 9-10, top panel) of two independent isolations. Red arrow point to a distinct band only visible in exosome and lyophilized parasite samples Lyophilized parasites were loaded as 800,000 parasites/well calculated based on parasite numbers prior to lyophilization. The 70 and 55 kDA bands of PageRuler™ Prestained Protein Ladder (Thermo Fisher Scientific, U.S.A.) were marked on the figures. As a negative control, exosome isolation protocol was done in the absence of *L. major* and this group was named as "mock".

3.2.11.2 Confirmation of Non-viability in Lyophilized Parasite Preparation

Bacteria can survive freeze-drying although the process requires carbon sources and skim milk to increase their survival rates (Harrison & Pelczar, 1963; Miyamoto-Shinohara et al., 2000). Our group had planned to use whole lyophilized parasites as a rich and complete antigen source. Therefore, we tested the viability of lyophilized parasites following resuspension. There was no sign of parasite survival based on observations of whole cultures in T25 flasks under a microscope. Quantification of parasites for 12-days using a hematocytometer suggested that zero parasites survived the process (Figure 3.32. bottom left panel). Moreover, flow cytometer counts showed the presence of eGFP positive events. However, eGFP+ event counts did not change during the 12-day sampling period (Figure 3.32. bottom right panel and top panel). These eGFP positive events turned out to be free-floating protein-lipid aggregates in the growth medium (Figure 3.33.). Furthermore, an *in vitro* infection experiment was performed to ensure that there were no live parasites in the growth medium. Microscopic and flow cytometric analysis confirmed that no infection took place (data not shown). In addition, mice that was vaccinated twice with lyophilized parasites showed no sign of cutaneous lesions at the site of injection (back of the neck, data not shown). In conclusion, *Leishmania major* parasites lyophilized in PBS did not survive the process, hence, they were used as an antigen source.

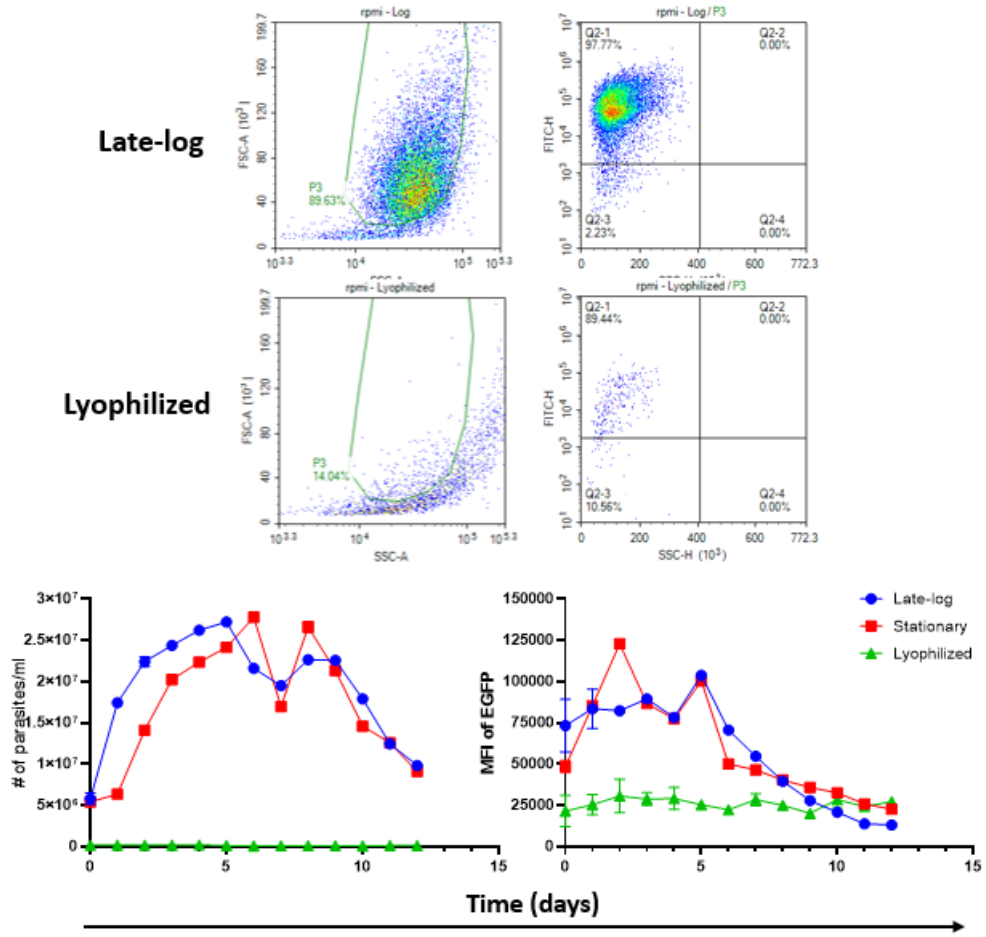

Figure 3.32. Viability assessment of lyophilized parasites.

Following resuspension, lyophilized parasites were seeded into growth medium alongside positive controls: late-logarithmic and stationary-phase parasites. The cultures were quantified for 12 days using a hematocytometer and flow cytometry. P3 designates viable parasite gate.

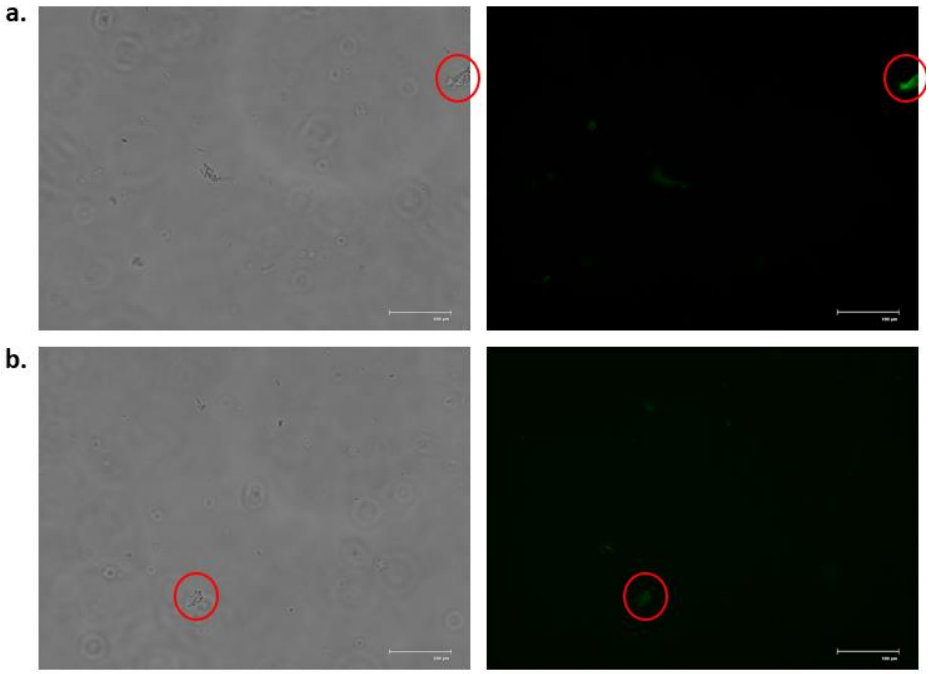

Figure 3.33. Fluorescent microscopy images of eGFP positive events.

Pictures of two examples (marked with red circles) of eGFP positive events detected by flow cytometry as shown in Figure 3.32. Whole cultures in T25 flasks were observed extensively and hundreds if not thousands of aggregated structures were observed.

3.2.11.3 Assessment of Protection Against *L. major* Parasite Challenge in BALB/c Mice Immunized with Different Vaccine Formulations

BALB/c (n=5 mice/group, n=7 for PBS-injected gorup) mice were immunized subcutaneously on days 0 and 14 with the following vaccine formulations: PBS, SLA, SLA+αGalCer, Exosomes, Exosomes+αGalCer, Lyophilized parasites, Lyophilized parasites+αGalCer. 15 days after the booster injection, each animal was challenged with live *L. major* parasites as described in Section 2.2.9.4.

Disease progression was assessed based on footpad swelling and parasite burden. Parasite loads were quantified utilizing luciferase activity of eGFP/Luc expressing *L. major* using the IVIS *in vivo* imager. Representative pictures of footpads

demonstrating lesions (left panels) and luciferase activities (right panels) are shown in Figure 3.34. PBS-administered group had the most swollen and inflamed footpads followed by exosome-administered group. The rest of the vaccinated groups had much less inflammation related swelling and redness in their footpads (Figure 3.34. top left and bottom left panels). Although each vaccinated group had lower means of footpad swelling (0.60-, 0.52-, 0.85-, 0.65-, 0.70- and 0.57-fold in the order shown in Figure 3.34.), only the footpad measurements of SLA+αGalCer and Lyo+αGalCer groups were found to be significantly lower than the PBS-administered control group. Similarly, each vaccinated group had lower means of luciferase activity (0.24-, 0.13-, 0.37-, 0.41-, 0.31- and 0.15-fold in the order shown in Figure 3.34.). However, only SLA, SLA+αGalCer and Lyo+αGalCer administered groups had significantly lower luciferase activity compared to PBS-administered group. Both the footpad measurements and parasite burdens (luciferase activity) showed the same trend in terms of disease progression.

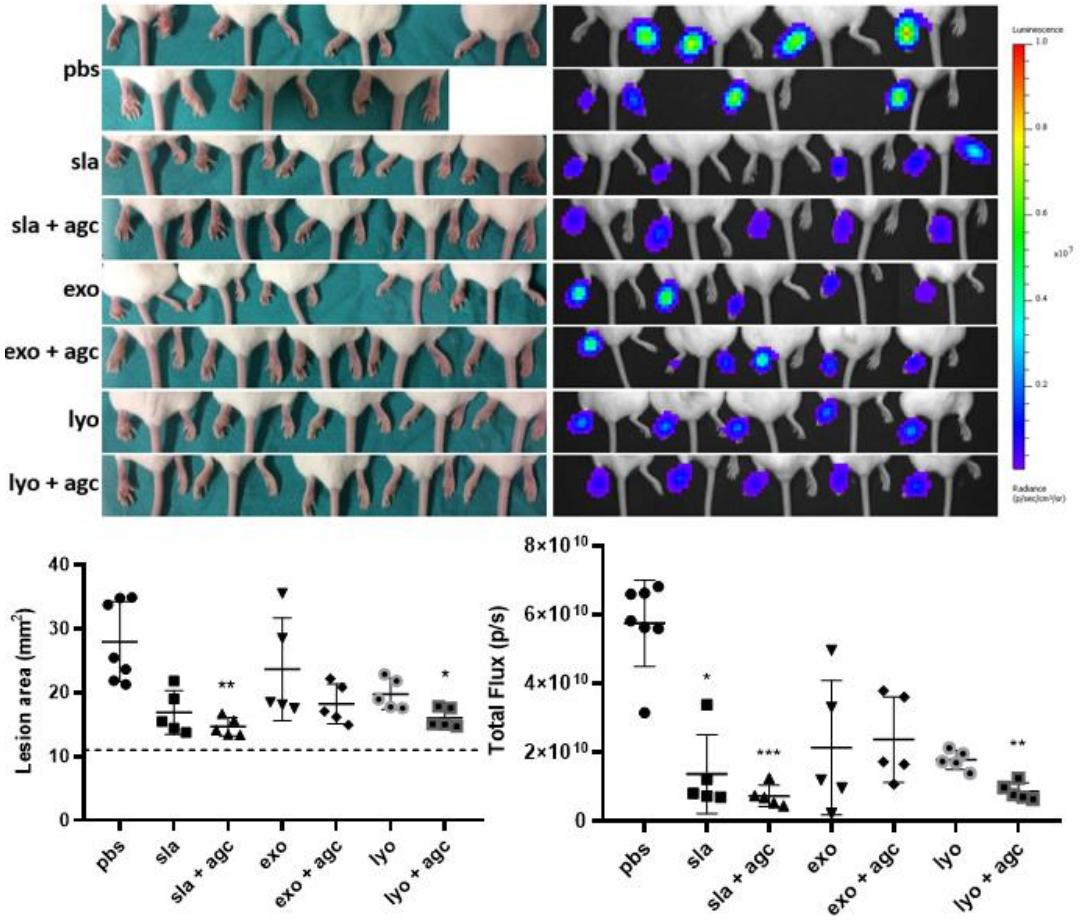

Figure 3.34. Assessment of disease progression based on footpad swellings and luciferase activities.

Pictures of footpads upon sacrification of mice 31 days after challenge, and a representative image of luciferase activity quantified using IVIS Lumina III (Perkin Elmer, U.S.A.) *in vivo* imager are shown on the top panel. On day 28, final footpad measurements and luciferase activities were quantified as depicted in the bottom panel. The dashed line represents the size of a healthy footpad calculated by taking the average of each mouse's footpad measurement prior to challenge. 5th mouse in the PBS-administered group, 3rd and 5th mice in the SLA-administered group, and the 2nd mouse in SLA+αGalCer-administered group were unfortunately had to be challenged on both of their footpads due to difficulty of the procedure. Each candidate group was compared to PBS-administered group using Kruskal-Wallis test followed by Dunn's multiple comparison test (*: p=0.0342, **: p=0.0013 for bottom left panel, *: p=0.0141, **: p=0.0014, ***: p=0.0003 for bottom right panel).

Furthermore, we thought the high standard deviation in some groups could be related to errors during the initial inoculum of parasites since the challenge was done in a concentrated solution ($9x10^6$ parasites/50 µl for each mouse). We suspected that slight variability during injection process could lead to considerable differences once the disease progressed. To test for this, we followed two groups by taking luciferase activity readings right after injection, on day 21 and finally on day 28. Our observations suggested that initial variability in administered volume did not correlate with parasite loads on day 21 and 28.

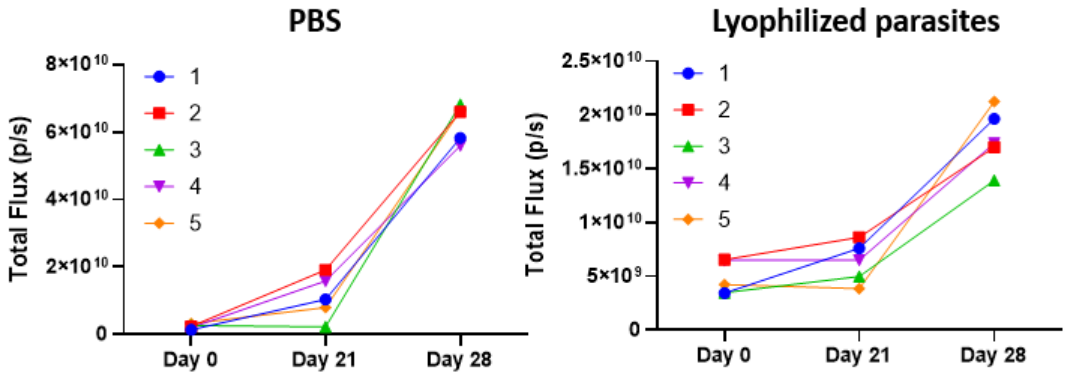

Figure 3.35. Evaluation of effect of variability in the initial inoculum on the progression of cutaneous Leishmaniasis.

Luciferase activities on Day 0, 21 and 28 were quantified using IVIS Lumina III (Perkin Elmer, U.S.A.) in vivo imager for each mouse of PBS and Lyo-administered groups.

Furthermore, we tested the level of protection vaccine formulations provided against parasite metastasis to popliteal lymph nodes as explained in Section 2.2.9.4.5. Unfortunately, a thorough analysis of parasite dissemination was not possible because luciferase activity was greatly reduced in severely swollen lymph nodes, which included PBS, Exo, and Exo+αGalCer-administered groups. Of note, swollen lymph nodes were approximately 10-15 times larger than a healthy lymph node (picture not shown), thus, leading to a big reduction in the diffusion rate of D-luciferin, slowing down the enzymatic reaction. However, it was still possible to compare SLA and Lyo-administered groups with their αGalCer added counterparts

because these groups had much smaller lymph nodes, removing the diffusion rate from the equation. Only Lyo+αGalCer-administered mice had significantly lower parasite loads in their lymph nodes compared to Lyo-administered group. Similarly, SLA+αGalCer mice had lower parasite burdens in their lymph nodes, though not significant, compared to SLA-administered group, potentially showing a protective effect of αGalCer against parasite dissemination. Possible mechanisms of action of antigen/adjuvant combinations are discussed in Section 3.2.11.5.

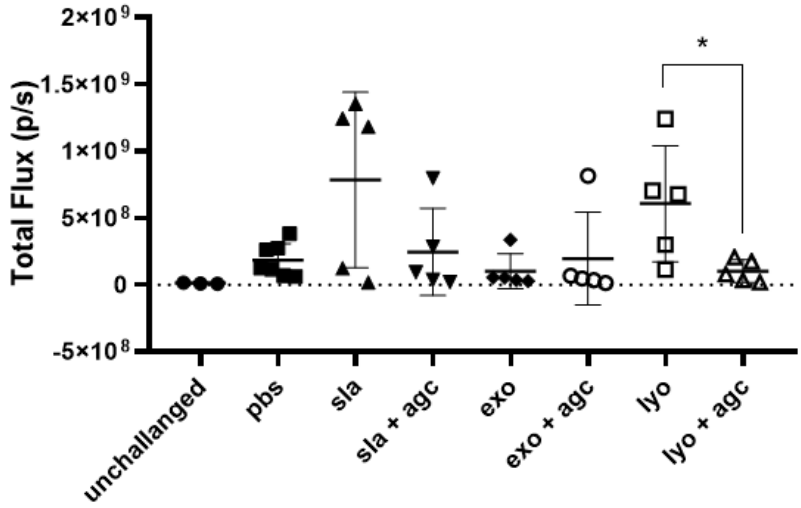

Figure 3.36. Assessment of parasite dissemination to popliteal lymph nodes as explained in Section 2.2.9.4.5.

Antigen alone groups were statistically compared to their antigen + adjuvant counterparts using Mann-Whitney test (*: p=0.0317).

3.2.11.4 Evaluation of SLA-specific Humoral Immunity Induced by Vaccine Formulations

IFNγ and IL4 are prototypical Th1 and Th2 cytokines, and they regulate B-cell proliferation and differentiation, affecting IgG2a and IgG1 class switching, respectively, in mice (Finkelman et al., 1990; Snapper & Paul, 1987; Toellner et al., 1998). Therefore, IgG2a and IgG1 antibody responses can be an early but indirect indicator of Th1 or Th2-mediated response to antigen-adjuvant combinations. Mouse

models of Leishmaniasis have shown the fundamental roles of helper T cell subtypes where a primarily Th1-mediated immunity was associated with resistant mouse strains such as C57Bl/6 while a primarily Th2 mediated immunity was associated with susceptible BALB/c mice (Heinzel et al., 1991; Scott et al., 1988), resulting in classical and alternative activation of macrophages, respectively (Bogdan et al., 1990; Chatelain et al., 1992; Heinzel, Schoenhaut, et al., 1993; Sypek et al., 1993). However, the role of humoral immune response against Leishmaniasis is unclear and highly complex. Production of high IgG antibody titers has been a strong indicator of parasite persistence, while the absence of immunoglobulins or B-cells resulted in resistance to *L. major* in susceptible BALB/c mice (Chen et al., 1993; Miles et al., 2005) and to *L. donovani* in C57Bl/6 mice (Smelt et al., 2000). Although FcγR-engagement can lead to activatory or inhibitory signals based on the subtype of FcγR and IgGs, immune complex formation can result in suppression of IL-12 and induction of IL-10 through low affinity FcγRs (Gallo et al., 2010; Guilliams et al., 2014). Moreover, it was found that both IgG1 and IgG2a/c induced similar levels of IL10 *in* vitro, albeit the former one utilized FcγRIII while the latter ones utilized primarily FcγRI and also FcγRIII to a lesser degree (Chu et al., 2010). Correspondingly, immune complex-FcγR mediated IL-10 production exacerbated cutaneous and mucocutaneous Leishmaniasis in mice infected with *L. amazonensis* and *L. Mexicana* (Buxbaum & Scott, 2005; Kima et al., 2000; Thomas & Buxbaum, 2008). These observations were not unique to mice, as delayed-type hypersensitivity (DTH) response in humans resulted in parasite elimination while immune complex-mediated disease exacerbation was associated with visceral Leishmaniasis (Basak et al., 1992; Haldar et al., 1983; Miles et al., 2005; Sundar et al., 1998) as well as local and diffuse cutaneous Leishmaniasis (as reviewed in Goncalves et al., 2020). Furthermore, this phenomena was not specific to Leishmaniasis either as the presence of immunoglobulins has been associated with suppressed DTH reactions, and it was termed as “immune deviation” (Asherson & Stone, 1965; Jerry et al., 1976; Kaplan & Streilein, 1977; McCurley et al., 1986; C. R. Parish et al., 1967; Christopher R. Parish, 1996) which can be an evolutionary strategy to prevent DTH-

mediated tissue destruction. For instance, B-cell deficient C57Bl/6 mice were highly resistant to visceral *Leishmaniasis* at the cost of neutrophil mediated hepatic pathology (Smelt et al., 2000).

In our trials, all of the vaccinated mice except for SLA-administered group had high IgG1 antibody titers, whereas SLA-administered group had an IgG2a dominated antibody production (Figure 3.37.). This was expected as BALB/c mice have a tendency of producing high IgG1 titers against *Leishmania major* (Ebrahimpoor et al., 2013; Rostamian et al., 2017). Although high IgG2a-inducing SLA-administered group showed significantly lower levels of parasite burden compared to PBS-administered group, even lower levels of parasite burdens were observed in SLA+αGalCer and Lyo+αGalCer-administered groups, which did not induce high levels of IgG2a (Figures 3.34. and 3.37.). In conclusion, our observations suggested that levels of IgG1 or IgG2a did not correlate with the progression of the disease, and were in support of the report published by Èphanie Honore et al. (1998) in which it was reported that high levels of IgG2a titer in BALB/c (V2 strain) mice was not associated with parasite control. Furthermore, α-GalCer stimulated NKT cells were reported to play a balancing role (Griewank et al., 2014) in cytokine milieu which can affect the class switching process. This is consistent with our findings as SLA-administered group had high levels of IgG2a titer, whereas SLA+αGalCer-administered group had a complete reversal of IgG2a/IgG1 ratio. Furthermore, this effect of αGalCer was not observed in other groups which did not have a skewed IgG2a/IgG1 ratio in the first place.

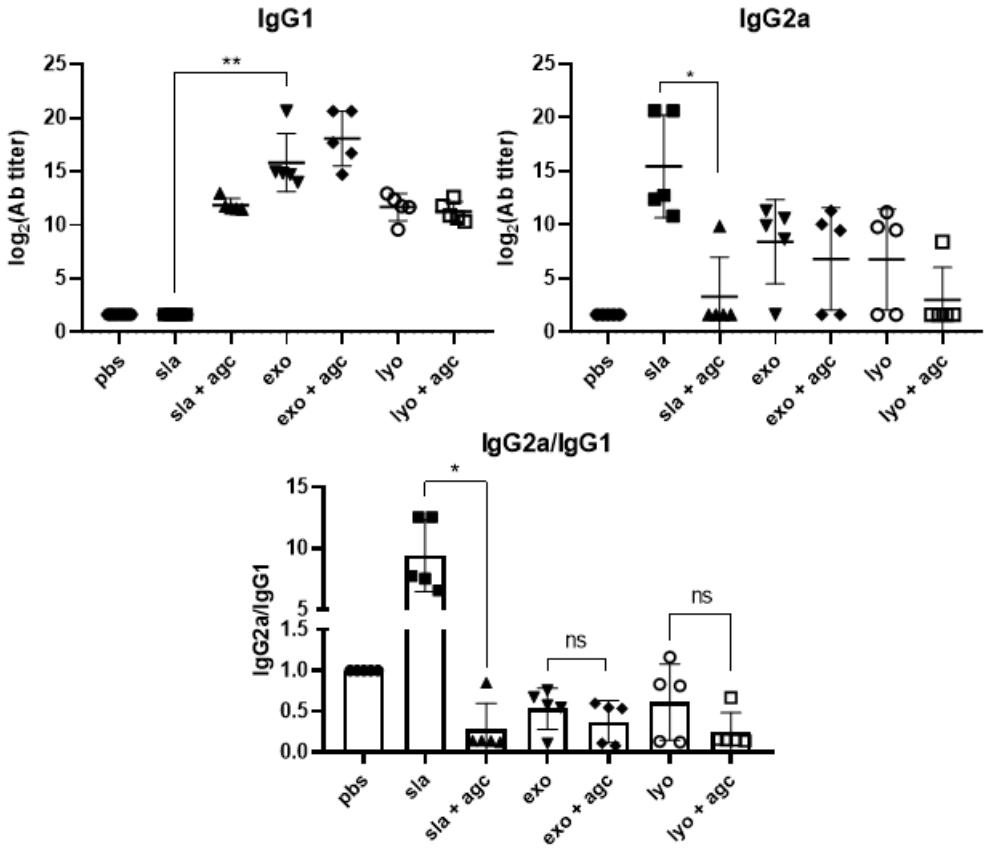

Figure 3.37. SLA specific IgG1 and IgG2a titers of immunized BALB/c mice.

The isolation of sera from immunized animals and IgG ELISA protocol are explained in Sections 2.2.9.4.1. and 2.2.9.4.2. The statistical comparison of groups was done using Kruskal-Wallis test followed by Dunn's multiple comparison test (top tight panel; *: p=0.0189, bottom panel *: p=0.0142, **: p=0.0051).

3.2.11.5 Evaluation of Cell-Mediated Immunity of Vaccinated Groups Against *L. major*

Th1-mediated immunity has been regarded as pivotal for resistance against both visceral and cutaneous Leishmaniasis while Th2-mediated immunity has been regarded as a susceptibility factor (reviewed in McMahon-Pratt & Alexander, 2004). Development of a Th1-mediated proinflammatory response is associated with cytokines IFNγ, TNFα, IL1, IL2 and IL12 accompanied by increased RNS and ROS

through upregulation of NADPH oxidase and iNOS (Atri et al., 2018; D. Sacks & Noben-Trauth, 2002; Tomiotto-Pellissier et al., 2018; Von Stebut et al., 2003). In contrast, development of a Th2-mediated anti-inflammatory response is associated with cytokines IL4, IL5, IL10, IL13 and TGFβ, accompanied by increased arginase activity, polyamine biosynthesis and downregulation of iNOS and TNFα (Gordon, 2003; Pascale Kropf et al., 2005; Muxel et al., 2018; D. Sacks & Noben-Trauth, 2002). While Th1-mediated immune response is important for controlling intracellular pathogens, Th2-mediated immune response is essential to fight against parasitic helminths, wound healing and prevention of septicemia at the cost of tolerating invaders to an extent (Allen & Wynn, 2011; Pasparakis et al., 2014). Below, cytokines released by T cell subsets Th1, Th2, Treg, Th9, Th17 and Th22 are discussed with a special emphasis on Th1 and Th2 in the context of Leishmaniasis.

IFNγ and TNFα classically activate macrophages and work synergistically to induce iNOS which is important for destruction of *L. major* amastigotes (Liew et al., 1997). Although Th1 response has been considered protective against *Leishmania spp.* (Heinzel et al., 1991; Scott et al., 1988), it has, also, been reported to exacerbate the disease. For instance, CD4+CD25-FoxP3- Th1 cells producing both IFNγ and IL10 were associated with disease exacerbation in mice infected with a virulent *L. major* strain or *L. donovani* (Anderson et al., 2007; Stäger et al., 2006). The production of IL10 by CD4+CD25-FoxP3- subclass of Th1 cells could be an evolutionary strategy of the host to counteract severe tissue inflammation in the absence of a proper Th2 response; however, it opens a door for exploitation by successful parasites like *Leishmania spp.* Furthermore, it is well documented that an excessive cell mediated immunity can lead to severe tissue damage and parasite persistence, which is a hallmark of mucocutaneous Leishmaniasis (Martin & Leibovich, 2005; Strazzulla et al., 2013).

IL4 and IL13 were associated with downregulation of Th1 cytokines, alternative activation of macrophages, increasing arginase and polyamine synthesis (de Waal Malefyt et al., 1993; Doherty et al., 1993; Hesse et al., 2001), and inhibition of leishmanicidal activity of macrophages *in vivo* (Pascale Kropf et al., 2005). In

support of these findings, IL13 deficient BALB/c mice were found to be resistant to *L. major* infection (Matthews et al., 2000). However, the role of Th2 cytokines in Leishmaniasis appear to be more complex than it seems. For instance, abrogation of CD4+ T cell specific IL4 signaling resulted in control of acute *L. major* infection, whereas global IL-4Rα deficiency led to parasite dissemination during chronic infection of BALB/c mice (Mohrs et al., 1999; Radwanska et al., 2007). Similar to CD4+ T cells, macrophage and neutrophil specific IL-4Rα deficiency delayed susceptibility in BALB/c mice by inhibiting alternative activation of macrophages (Hölscher et al., 2006). Furthermore, the protective role of IL4 signaling was reported to be APC dependent as dendritic cell specific IL-4Rα-deficient BALB/c mice succumbed to parasitemia. Surprisingly, the observed protective effect of IL4 signaling was associated with the induction of IL12 by IL4 signaling in dendritic cells, ultimately favoring a Th1 response (Alexander & Brombacher, 2012; Biedermann et al., 2001), which is in favor of primate vaccination trials utilizing rIL12 and ALUM in which the absence of ALUM decreased protective effects in *L. amazonensis* infection in rhesus macaques (Kenney et al., 1999) or even rendered the vaccination ineffective against *L. major* infection in vervet monkeys (Gicheru et al., 2001). Furthermore, another study found no effect of IL4 deficiency on disease progression and Th1 polarization in BALB/c mice (Noben-Trauth et al., 1996). Subsequently, it was found that distinct parasite isolates can affect disease progression differently in IL4 deficient BALB/c mice (P. Kropf et al., 2003). Similar protective effects of IL4 signaling were found in *L. donovani* infection as IL-4Rα-deficient BALB/c mice had higher hepatic parasite burdens and decreased protective granuloma formation compared to IL4-deficient mice, suggesting protective roles of IL4 and IL13, both of which are recognized through IL-4Rα (Alexander et al., 2000; Stäger, Alexander, Carter, et al., 2003). Similar to *L. major* infection, the protective role of IL4 signaling was not due to macrophages, neutrophils, CD4+ T cells or CD8+ T cells, pointing to a possible role of dendritic cells once again (Alexander & Brombacher, 2012; McFarlane et al., 2011). Further vaccination trials with promising candidates showed increased IL4 and IL13 association and requirement

to insure a protective type-1 response (Basu et al., 2005, 2007; Stäger, Alexander, Kirby, et al., 2003). Moreover, IL4 and IL13 were found to inhibit Th17 differentiation and IL17 induced immunopathology (Newcomb et al., 2009), a susceptibility factor for *Leishmaniasis* (discussed in the next paragraphs).

In our experiments, results of SLA-pulsed splenocytes showed lower levels of IFNγ and TNFα in groups with the lowest parasite loads: SLA and lyophilized parasite-based candidates (Figures 3.34. and 3.38.). Groups vaccinated with exosome-based candidates had higher levels of IFNγ and TNFα, but also had higher parasite loads on their footpads. Similar to exosome-administered groups, PBS administered group had very high levels of IFNγ and TNFα, but had the highest parasite load by far, contradicting the notion that a Th1 dominant response is necessary for controlling intracellular amastigotes. On the Th2 cytokine spectrum (IL4, IL5, IL10 and IL13), unvaccinated group had the lowest levels of IL5, and similar levels of IL4 and IL13 compared to SLA and lyophilized parasite-administered groups. Exosome-administered groups, on the other hand, had the highest levels of Th2 cytokines (Figure 3.38.). These results were, also, inconsistent with the literature because the low levels of Th2 cytokines did not correlate with lower parasite burdens. A closer look at Th1 and Th2 cytokines revealed an almost perfect correlation between parasite burdens and Th1/Th2 balance, calculated by the ratio of prototypical Th1 and Th2 cytokines IFNγ and IL4, respectively (Figure 3.39.). This analysis revealed that groups with balanced Th1/Th2 levels controlled parasitemia much better than PBS-administered group. In conclusion, our results demonstrated uncontrolled proinflammatory Th1 response and the beginning of formation of necrotic footpad tissues accompanied by high levels of parasite burdens in unvaccinated group, which has been extensively reported for mucocutaneous Leishmaniasis (Antonelli et al., 2004, 2005; Bacellar et al., 2002; Follador et al., 2002). Furthermore, our results underline the importance of a balanced Th1/Th2 response against *L. major* infection in controlling tissue destruction possibly through a balanced reaction of classically and alternatively activated macrophages which is essential to achieve wound healing and homeostasis (Hesse et al., 2001; Munder et al., 1998). Although BALB/c

infection model we utilized mimicked excessive cell mediated immunity typically seen in mucocutaneous Leishmaniasis more closely than traditional cutaneous Leishmaniasis model, we think that it may be related to the specific *L. major* strain we used which was a patient isolate. This hypothesis would not be unreasonable as distinct patient isolates of the same species of *Leishmania* were reported to trigger inflammatory responses differently (P. Kropf et al., 2003; Teixeira et al., 2005).

Another Th2 cytokine IL10 suppresses macrophage activation and dendritic cell maturation. It can, also, be secreted by other T cells: mainly Treg and even Th1 cells as an immunoregulatory mechanism to prevent excessive inflammation (O'Garra & Vieira, 2007). Decreased IL4 and IL10 and increased IFNγ is associated with clinical cure of human cutaneous Leishmaniasis patients (Lúcio Roberto Castellano et al., 2009). Moreover,` IL10 depletion led to sterile cure of *L. major* infected C57Bl/6 model (Belkaid et al., 2001). On a different perspective, presence of CD4+CD25+ Tregs and IL10 was found to be important for concomitant immunity procured by continuous antigen supply of remaining *L. major* amastigotes in the skin of C57Bl/6 mice at the risk of disease reactivation (Belkaid, Piccirillo, et al., 2002). Also, presence of IL10 is favorable, and partial rather than complete blockage of IL10 is recommended as a therapeutic strategy in *Leishmania braziliensis* infections to modulate immunopathology in mucocutaneous Leishmaniasis (Lucio Roberto Castellano et al., 2015; Gomes-Silva et al., 2007). In our experiment, the level of IL10 closely mimicked other Th2 cytokines IL4 and IL13, and it was revealed that high levels of IL10 did not correlate with parasite burdens (Figures 3.34. and 3.38.) as observed in Exo+αGalCer-administered group which had significantly higher levels of IL10 while having lower parasite burdens compared to unvaccinated group. However, we were unable to test the long-term effects of high levels of IL10 on parasite persistence, and in prevention of development of severe necrotic lesions due to the relatively short amount of time required for disease progression (31 days) in our model.

Another proinflammatory cytokine, IL6, does not seem to play a pivotal role in Leishmaniasis since IL6 deficient BALB/c mice had decreased Th1 and Th2

cytokines but the progression of cutaneous lesions were not affected (Titus et al., 2001). Similarly, contradictory results on IL2 were published on Leishmaniasis suggesting that IL2 can induce both Th1 and Th2 cells to produce IFNγ and IL4, respectively, classically or alternatively activating macrophages leading to parasite clearance or persistence (Heinzel, Rerko, et al., 1993; Oliveira et al., 2015; X. Wang & Mosmann, 2001). Our results suggested that IL6 and IL2 levels did not correlate with disease progression (Figures 3.34. and 3.38.), which was reasonable based on aforementioned reports.

IL22, a member of IL10 family of cytokines, was reported to protect against tissue damage in *L. major* infection of both BALB/c and C57Bl/6 mice (Gimblet et al., 2015; Hezarjaribi et al., 2014). We observed high levels of IL22 in Exo+αGalCer-administered group. In line with the aforementioned reports, we observed less swollen and inflamed footpads in this group compared to Exo-administered group underlying the effect of αGalCer in balancing the initial cytokine milieu and immune response (Figure 3.34. and 3.38.)

The prototypical cytokine of Th17 cells, IL17, was associated with protection of mucosal surfaces and it was reported to have protective effects in mucocutaneous Leishmaniasis (Alexander & Brombacher, 2012). However, IL17 exacerbated cutaneous lesions of *L. major* infected BALB/c and C57Bl/6 mice (Gonzalez-Lombana et al., 2013; Kostka et al., 2009) and *L. braziliensis* infected MCL patients (Bacallar et al., 2009), through neutrophil mediated tissue damage (Boaventura et al., 2010). In our experiment, mice with the highest IL-17a levels (PBS and Exo-administered groups) were the ones with the most inflamed footpads (Figure 3.34. and 3.38.) although the variation within the groups was too high for this cytokine and levels of IL17a were almost undetectable in majority of mice, preventing a thorough analysis in our experimental model.

IL9 is reported to provide a protective immunity against intestinal parasites and cause pathology in atopic allergic reactions (Faulkner et al., 1998). While the main source of IL9 is considered Th9 cells, it was, also, produced by Th17 and Treg cells.

Persistent high levels of IL9 were associated with susceptibility in BALB/c mice whereas IL9 depletion resulted in resistance to *L. major* infection (Arendse et al., 2005; Gessner et al., 1993; Nashed et al., 2000). Although, we did not see persistent high levels of IL9 in unvaccinated group like it was suggested, groups vaccinated with exosome-based candidates showed highest levels of IL9 (Figure 3.38.). Although Exo and Exo+αGalCer-administered groups had lower levels of parasite burdens in their footpads compared to unvaccinated group, they still had slightly higher levels of parasite burdens compared to groups vaccinated with SLA and lyophilized parasite-based vaccine candidates (Figure 3.34.) which may have partly resulted from higher levels of IL9 secretion.

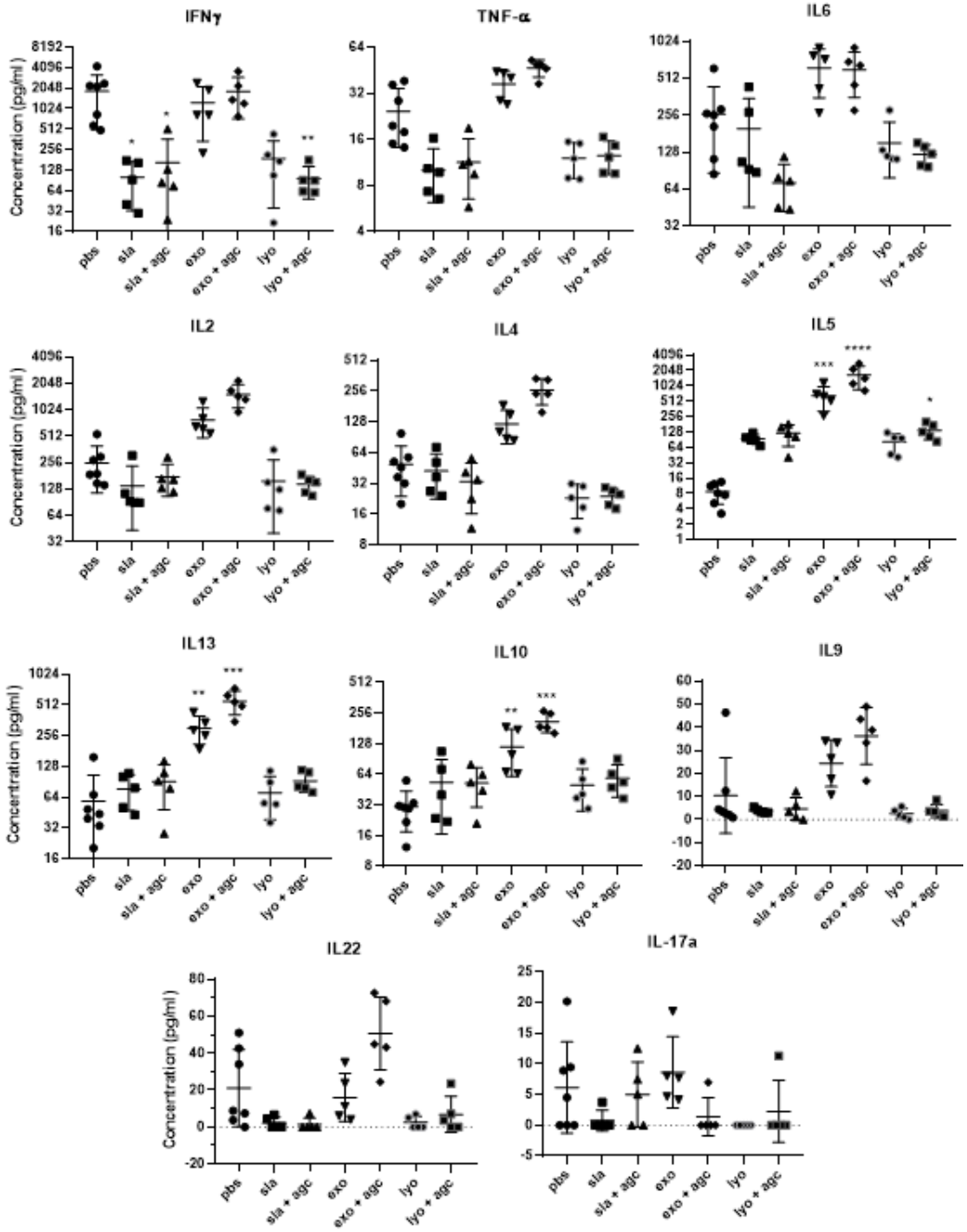

Figure 3.38. SLA specific Th1, Th2, Th9, Th17 and Th22 cytokine levels of mice immunized with exosome, SLA or lyophilized parasite-based vaccine candidates.

Spleens of mice were extracted, and purified splenocytes were pulsed with SLA. Following a 48-hour incubation period, cytometric bead array was performed to supernatants of pulsed splenocytes followed by flow cytometric analysis according to the manufacturer's instructions. All groups were statistically compared to splenocytes of PBS-

Figure 3.38. (continued) SLA specific Th1, Th2, Th9, Th17 and Th22 cytokine levels of mice immunized with exosome, SLA or lyophilized parasite-based vaccine candidates.

administered group for each respective cytokine using Kruskal-Wallis followed by Dunn's multiple comparison test (for IFNγ *: p<0.0162, **: p=0.0095, for IL5 *: p=0.0399, ***: p=0.0002, ****: p<0.0001, for IL13 **: p=0.0049, ***: p=0.0003, for IL10 **: p=0.0084, ***: p=0.0002).

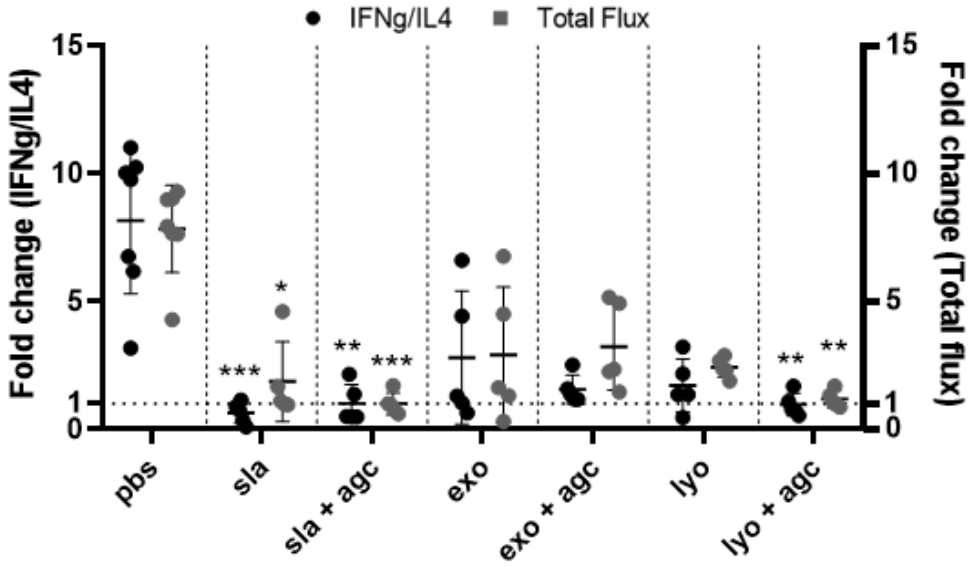

Figure 3.39. Evaluation of Th1/Th2 balance on controlling parasitemia.

SLA+αGalCer group provided the best protection against *L. major* based on parasite burdens. The cytokine profile of this group was assumed as the reason of high level of protection in an attempt to understand the observed effects by deduction. Therefore, means of this group for IFNγ/IL4 ratio and Total flux was levelled to 1, separately. The levels of IFNγ/IL4 ratio and Total flux of each mouse of every group was reported as fold change based on these two means and shown side by side. All groups were statistically compared to PBS-administered group in their respective subcategory (IFNγ/IL4 ratio or Total flux) using Kruskal-Wallis followed by Dunn's multiple comparison test (** (sla+agc): p=0.0054, ** (lyo+agc): p=0.0076, ***: p=0.0004 for IFNg/IL4, *: p=0.0141, **: p=0.0014, ***: p=0.0003 for Total flux)

In conclusion, the footpad swellings of SLA+αGalCer, Lyo+αGalCer and Exo+αGalCer groups were consistently lower than their antigen alone counterparts (Figure 3.34.), indicating healthy wound healing processes. Similarly, exosome and lyophilized parasites with αGalCer had a better balance of Th1/Th2 ratio, and lower parasite burdens were observed in Lyo+αGalCer group. αGalCer was reported to compete for CD1d receptor on NKT cells against LPG and GILP binding (Amprey et al., 2004; Belo et al., 2017). By binding to this receptor, α-GalCer not only induced NKT cells to release cytokines such as IFN-γ, IL-4, 10, 13 and 17 (Macho-Fernandez & Brigl, 2015; Michel et al., 2008; Moreira-Teixeira et al., 2011, 2012), but it also prevented the dampening effect of LPG and GILPs on cytokine release of NKT cells through competition (Amprey et al., 2004; Belo et al., 2017). Lyophilized whole parasites can be considered as the richest source of LPG and GILPs. It is possible that in the presence of αGalCer, LPG and GILPs from lyophilized parasites could not exploit NKT cell response to their advantage which ultimately may have resulted in lower parasite burdens. Exosomes are also rich sources of LPGs and GILPs; however, positive effect of αGalCer on parasite burdens was not obvious in exosome-based candidates. It is possible that high levels of FBS contamination in exosome isolates may have clouded the true potential of exosome-based candidates, as our previous vaccination trials suggested very high levels of protection procured by exosome-based vaccines (Ayanoğlu, PhD Thesis, 2019). Application of a purification procedure following differential centrifugation for exosomes could yield exciting results for their immunogenic potential. Until then, SLA and lyophilized parasite-based vaccine candidates combined with αGalCer are the most promising ones based on low levels of parasite burdens and excellent wound healing characteristics in BALB/c mice. Finally, long-term protection against cutaneous Leishmaniasis, historically, can only be achieved by discontinued Leishmanization and second-generation Leishmanization (using CRISPR attenuated live strains) based vaccinations both of which rely on continuous antigen supply by live parasites, from the primary infection, residing typically in the lymph nodes asymptomatically. Regularly repeated vaccinations with lyophilized parasites may be a safer alternative

to second generation Leishmanization trials as the procedure leave no parasite alive while providing a complete antigen repertoire without heat denaturation. However, the long-term success of such candidates relies on generation of central, effector and tissue resident memory T-cells whereas live vaccines used in second-generation Leishmanization trials have the advantage of continuous supply of protective short-lived effector CD4+Ly6C+ T-cells (Pacheco-Fernandez et al., 2021; Peters et al., 2014; Zhang et al., 2020).

CHAPTER 4

CONCLUSION AND FUTURE PERSPECTIVES

There have been extensive research on exploatitaion of the host immune response by *Leishmania spp.* to achieve persistance. Evidence suggests that Leishmania evade immunity through manipulation of the adaptive immune response at the cellular level and subversion of the signaling pathways at the intracellular level. Examples include subversion of TLR, IFN-γR and NLRP signaling and downstream transcription factors such as NFκB and STAT1 as well as hijaking of intracellular transportation and cytoskeletal elements. Nevertheless, contribution of another important pathogen sensing pathway dedicated tosensing cytosolic dsDNA (cGAS-STING-TBK1 pathway), have been largely ignored.

In this thesis, we first optimized an *in vitro* infection model by targeting variables that might impact the infection process in order to achieve a reliable *in vitro* infection model that closely mimicked natural infection of macrophages. The tested variables consisted of strategies used in development of stationary phase parasites, the time of co-incubation of parasites with THP1 cells to achieve maximum infection levels without false positive results, the media types in which prolonged infection model took place, determination of the effect of opsonization on prolonged infection model, and determination of the level of PMA-induced differentiation to achieve high parasite loads as well as equalizing phagocytic capacities of KO-THP1 cells with WT-THP1 cells. Subsequent experiments suggested a deleterious role of the cGAS-STING-TBK1 pathway based on apparent resistance observed in KO-THP1 cells and WT-THP1 cells treated with TBK1 inhibitors to *L. major* infection. Gene expression analyses showed increased cytotoxic and proinflammatory capacities of cGAS- and TBK1-KO cells compared to WT cells, providing a possible explanation for their resistance to *L. major* infection. It was also found that the observed aggravation of infection of WT cells were independent of type I IFNs. This suggest

that cGAS-STING-TBK1 pathway is either involved in the exploitation of THP1 cells in a non-canonical manner, or *L. major* parasites developed strategies to fine-tune the ISG response in a manner in which they degrade or render host-protective elements inefficient while allowing host susceptibility factors to work to their benefit. Hence, the absence of type I IFNs points to a possible protective role in *L. major* infection when the results are interpreted in a deductive manner. Unfortunately, these studies only scratched the surface of the role of cGAS-STING-TBK1 pathway in Leishmaniasis, and further experiments are required to fully understand the downstream elements resulting in susceptibility to *L. major*. Furthermore, Amlexanox likely plays a dual role where its inhibition of TBK1 and F-actin polymerization work synergistically to prevent amastigote proliferation. However, *in vivo* trials of Amlexanox, other TBK1 inhibitors and utilization of KO-mouse models are required to move onto clinical trials in cutaneous Leishmaniasis patients.

Despite numerous vaccination trials, there is still no licensed vaccines for Leishmaniasis in humans. We utilized different *Leishmania* antigen compositions (lyophilized whole parasites, soluble *Leishmania* antigens and *Leishmania* exosomes) in terms of their protective effects when used as vaccines. We also, capitalized on early involvement of NKT cells by combining the aforementioned antigen compositions with the prototypical NKT cell adjuvant α-galactosylceramide. All of the antigen formulations provided considerable protection, which was assessed based on parasite loads and development of lesions. However, SLA and lyophilized parasites in combination with α-galactosylceramide were the most promising candidates as they provided the most significantly reduction in parasite loads and lesion sizes. Due to the relatively short period of time it takes for severe lesions to develop in the unvaccinated group, it was not possible to assess whether these promising candidates could have ultimately induced elimination of the parasites since even in the resistant mouse strains, self-healing takes 5-9 weeks. Nevertheless, the results suggest that the promising antigen-adjuvant combinations used in this study deserves further investigation.

REFERENCES

Agramonte-Hevia, J., González-Arenas, A., Barrera, D., & Velasco-Velázquez, M. (2002). Gram-negative bacteria and phagocytic cell interaction mediated by complement receptor 3. *FEMS Immunology and Medical Microbiology*, *34*(4), 355–366. https://doi.org/10.1016/S0928-8244(02)00408-X

Alexander, J., & Brombacher, F. (2012). T helper1/T helper2 cells and resistance/susceptibility to Leishmania infection: Is this paradigm still relevant? *Frontiers in Immunology*, *3*(APR), 1–13. https://doi.org/10.3389/fimmu.2012.00080

Alexander, J., Carter, K. C., Al-Fasi, N., Satoskar, A., & Brombacher, F. (2000). Endogenous IL-4 is necessary for effective drug therapy against visceral leishmaniasis. *European Journal of Immunology*, *30*(10), 2935–2943. https://doi.org/10.1002/1521-4141

Allen, J. E., & Wynn, T. A. (2011). Evolution of Th2 Immunity: A Rapid Repair Response to Tissue Destructive Pathogens. *PLOS Pathogens*, *7*(5), e1002003. https://doi.org/10.1371/JOURNAL.PPAT.1002003

Amprey, J. L., Im, J. S., Turco, S. J., Murray, H. W., Illarionov, P. A., Besra, G. S., Porcelli, S. A., & Späth, G. F. (2004). A subset of liver NK T cells is activated during Leishmania donovani infection by CD1d-bound lipophosphoglycan. *Journal of Experimental Medicine*, *200*(7), 895–904. https://doi.org/10.1084/jem.20040704

Anderson, C. F., Oukka, M., Kuchroo, V. J., & Sacks, D. (2007). CD4+CD25-Foxp3- Th1 cells are the source of IL-10-mediated immune suppression in chronic cutaneous leishmaniasis. *Journal of Experimental Medicine*, *204*(2), 285–297. https://doi.org/10.1084/jem.20061886

Andrade, W. A., Agarwal, S., Mo, S., Shaffer, S. A., Dillard, J. P., Schmidt, T., Hornung, V., Fitzgerald, K. A., Kurt-Jones, E. A., & Golenbock, D. T. (2016). Type I Interferon Induction by Neisseria gonorrhoeae: Dual Requirement of

Cyclic GMP-AMP Synthase and Toll-like Receptor 4. *Cell Reports*, *15*(11), 2438–2448. https://doi.org/10.1016/J.CELREP.2016.05.030

Antonelli, L. R. V., Dutra, W. O., Almeida, R. P., Bacellar, O., Carvalho, E. M., & Gollob, K. J. (2005). Activated inflammatory T cells correlate with lesion size in human cutaneous leishmaniasis. *Immunology Letters*, *101*(2), 226–230. https://doi.org/10.1016/J.IMLET.2005.06.004

Antonelli, L. R. V., Dutra, W. O., Almeida, R. P., Bacellar, O., & Gollob, K. J. (2004). Antigen specific correlations of cellular immune responses in human leishmaniasis suggests mechanisms for immunoregulation. *Clinical and Experimental Immunology*, *136*(2), 341–348. https://doi.org/10.1111/J.1365-2249.2004.02426.X

Arendse, B., Snick, J. Van, & Brombacher, F. (2005). IL-9 Is a Susceptibility Factor in Leishmania major Infection by Promoting Detrimental Th2/Type 2 Responses. *The Journal of Immunology*, *174*(4), 2205–2211. https://doi.org/10.4049/JIMMUNOL.174.4.2205

Aronson, N., Herwaldt, B. L., Libman, M., Pearson, R., Lopez-Velez, R., Weina, P., Carvalho, E. M., Ephros, M., Jeronimo, S., & Magill, A. (2016). Diagnosis and Treatment of Leishmaniasis: Clinical Practice Guidelines by the Infectious Diseases Society of America (IDSA) and the American Society of Tropical Medicine and Hygiene (ASTMH). *Clinical Infectious Diseases : An Official Publication of the Infectious Diseases Society of America*, *63*(12), e202–e264. https://doi.org/10.1093/cid/ciw670

Asherson, G. L., & Stone, S. H. (1965). Selective and specific inhibition of 24 hour skin reactions in the guinea-pig: I. Immune deviation: description of the phenomenon and the effect of splenectomy. *Immunology*, *9*(3), 205. /pmc/articles/PMC1423579/?report=abstract

Atri, C., Guerfali, F. Z., & Laouini, D. (2018). Role of Human Macrophage Polarization in Inflammation during Infectious Diseases. *International Journal of Molecular Sciences 2018, Vol. 19, Page 1801*, *19*(6), 1801.

https://doi.org/10.3390/IJMS19061801

Awasthi, A., Mathur, R., Khan, A., Joshi, B. N., Jain, N., Sawant, S., Boppana, R., Mitra, D., & Saha, B. (2003). CD40 signaling is impaired in L. major-infected macrophages and is rescued by a p38MAPK activator establishing a host-protective memory T cell response. *The Journal of Experimental Medicine*, *197*(8), 1037–1043. https://doi.org/10.1084/JEM.20022033

Ayanoğlu, İ. C. (2019). *The Contribution of Kinetoplast DNA to Leishmania Major Experimental Infection and Evaluation of Leishmania Extracellular Vesicle Based Vaccine Against Cutaneous Leishmaniasis in BALB/C Mice*. Middle East Technical University.

Bacallar, O., Faria, D., Nascimento, M., Cardoso, T. M., Gollob, K. J., Dutra, W. O., Scott, P., & Carvalho, E. M. (2009). Interleukin 17 production among patients with American cutaneous leishmaniasis. *The Journal of Infectious Diseases*, *200*(1), 75–78. https://doi.org/10.1086/599380

Bacellar, O., Lessa, H., Schriefer, A., Machado, P., De Jesus, A. R., Dutra, W. O., Gollob, K. J., & Carvalho, E. M. (2002). Up-regulation of Th1-type responses in mucosal leishmaniasis patients. *Infection and Immunity*, *70*(12), 6734–6740. https://doi.org/10.1128/IAI.70.12.6734-6740.2002

Bajénoff, M., Breart, B., Huang, A. Y. C., Qi, H., Cazareth, J., Braud, V. M., Germain, R. N., & Glaichenhaus, N. (2006). Natural killer cell behavior in lymph nodes revealed by static and real-time imaging. *The Journal of Experimental Medicine*, *203*(3), 619. https://doi.org/10.1084/JEM.20051474

Barman, H., Walch, M., Latinovic-Golic, S., Dumrese, C., Dolder, M., Groscurth, P., & Ziegler, U. (2006). Cholesterol in negatively charged lipid bilayers modulates the effect of the antimicrobial protein granulysin. *The Journal of Membrane Biology*, *212*(1), 29–39. https://doi.org/10.1007/S00232-006-0040-3

Basak, S. K., Saha, B., Bhattacharya, A., & Roy, S. (1992). Immunobiological studies on experimental visceral leishmaniasis. II. Adherent cell-mediated

down-regulation of delayed-type hypersensitivity response and up-regulation of B cell activation. *European Journal of Immunology*, *22*(8), 2041–2045. https://doi.org/10.1002/EJI.1830220813

Basmaciyan, L., Azas, N., & Casanova, M. (2018). Different apoptosis pathways in Leishmania parasites. *Cell Death Discovery*, *4*(1), 4–6. https://doi.org/10.1038/s41420-018-0092-z

Basu, R., Bhaumik, S., Basu, J. M., Naskar, K., De, T., & Roy, S. (2005). Kinetoplastid Membrane Protein-11 DNA Vaccination Induces Complete Protection against Both Pentavalent Antimonial-Sensitive and -Resistant Strains of Leishmania donovani That Correlates with Inducible Nitric Oxide Synthase Activity and IL-4 Generation: Evidence for Mixed Th1- and Th2-Like Responses in Visceral Leishmaniasis. *The Journal of Immunology*, *174*(11), 7160–7171. https://doi.org/10.4049/JIMMUNOL.174.11.7160

Basu, R., Bhaumik, S., Haldar, A. K., Naskar, K., De, T., Dana, S. K., Walden, P., & Roy, S. (2007). Hybrid cell vaccination resolves Leishmania donovani infection by eliciting a strong CD8+ cytotoxic T-lymphocyte response with concomitant suppression of interleukin-10 (IL-10) but not IL-4 or IL-13. *Infection and Immunity*, *75*(12), 5956–5966. https://doi.org/10.1128/IAI.00944-07

Bates, P. A. (2008). Leishmania sand fly interaction: progress and challenges. *Current Opinion in Microbiology*, *11*(4), 340. https://doi.org/10.1016/J.MIB.2008.06.003

Becker, L., Liu, N. C., Averill, M. M., Yuan, W., Pamir, N., Peng, Y., Irwin, A. D., Fu, X., Bornfeldt, K. E., & Heinecke, J. W. (2012). Unique Proteomic Signatures Distinguish Macrophages and Dendritic Cells. *PLOS ONE*, *7*(3), e33297. https://doi.org/10.1371/JOURNAL.PONE.0033297

Belkaid, Y., Hoffmann, K. F., Mendez, S., Kamhawi, S., Udey, M. C., Wynn, T. A., & Sacks, D. L. (2001). The role of interleukin (IL)-10 in the persistence of Leishmania major in the skin after healing and the therapeutic potential of

anti-IL-10 receptor antibody for sterile cure. *The Journal of Experimental Medicine*, *194*(10), 1497–1506. https://doi.org/10.1084/JEM.194.10.1497

Belkaid, Y., Piccirillo, C. a, & Mendez, S. (2002). CD4+ CD25+ regulatory T cells control Leishmania major persistence and immunity. *Nature*, *420*(September), 633–637. https://doi.org/10.1038/nature01199.1.

Belkaid, Y., Von Stebut, E., Mendez, S., Lira, R., Caler, E., Bertholet, S., Udey, M. C., & Sacks, D. (2002). CD8+ T cells are required for primary immunity in C57BL/6 mice following low-dose, intradermal challenge with Leishmania major. *Journal of Immunology (Baltimore, Md. : 1950)*, *168*(8), 3992–4000. https://doi.org/10.4049/JIMMUNOL.168.8.3992

Belo, R., Santarém, N., Pereira, C., Pérez-Cabezas, B., Macedo, F., Leite-de-Moraes, M., & Cordeiro-da-Silva, A. (2017). Leishmania infantum exoproducts inhibit human invariant NKT cell expansion and activation. *Frontiers in Immunology*, *8*(JUN). https://doi.org/10.3389/fimmu.2017.00710

Besteiro, S., Williams, R. A. M., Morrison, L. S., Coombs, G. H., & Mottram, J. C. (2006). Endosome sorting and autophagy are essential for differentiation and virulence of Leishmania major. *Journal of Biological Chemistry*, *281*(16), 11384–11396. https://doi.org/10.1074/jbc.M512307200

Biedermann, T., Zimmermann, S., Himmelrich, H., Gumy, A., Egeter, O., Sakrauski, A. K., Seegmüller, I., Voigt, H., Launois, P., Levine, A. D., Wagner, H., Heeg, K., Louis, J. A., & Röcken, M. (2001). IL-4 instructs TH1 responses and resistance to Leishmania major in susceptible BALB/c mice. *Nature Immunology*, *2*(11), 1054–1060. https://doi.org/10.1038/NI725

Blanchette, J., Abu-Dayyeh, I., Hassani, K., Whitcombe, L., & Olivier, M. (2009). Regulation of macrophage nitric oxide production by the protein tyrosine phosphatase Src homology 2 domain phosphotyrosine phosphatase 1 (SHP-1). *Immunology*, *127*(1), 123. https://doi.org/10.1111/J.1365-2567.2008.02929.X

Blanchette, J., Racette, N., Faure, R., Siminovitch, K. A., & Olivier, M. (1999). Leishmania-induced increases in activation of macrophage SHP-1 tyrosine

phosphatase are associated with impaired IFN-γ-triggered JAK2 activation. *European Journal of Immunology*, *29*(11), 3737–3744. https://doi.org/10.1002/(SICI)1521-4141(199911)29:11<3737::AID-IMMU3737>3.0.CO;2-S

Boaventura, V. S., Santos, C. S., Cardoso, C. R., De Andrade, J., Dos Santos, W. L. C., Clarêncio, J., Silva, J. S., Borges, V. M., Barral-Netto, M., Brodskyn, C. I., & Barral, A. (2010). Human mucosal leishmaniasis: neutrophils infiltrate areas of tissue damage that express high levels of Th17-related cytokines. *European Journal of Immunology*, *40*(10), 2830–2836. https://doi.org/10.1002/EJI.200940115

Bogdan, C., Moll, H., Solbach, W., & Röllinghoff, M. (1990). Tumor necrosis factor-alpha in combination with interferon-gamma, but not with interleukin 4 activates murine macrophages for elimination of Leishmania major amastigotes. *European Journal of Immunology*, *20*(5), 1131–1135. https://doi.org/10.1002/EJI.1830200528

Brittingham, A., Morrison, C. J., McMaster, W. R., McGwire, B. S., Chang, K. P., & Mosser, D. M. (1995). Role of the Leishmania surface protease gp63 in complement fixation, cell adhesion, and resistance to complement-mediated lysis. *The Journal of Immunology*, *155*(6).

Brossay, L., Chioda, M., Burdin, N., Koezuka, Y., Casorati, G., Dellabona, P., & Kronenberg, M. (1998). CD1d-mediated recognition of an alpha-galactosylceramide by natural killer T cells is highly conserved through mammalian evolution. *The Journal of Experimental Medicine*, *188*(8), 1521–1528. https://doi.org/10.1084/JEM.188.8.1521

Buxbaum, L. U., & Scott, P. (2005). Interleukin 10- and Fcgamma receptor-deficient mice resolve Leishmania mexicana lesions. *Infection and Immunity*, *73*(4), 2101–2108. https://doi.org/10.1128/IAI.73.4.2101-2108.2005

Cameron, P., McGachy, A., Anderson, M., Paul, A., Coombs, G. H., Mottram, J. C., Alexander, J., & Plevin, R. (2004). Inhibition of lipopolysaccharide-

induced macrophage IL-12 production by Leishmania mexicana amastigotes: the role of cysteine peptidases and the NF-kappaB signaling pathway. *Journal of Immunology (Baltimore, Md. : 1950)*, *173*(5), 3297–3304. https://doi.org/10.4049/JIMMUNOL.173.5.3297

Castellano, Lucio Roberto, Argiro, L., Dessein, H., Dessein, A., Da Silva, M. V., Correia, D., & Rodrigues, V. (2015). Potential Use of Interleukin-10 Blockade as a Therapeutic Strategy in Human Cutaneous Leishmaniasis. *Journal of Immunology Research*, *2015*. https://doi.org/10.1155/2015/152741

Castellano, Lúcio Roberto, Filho, D. C., Argiro, L., Dessein, H., Prata, A., Dessein, A., & Rodrigues, V. (2009). Th1/Th2 immune responses are associated with active cutaneous leishmaniasis and clinical cure is associated with strong interferon-gamma production. *Human Immunology*, *70*(6), 383–390. https://doi.org/10.1016/J.HUMIMM.2009.01.007

Centers for Disease Control and Prevention. (2020). *CDC - Leishmaniasis - Epidemiology & Risk Factors*.

Chagas, A. C., Oliveira, F., Debrabant, A., Valenzuela, J. G., Ribeiro, J. M. C., & Calvo, E. (2014). Lundep, a Sand Fly Salivary Endonuclease Increases Leishmania Parasite Survival in Neutrophils and Inhibits XIIa Contact Activation in Human Plasma. *PLOS Pathogens*, *10*(2), e1003923. https://doi.org/10.1371/JOURNAL.PPAT.1003923

Chakraborty, D., Banerjee, S., Sen, A., Banerjee, K. K., Das, P., & Roy, S. (2005). Leishmania donovani affects antigen presentation of macrophage by disrupting lipid rafts. *Journal of Immunology (Baltimore, Md. : 1950)*, *175*(5), 3214–3224. https://doi.org/10.4049/JIMMUNOL.175.5.3214

Charmoy, Melanie, Hurrell, B. P., Romano, A., Lee, S. H., Ribeiro-Gomes, F., Riteau, N., Mayer-Barber, K., Tacchini-Cottier, F., & Sacks, D. L. (2016). The Nlrp3 inflammasome, IL-1β, and neutrophil recruitment are required for susceptibility to a nonhealing strain of Leishmania major in C57BL/6 mice. *European Journal of Immunology*, *46*(4), 897–911.

https://doi.org/10.1002/EJI.201546015

Charmoy, Mélanie, Megnekou, R., Allenbach, C., Zweifel, C., Perez, C., Monnat, K., Breton, M., Ronet, C., Launois, P., & Tacchini-Cottier, F. (2007). Leishmania major induces distinct neutrophil phenotypes in mice that are resistant or susceptible to infection. *Journal of Leukocyte Biology*, *82*(2), 288–299. https://doi.org/10.1189/JLB.0706440

Chatelain, R., Varkila, K., & Coffman, R. L. (1992). IL-4 induces a Th2 response in Leishmania major-infected mice. *The Journal of Immunology*, *148*(4).

Chaudhuri, G., & Chang, K. P. (1988). Acid protease activity of a major surface membrane glycoprotein (gp63) from Leishmania mexicana promastigotes. *Molecular and Biochemical Parasitology*, *27*(1), 43–52. https://doi.org/10.1016/0166-6851(88)90023-0

Chaves, M. M., Lee, S. H., Kamenyeva, O., Ghosh, K., Peters, N. C., & Sacks, D. (2020). The role of dermis resident macrophages and their interaction with neutrophils in the early establishment of Leishmania major infection transmitted by sand fly bite. *PLoS Pathogens*, *16*(11), 1–24. https://doi.org/10.1371/journal.ppat.1008674

Chen, J., Trounstine, M., Alt, F. W., Young, F., Kurahara, C., Loring, J. F., & Huszar, D. (1993). Immunoglobulin gene rearrangement in B cell deficient mice generated by targeted deletion of the JH locus. *International Immunology*, *5*(6), 647–656. https://doi.org/10.1093/INTIMM/5.6.647

Choudhuri, S., & Garg, N. J. (2020). PARP1-cGAS-NF-κB pathway of proinflammatory macrophage activation by extracellular vesicles released during Trypanosoma cruzi infection and Chagas disease. *PLOS Pathogens*, *16*(4), e1008474. https://doi.org/10.1371/JOURNAL.PPAT.1008474

Chu, N., Thomas, B. N., Patel, S. R., & Buxbaum, L. U. (2010). IgG1 Is Pathogenic in Leishmania mexicana Infection. *The Journal of Immunology*, *185*(11), 6939–6946. https://doi.org/10.4049/JIMMUNOL.1002484

Contreras, I., Gómez, M. A., Nguyen, O., Shio, M. T., McMaster, R. W., & Olivier, M. (2010). Leishmania-induced inactivation of the macrophage transcription factor AP-1 is mediated by the parasite metalloprotease GP63. *PLoS Pathogens*, *6*(10). https://doi.org/10.1371/JOURNAL.PPAT.1001148

Courret, N., Fréhel, C., Gouhier, N., Pouchelet, M., Prina, E., Roux, P., & Antoine, J. C. (2002). Biogenesis of Leishmania-harbouring parasitophorus vacuoles following phagocytosis of the metacyclic promastigote or amastigote stages of the parasites. *Journal of Cell Science*, *115*(11), 2303–2316.

Crauwels, P., Bohn, R., Thomas, M., Gottwalt, S., Jäckel, F., Krämer, S., Bank, E., Tenzer, S., Walther, P., Bastian, M., & Van Zandbergen, G. (2015). Apoptotic-like Leishmania exploit the host´s autophagy machinery to reduce T-cell-mediated parasite elimination. *Autophagy*, *11*(2), 285–297. https://doi.org/10.1080/15548627.2014.998904

Cuervo, P., Sabóia-Vahia, L., Costa Silva-Filho, F., Fernandes, O., Cupolillo, E., & De Jesus, J. B. (2006). A zymographic study of metalloprotease activities in extracts and extracellular secretions of Leishmania (Viannia) braziliensis strains. *Parasitology*, *132*(2), 177–185. https://doi.org/10.1017/S0031182005008942

Czop, J. K., & Kay, J. (1991). Isolation and characterization of β-glucan receptors on human mononuclear phagocytes. *Journal of Experimental Medicine*, *173*(6), 1511–1520. https://doi.org/10.1084/jem.173.6.1511

Das, S., Kumar, A., Mandal, A., Abhishek, K., Verma, S., Kumar, A., & Das, P. (2019). Nucleic acid sensing activates the innate cytosolic surveillance pathway and promotes parasite survival in visceral leishmaniasis. *Scientific Reports*, *9*(1), 1–19. https://doi.org/10.1038/s41598-019-45800-0

Das, S., Pandey, K., Kumar, A., Sardar, A. H., Purkait, B., Kumar, M., Kumar, S., Ravidas, V. N., Roy, S., Singh, D., & Das, P. (2012). TGF-β1 re-programs TLR4 signaling in L. donovani infection: enhancement of SHP-1 and ubiquitin-editing enzyme A20. *Immunology and Cell Biology*, *90*(6), 640–654.

https://doi.org/10.1038/ICB.2011.80

De Souza Leao, S., Lang, T., Prina, E., Hellio, R., & Antoine, J. C. (1995). Intracellular Leishmania amazonensis amastigotes internalize and degrade MHC class II molecules of their host cells. *Journal of Cell Science*, *108*(10), 3219–3231. https://doi.org/10.1242/JCS.108.10.3219

de Veer, M. J., Curtis, J. M., Baldwin, T. M., DiDonato, J. A., Sexton, A., McConville, M. J., Handman, E., & Schofield, L. (2003). MyD88 is essential for clearance of Leishmania major: possible role for lipophosphoglycan and Toll-like receptor 2 signaling. *European Journal of Immunology*, *33*(10), 2822–2831. https://doi.org/10.1002/EJI.200324128

de Waal Malefyt, R., Figdor, C. G., Huijbens, R., Mohan-Peterson, S., Bennett, B., Culpepper, J., Dang, W., Zurawski, G., & de Vries, J. E. (1993). Effects of IL-13 on phenotype, cytokine production, and cytotoxic function of human monocytes. Comparison with IL-4 and modulation by IFN-gamma or IL-10. *The Journal of Immunology*, *151*(11).

Decout, A., Katz, J. D., Venkatraman, S., & Ablasser, A. (2021). The cGAS–STING pathway as a therapeutic target in inflammatory diseases. *Nature Reviews Immunology*, *21*(9), 548–569. https://doi.org/10.1038/s41577-021-00524-z

Desjardins, M., & Descoteaux, A. (1997). Inhibition of phagolysosomal biogenesis by the Leishmania lipophosphoglycan. *Journal of Experimental Medicine*, *185*(12), 2061–2068. https://doi.org/10.1084/jem.185.12.2061

Doherty, T. M., Kastelein, R., Menon, S., Andrade, S., & Coffman, R. L. (1993). Modulation of murine macrophage function by IL-13. *The Journal of Immunology*, *151*(12).

Dostálová, A., & Volf, P. (2012). Leishmania development in sand flies: parasite-vector interactions overview. *Parasites & Vectors 2012 5:1*, *5*(1), 1–12. https://doi.org/10.1186/1756-3305-5-276

Dotiwala, F., Mulik, S., Polidoro, R. B., Ansara, J. A., Burleigh, B. A., Walch, M., Gazzinelli, R. T., & Lieberman, J. (2016). Killer lymphocytes use granulysin, perforin and granzymes to kill intracellular parasites. *Nature Medicine*, *22*(2), 210–216. https://doi.org/10.1038/nm.4023

Ebrahimpoor, S., Pakzad, S.-R., & Ajdary, S. (2013). IgG1 and IgG2a Profile of Serum Antibodies to Leishmania major Amastigote in BALB/c and C57BL/6Mice. *Iranian Journal of Allergy, Asthma and Immunology*, *12*(4), 361–367. https://ijaai.tums.ac.ir/index.php/ijaai/article/view/491

Èphanie Honore, S., Jean-Franc, Y., Ois Garin, °, Sulahian, A., Gangneux, J.-P., & Derouin, F. (1998). Influence of the host and parasite strain in a mouse model of visceral Leishmania infantum infection. *FEMS Immunology & Medical Microbiology*, *21*(3), 231–239. https://doi.org/10.1111/J.1574-695X.1998.TB01170.X

Faria, M. S., Reis, F. C. G., Azevedo-Pereira, R. L., Morrison, L. S., Mottram, J. C., & Lima, A. P. C. A. (2011). Leishmania inhibitor of serine peptidase prevents TLR4 activation by neutrophil elastase promoting parasite survival in murine macrophages. *Journal of Immunology (Baltimore, Md. : 1950)*, *186*(1), 411. https://doi.org/10.4049/JIMMUNOL.1002175

Faulkner, H., Renauld, J. C., Van Snick, J., & Grencis, R. K. (1998). Interleukin-9 enhances resistance to the intestinal nematode Trichuris muris. *Infection and Immunity*, *66*(8), 3832–3840. https://doi.org/10.1128/IAI.66.8.3832-3840.1998

Felipe, I., Bochio, E. E., Martins, N. B., & Pacheco, C. (1991). Inhibition of macrophage phagocytosis of Escherichia coli by mannose and mannan. *Brazilian Journal of Medical and Biological Research*, *24*(9), 919–924. https://pubmed.ncbi.nlm.nih.gov/1797285/

Finkelman, F. D., Holmes, J., Katona, I. M., Urban, J. F., Beckmann, M. P., Park, L. S., Schooley, K. A., Coffman, R. L., Mosmann, T. R., & Paul, W. E. (1990). Lymphokine control of in vivo immunoglobulin isotype selection.

Annual Review of Immunology, *8*, 303–330. https://doi.org/10.1146/ANNUREV.IY.08.040190.001511

Follador, I., Araújo, C., Bacellar, O., Araújo, C. B., Carvalho, L. P., Almeida, R. P., & Carvalho, E. M. (2002). Epidemiologic and immunologic findings for the subclinical form of Leishmania braziliensis infection. *Clinical Infectious Diseases : An Official Publication of the Infectious Diseases Society of America*, *34*(11). https://doi.org/10.1086/340261

Forget, G., Gregory, D. J., & Olivier, M. (2005). Proteasome-mediated degradation of STAT1alpha following infection of macrophages with Leishmania donovani. *The Journal of Biological Chemistry*, *280*(34), 30542–30549. https://doi.org/10.1074/JBC.M414126200

Fruth, U., Solioz, N., & Louis, J. A. (1993). Leishmania major interferes with antigen presentation by infected macrophages. *The Journal of Immunology*, *150*(5).

Fu, Y. L., & Harrison, R. E. (2021). Microbial Phagocytic Receptors and Their Potential Involvement in Cytokine Induction in Macrophages. *Frontiers in Immunology*, *12*(April). https://doi.org/10.3389/fimmu.2021.662063

Gabriel, C., McMaster, W. R., Girard, D., & Descoteaux, A. (2010). Leishmania donovani Promastigotes Evade the Antimicrobial Activity of Neutrophil Extracellular Traps. *The Journal of Immunology*, *185*(7), 4319–4327. https://doi.org/10.4049/JIMMUNOL.1000893

Gallo, P., Gonçalves, R., & Mosser, D. M. (2010). The influence of IgG Density and Macrophage Fc (gamma) Receptor Cross-linking on Phagocytosis and IL-10 Production. *Immunology Letters*, *133*(2), 70. https://doi.org/10.1016/J.IMLET.2010.07.004

Gaur, U., Roberts, S. C., Dalvi, R. P., Corraliza, I., Ullman, B., & Wilson, M. E. (2007). An Effect of Parasite-Encoded Arginase on the Outcome of Murine Cutaneous Leishmaniasis. *The Journal of Immunology*, *179*(12), 8446–8453. https://doi.org/10.4049/JIMMUNOL.179.12.8446

Gawish, R., Martins, R., Böhm, B., Wimberger, T., Sharif, O., Lakovits, K., Schmidt, M., & Knapp, S. (2015). Triggering receptor expressed on myeloid cells-2 fine-tunes inflammatory responses in murine Gram-negative sepsis. *FASEB Journal : Official Publication of the Federation of American Societies for Experimental Biology*, *29*(4), 1247–1257. https://doi.org/10.1096/FJ.14-260067

Gessner, A., Blum, H., & Röllinghoff, M. (1993). Differential regulation of IL-9-expression after infection with Leishmania major in susceptible and resistant mice. *Immunobiology*, *189*(5), 419–435. https://doi.org/10.1016/S0171-2985(11)80414-6

Gicheru, M. M., Olobo, J. O., Anjili, C. O., Orago, A. S., Modabber, F., & Scott, P. (2001). Vervet monkeys vaccinated with killed Leishmania major parasites and interleukin-12 develop a type 1 immune response but are not protected against challenge infection. *Infection and Immunity*, *69*(1), 245–251. https://doi.org/10.1128/IAI.69.1.245-251.2001

Gimblet, C., Loesche, M. A., Carvalho, L., Carvalho, E. M., Grice, E. A., Artis, D., & Scott, P. (2015). IL-22 Protects against Tissue Damage during Cutaneous Leishmaniasis. *PLOS ONE*, *10*(8), e0134698. https://doi.org/10.1371/JOURNAL.PONE.0134698

Goldman, R. (1988). Characteristics of the beta-glucan receptor of murine macrophages. *Experimental Cell Research*, *174*(2), 481–490. https://doi.org/10.1016/0014-4827(88)90317-5

Gomes-Silva, A., De Cássia Bittar, R., Dos Santos Nogueira, R., Amato, V. S., Da Silva Mattos, M., Oliveira-Neto, M. P., Coutinho, S. G., & Da-Cruz, A. M. (2007). Can interferon-γ and interleukin-10 balance be associated with severity of human Leishmania (Viannia) braziliensis infection? *Clinical and Experimental Immunology*, *149*(3), 440. https://doi.org/10.1111/J.1365-2249.2007.03436.X

Gomez, M. A., Contreras, I., Hallé, M., Tremblay, M. L., McMaster, R. W., &

Olivier, M. (2009). Leishmania GP63 alters host signaling through cleavage-activated protein tyrosine phosphatases. *Science Signaling*, *2*(90), 1–13. https://doi.org/10.1126/scisignal.2000213

Goncalves, R., Christensen, S. M., & Mosser, D. M. (2020). Humoral immunity in leishmaniasis – Prevention or promotion of parasite growth? *Cytokine: X*, *2*(4), 100046. https://doi.org/10.1016/j.cytox.2020.100046

Goncalves, R., Zhang, X., Cohen, H., Debrabant, A., & Mosser, D. M. (2011). Platelet activation attracts a subpopulation of effector monocytes to sites of Leishmania major infection. *The Journal of Experimental Medicine*, *208*(6), 1253. https://doi.org/10.1084/JEM.20101751

Gonzalez-Lombana, C., Gimblet, C., Bacellar, O., Oliveira, W. W., Passos, S., Carvalho, L. P., Goldschmidt, M., Carvalho, E. M., & Scott, P. (2013). IL-17 mediates immunopathology in the absence of IL-10 following Leishmania major infection. *PLoS Pathogens*, *9*(3). https://doi.org/10.1371/JOURNAL.PPAT.1003243

González, C., Wang, O., Strutz, S. E., González-Salazar, C., Sánchez-Cordero, V., & Sarkar, S. (2010). Climate Change and Risk of Leishmaniasis in North America: Predictions from Ecological Niche Models of Vector and Reservoir Species. *PLOS Neglected Tropical Diseases*, *4*(1), e585. https://doi.org/10.1371/JOURNAL.PNTD.0000585

Gordon, S. (2003). Alternative activation of macrophages. *Nature Reviews. Immunology*, *3*(1), 23–35. https://doi.org/10.1038/NRI978

Gossage, S. M., Rogers, M. E., & Bates, P. A. (2003). Two separate growth phases during the development of Leishmania in sand flies: implications for understanding the life cycle. *International Journal for Parasitology*, *33*(10), 1027. https://doi.org/10.1016/S0020-7519(03)00142-5

Gregory, D. J., Godbout, M., Contreras, I., Forget, G., & Olivier, M. (2008). A novel form of NF-kappaB is induced by Leishmania infection: involvement in macrophage gene expression. *European Journal of Immunology*, *38*(4), 1071–

1081. https://doi.org/10.1002/EJI.200737586

Griewank, K. G., Lorenz, B., Fischer, M. R., Boon, L., Lopez Kostka, S., & von Stebut, E. (2014). Immune Modulating Effects of NKT Cells in a Physiologically Low Dose Leishmania major Infection Model after αGalCer Analog PBS57 Stimulation. *PLoS Neglected Tropical Diseases*, *8*(6). https://doi.org/10.1371/journal.pntd.0002917

Guilliams, M., Bruhns, P., Saeys, Y., Hammad, H., & Lambrecht, B. N. (2014). The function of Fcγ receptors in dendritic cells and macrophages. *Nature Reviews Immunology 2014 14:2*, *14*(2), 94–108. https://doi.org/10.1038/nri3582

Guimarães-Costa, A. B., Nascimento, M. T. C., Froment, G. S., Soares, R. P. P., Morgado, F. N., Conceição-Silva, F., & Saraiva, E. M. (2009). Leishmania amazonensis promastigotes induce and are killed by neutrophil extracellular traps. *Proceedings of the National Academy of Sciences of the United States of America*, *106*(16), 6748–6753. https://doi.org/10.1073/PNAS.0900226106

Haldar, J. P., Ghose, S., Saha, K. C., & Ghose, A. C. (1983). Cell-mediated immune response in Indian kala-azar and post-kala-azar dermal leishmaniasis. *Infection and Immunity*, *42*(2), 702. https://doi.org/10.1128/iai.42.2.702-707.1983

Harrington, V., & Gurung, P. (2020). Reconciling protective and pathogenic roles of the NLRP3 inflammasome in leishmaniasis. *Immunological Reviews*, *297*(1), 53. https://doi.org/10.1111/IMR.12886

Harrison, A. P., & Pelczar, M. J. (1963). Damage and survival of bacteria during freeze-drying and during storage over a ten-year period. *Journal of General Microbiology*, *30*(3), 395–400. https://doi.org/10.1099/00221287-30-3-395/CITE/REFWORKS

Hassani, K., Shio, M. T., Martel, C., Faubert, D., & Olivier, M. (2014). Absence of Metalloprotease GP63 Alters the Protein Content of Leishmania Exosomes. *PLOS ONE*, *9*(4), e95007. https://doi.org/10.1371/JOURNAL.PONE.0095007

Heinzel, F. P., Rerko, R. M., Hatam, F., & Locksley, R. M. (1993). IL-2 is necessary for the progression of leishmaniasis in susceptible murine hosts. *The Journal of Immunology*, *150*(9).

Heinzel, F. P., Sadick, M. D., Holaday, B. J., Coffman, R. L., & Locksley, R. M. (1989). Reciprocal expression of interferon gamma or interleukin 4 during the resolution or progression of murine leishmaniasis. Evidence for expansion of distinct helper T cell subsets. *The Journal of Experimental Medicine*, *169*(1), 59–72. https://doi.org/10.1084/JEM.169.1.59

Heinzel, F. P., Sadick, M. D., Mutha, S. S., & Locksley, R. M. (1991). Production of interferon gamma, interleukin 2, interleukin 4, and interleukin 10 by CD4+ lymphocytes in vivo during healing and progressive murine leishmaniasis. *Proceedings of the National Academy of Sciences of the United States of America*, *88*(16), 7011–7015. https://doi.org/10.1073/PNAS.88.16.7011

Heinzel, F. P., Schoenhaut, D. S., Rerko, R. M., Rosser, L. E., & Gately, M. K. (1993). Recombinant interleukin 12 cures mice infected with Leishmania major. *The Journal of Experimental Medicine*, *177*(5), 1505–1509. https://doi.org/10.1084/JEM.177.5.1505

Hermoso, T., Fishelson, Z., Becker, S. I., Hirschberg, K., & Jaffe, C. L. (1991). Leishmanial protein kinases phosphorylate components of the complement system. *The EMBO Journal*, *10*(13), 4061. https://doi.org/10.1002/j.1460-2075.1991.tb04982.x

Hesse, M., Modolell, M., La Flamme, A. C., Schito, M., Fuentes, J. M., Cheever, A. W., Pearce, E. J., & Wynn, T. A. (2001). Differential regulation of nitric oxide synthase-2 and arginase-1 by type 1/type 2 cytokines in vivo: granulomatous pathology is shaped by the pattern of L-arginine metabolism. *Journal of Immunology (Baltimore, Md. : 1950)*, *167*(11), 6533–6544. https://doi.org/10.4049/JIMMUNOL.167.11.6533

Hezarjaribi, H. Z., Ghaffarifar, F., Dalimi, A., & Sharifi, Z. (2014). Evaluation of protective effect of IL-22 and IL-12 on cutaneous leishmaniasis in BALB/c

mice. *Asian Pacific Journal of Tropical Medicine*, *7*(12), 940–945. https://doi.org/10.1016/S1995-7645(14)60166-8

Hisaeda, H, Sakai, T., Ishikawa, H., Maekawa, Y., Yasutomo, K., Good, R. A., & Himeno, K. (1997). Heat shock protein 65 induced by gammadelta T cells prevents apoptosis of macrophages and contributes to host defense in mice infected with Toxoplasma gondii. *The Journal of Immunology*, *159*(5).

Hisaeda, Hajime, & Himeno, K. (1997). The role of host-derived heat-shock protein in immunity against Toxoplasma gondii infection. *Parasitology Today (Personal Ed.)*, *13*(12), 465–468. https://doi.org/10.1016/S0169-4758(97)01128-9

Holm, Å., Tejle, K., Magnusson, K. E., Descoteaux, A., & Rasmusson, B. (2001). Leishmania donovani lipophosphoglycan causes periphagosomal actin accumulation: correlation with impaired translocation of PKCα and defective phagosome maturation. *Cellular Microbiology*, *3*(7), 439–447. https://doi.org/10.1046/J.1462-5822.2001.00127.X

Hölscher, C., Arendse, B., Schwegmann, A., Myburgh, E., & Brombacher, F. (2006). Impairment of Alternative Macrophage Activation Delays Cutaneous Leishmaniasis in Nonhealing BALB/c Mice. *The Journal of Immunology*, *176*(2), 1115–1121. https://doi.org/10.4049/JIMMUNOL.176.2.1115

Hsiao, C. H. C., Yao, C., Storlie, P., Donelson, J. E., & Wilson, M. E. (2008). The major surface protease (MSP or GP63) in the intracellular amastigote stage of Leishmania chagasi. *Molecular and Biochemical Parasitology*, *157*(2), 148–159. https://doi.org/10.1016/J.MOLBIOPARA.2007.10.008

Hurrell, B. P., Schuster, S., Grün, E., Coutaz, M., Williams, R. A., Held, W., Malissen, B., Malissen, M., Yousefi, S., Simon, H. U., Müller, A. J., & Tacchini-Cottier, F. (2015). Rapid Sequestration of Leishmania mexicana by Neutrophils Contributes to the Development of Chronic Lesion. *PLOS Pathogens*, *11*(5), e1004929. https://doi.org/10.1371/JOURNAL.PPAT.1004929

Ishikawa, H., Hisaeda, H., Taniguchi, M., Nakayama, T., Sakai, T., Maekawa, Y., Nakano, Y., Zhang, M., Zhang, T., Nishitani, M., Takashima, M., & Himeno, K. (2000). CD4+ Vα14 NKT cells play a crucial role in an early stage of protective immunity against infection with Leishmania major. *International Immunology*, *12*(9), 1267–1274. https://doi.org/10.1093/intimm/12.9.1267

Isnard, A., Shio, M. T., & Olivier, M. (2012). Impact of Leishmania metalloprotease GP63 on macrophage signaling. *Frontiers in Cellular and Infection Microbiology*, *2*, 72. https://doi.org/10.3389/FCIMB.2012.00072/BIBTEX

Jablonski, K. A., Amici, S. A., Webb, L. M., Ruiz-Rosado, J. D. D., Popovich, P. G., Partida-Sanchez, S., & Guerau-De-arellano, M. (2015). Novel Markers to Delineate Murine M1 and M2 Macrophages. *PLOS ONE*, *10*(12), e0145342. https://doi.org/10.1371/JOURNAL.PONE.0145342

Jaramillo, M., Gomez, M. A., Larsson, O., Shio, M. T., Topisirovic, I., Contreras, I., Luxenburg, R., Rosenfeld, A., Colina, R., McMaster, R. W., Olivier, M., Costa-Mattioli, M., & Sonenberg, N. (2011). Leishmania repression of host translation through mTOR cleavage is required for parasite survival and infection. *Cell Host and Microbe*, *9*(4), 331–341. https://doi.org/10.1016/j.chom.2011.03.008

Jerry, L. M., Rowden, G., Cano, P. O., Phillips, T. M., Deutsch, G. F., Capek, A., Hartmann, D., & Lewis, M. G. (1976). Immune complexes in human melanoma: a consequence of deranged immune regulation. *Scandinavian Journal of Immunology*, *5*(6–7), 845–859. https://doi.org/10.1111/J.1365-3083.1976.TB03034.X

Joshi, P. B., Kelly, B. L., Kamhawi, S., Sacks, D. L., & McMaster, W. R. (2002). Targeted gene deletion in Leishmania major identifies leishmanolysin (GP63) as a virulence factor. *Molecular and Biochemical Parasitology*, *120*(1), 33–40. https://doi.org/10.1016/S0166-6851(01)00432-7

Joshi, P. B., Sacks, D. L., Modi, G., & McMaster, W. R. (1998). Targeted gene

deletion of Leishmania major genes encoding developmental stage-specific leishmanolysin (GP63). *Molecular Microbiology*, *27*(3), 519–530. https://doi.org/10.1046/J.1365-2958.1998.00689.X

Kaplan, H. J., & Streilein, J. W. (1977). Immune Response to Immunization Via the Anterior Chamber of the Eye. *The Journal of Immunology*, *118*(3).

Karmakar, S., Bhaumik, S. K., Paul, J., & De, T. (2012). TLR4 and NKT cell synergy in immunotherapy against visceral leishmaniasis. *PLoS Pathogens*, *8*(4). https://doi.org/10.1371/JOURNAL.PPAT.1002646

Karmakar, S., Paul, J., & De, T. (2011). Leishmania donovani glycosphingolipid facilitates antigen presentation by inducing relocation of CD1d into lipid rafts in infected macrophages. *European Journal of Immunology*, *41*(5), 1376–1387. https://doi.org/10.1002/EJI.201040981

Kenney, R. T., Sacks, D. L., Sypek, J. P., Vilela, L., Gam, A. A., & Evans-Davis, K. (1999). Protective immunity using recombinant human IL-12 and alum as adjuvants in a primate model of cutaneous leishmaniasis. *Journal of Immunology (Baltimore, Md. : 1950)*, *163*(8), 4481–4488. http://www.ncbi.nlm.nih.gov/pubmed/10510390

Khouri, R., Bafica, A., Silva, M. da P. P., Noronha, A., Kolb, J.-P., Wietzerbin, J., Barral, A., Barral-Netto, M., & Van Weyenbergh, J. (2009). IFN-β Impairs Superoxide-Dependent Parasite Killing in Human Macrophages: Evidence for a Deleterious Role of SOD1 in Cutaneous Leishmaniasis. *The Journal of Immunology*, *182*(4), 2525–2531. https://doi.org/10.4049/jimmunol.0802860

Kima, P. E., Constant, S. L., Hannum, L., Colmenares, M., Lee, K. S., Haberman, A. M., Shlomchik, M. J., & McMahon-Pratt, D. (2000). Internalization of Leishmania mexicana complex amastigotes via the Fc receptor is required to sustain infection in murine cutaneous leishmaniasis. *The Journal of Experimental Medicine*, *191*(6), 1063–1067. https://doi.org/10.1084/JEM.191.6.1063

Kima, P. E., Soong, L., Chicharro, C., Ruddle, N. H., & McMahon-Pratt, D.

(1996). Leishmania-infected macrophages sequester endogenously synthesized parasite antigens from presentation to CD4+ T cells. *European Journal of Immunology*, *26*(12), 3163–3169. https://doi.org/10.1002/EJI.1830261249

Kostka, S. L., Dinges, S., Griewank, K., Iwakura, Y., Udey, M. C., & Stebut, E. von. (2009). IL-17 promotes progression of cutaneous leishmaniasis in susceptible mice. *Journal of Immunology (Baltimore, Md. : 1950)*, *182*(5), 3039. https://doi.org/10.4049/JIMMUNOL.0713598

Kropf, P., Herath, S., Weber, V., Modolell, M., & Müller, I. (2003). Factors influencing Leishmania major infection in IL-4-deficient BALB/c mice. *Parasite Immunology*, *25*(8–9), 439–447. https://doi.org/10.1111/J.1365-3024.2003.00655.X

Kropf, Pascale, Fuentes, J. M., Fähnrich, E., Arpa, L., Herath, S., Weber, V., Soler, G., Celada, A., Modolell, M., & Müller, I. (2005). Arginase and polyamine synthesis are key factors in the regulation of experimental leishmaniasis in vivo. *FASEB Journal : Official Publication of the Federation of American Societies for Experimental Biology*, *19*(8), 1000–1002. https://doi.org/10.1096/FJ.04-3416FJE

Krovi, S. H., & Gapin, L. (2018). Invariant natural killer T cell subsets-more than just developmental intermediates. *Frontiers in Immunology*, *9*(JUN), 1–17. https://doi.org/10.3389/fimmu.2018.01393

Kulkarni, M. M., McMaster, W. R., Kamysz, E., Kamysz, W., Engman, D. M., & McGwire, B. S. (2006). The major surface-metalloprotease of the parasitic protozoan, Leishmania, protects against antimicrobial peptide-induced apoptotic killing. *Molecular Microbiology*, *62*(5), 1484–1497. https://doi.org/10.1111/J.1365-2958.2006.05459.X

Kumar, R., Bunn, P. T., Singh, S. S., Ng, S. S., Montes de Oca, M., De Labastida Rivera, F., Chauhan, S. B., Singh, N., Faleiro, R. J., Edwards, C. L., Frame, T. C. M., Sheel, M., Austin, R. J., Lane, S. W., Bald, T., Smyth, M. J., Hill, G.

R., Best, S. E., Haque, A., … Engwerda, C. R. (2020). Type I Interferons Suppress Anti-parasitic Immunity and Can Be Targeted to Improve Treatment of Visceral Leishmaniasis. *Cell Reports*, *30*(8), 2512-2525.e9. https://doi.org/10.1016/j.celrep.2020.01.099

Landriscina, M., Prudovsky, I., Carreira, C. M., Soldi, R., Tarantini, F., & Maciag, T. (2000). Amlexanox reversibly inhibits cell migration and proliferation and induces the Src-dependent disassembly of actin stress fibers in vitro. *Journal of Biological Chemistry*, *275*(42), 32753–32762. https://doi.org/10.1074/jbc.M002336200

Lécuyer, M. A., Saint-Laurent, O., Bourbonnière, L., Larouche, S., Larochelle, C., Michel, L., Charabati, M., Abadier, M., Zandee, S., Jahromi, N. H., Gowing, E., Pittet, C., Lyck, R., Engelhardt, B., & Prat, A. (2017). Dual role of ALCAM in neuroinflammation and blood-brain barrier homeostasis. *Proceedings of the National Academy of Sciences of the United States of America*, *114*(4), E524–E533. https://doi.org/10.1073/PNAS.1614336114/-/DCSUPPLEMENTAL

Liehl, P., Zuzarte-Luís, V., Chan, J., Zillinger, T., Baptista, F., Carapau, D., Konert, M., Hanson, K. K., Carret, C., Lassnig, C., Müller, M., Kalinke, U., Saeed, M., Chora, A. F., Golenbock, D. T., Strobl, B., Prudêncio, M., Coelho, L. P., Kappe, S. H., … Mota, M. M. (2014). Host-cell sensors for Plasmodium activate innate immunity against liver-stage infection. *Nature Medicine*, *20*(1), 47–53. https://doi.org/10.1038/NM.3424

Lieke, T., Nyln, S., Eidsmo, L., Schmetz, C., Berg, L., & Akuffo, H. (2011). The interplay between Leishmania promastigotes and human Natural Killer cells in vitro leads to direct lysis of Leishmania by NK cells and modulation of NK cell activity by Leishmania promastigotes. *Parasitology*, *138*(14), 1898–1909. https://doi.org/10.1017/S0031182011001363

Liew, F. Y., Wei, X. Q., & Proudfoot, L. (1997). Cytokines and nitric oxide as effector molecules against parasitic infections. *Philosophical Transactions of*

the Royal Society B: Biological Sciences, *352*(1359), 1311. https://doi.org/10.1098/RSTB.1997.0115

Lodge, R., & Descoteaux, A. (2005a). Leishmania donovani promastigotes induce periphagosomal F-actin accumulation through retention of the GTPase Cdc42. *Cellular Microbiology*, *7*(11), 1647–1658. https://doi.org/10.1111/j.1462-5822.2005.00582.x

Lodge, R., & Descoteaux, A. (2005b). Modulation of phagolysosome biogenesis by the lipophosphoglycan of Leishmania. *Clinical Immunology*, *114*(3 SPEC. ISS.), 256–265. https://doi.org/10.1016/j.clim.2004.07.018

Macho-Fernandez, E., & Brigl, M. (2015). The Extended Family of CD1d-Restricted NKT Cells: Sifting through a Mixed Bag of TCRs, Antigens, and Functions. *Frontiers in Immunology*, *0*(JUL), 362. https://doi.org/10.3389/FIMMU.2015.00362

Majumdar, T., Chattopadhyay, S., Ozhegov, E., Dhar, J., Goswami, R., Sen, G. C., & Barik, S. (2015). Induction of Interferon-Stimulated Genes by IRF3 Promotes Replication of Toxoplasma gondii. *PLoS Pathogens*, *11*(3), 1–22. https://doi.org/10.1371/journal.ppat.1004779

Mann, S., Frasca, K., Scherrer, S., Henao-Martínez, A. F., Newman, S., Ramanan, P., & Suarez, J. A. (2021). A Review of Leishmaniasis: Current Knowledge and Future Directions. *Current Tropical Medicine Reports*, *8*(2), 121–132. https://doi.org/10.1007/s40475-021-00232-7

Marth, T., & Kelsall, B. L. (1997). Regulation of interleukin-12 by complement receptor 3 signaling. *The Journal of Experimental Medicine*, *185*(11), 1987–1995. https://doi.org/10.1084/JEM.185.11.1987

Martin, P., & Leibovich, S. J. (2005). Inflammatory cells during wound repair: the good, the bad and the ugly. *Trends in Cell Biology*, *15*(11), 599–607. https://doi.org/10.1016/J.TCB.2005.09.002

Matheoud, D., Moradin, N., Bellemare-Pelletier, A., Shio, M. T., Hong, W. J.,

Olivier, M., Gagnon, É., Desjardins, M., & Descoteaux, A. (2013). Leishmania evades host immunity by inhibiting antigen cross-presentation through direct cleavage of the SNARE VAMP8. *Cell Host and Microbe, 14*(1), 15–25. https://doi.org/10.1016/j.chom.2013.06.003

Matte, C., Casgrain, P. A., Séguin, O., Moradin, N., Hong, W. J., & Descoteaux, A. (2016). Leishmania major Promastigotes Evade LC3-Associated Phagocytosis through the Action of GP63. *PLoS Pathogens*, *12*(6), 1–17. https://doi.org/10.1371/journal.ppat.1005690

Matthews, D. J., Emson, C. L., McKenzie, G. J., Jolin, H. E., Blackwell, J. M., & McKenzie, A. N. J. (2000). IL-13 Is a Susceptibility Factor for Leishmania major Infection. *The Journal of Immunology*, *164*(3), 1458–1462. https://doi.org/10.4049/JIMMUNOL.164.3.1458

Mattner, J., Donhauser, N., Werner-Felmayer, G., & Bogdan, C. (2006). NKT cells mediate organ-specific resistance against Leishmania major infection. *Microbes and Infection*, *8*(2), 354–362. https://doi.org/10.1016/j.micinf.2005.07.002

Maurya, R., Mehrotra, S., Prajapati, V. K., Nylén, S., Sacks, D., & Sundar, S. (2010). Evaluation of blood agar microtiter plates for culturing Leishmania parasites to titrate parasite burden in spleen and peripheral blood of patients with visceral leishmaniasis. *Journal of Clinical Microbiology*, *48*(5), 1932–1934. https://doi.org/10.1128/JCM.01733-09

Mbow, M. L., Dekrey, G. K., & Titus, R. G. (2001). Leishmania major induces differential expression of costimulatory molecules on mouse epidermal cells. *European Journal of Immunology*, *31*, 1400–1409. https://doi.org/10.1002/1521-4141(200105)31:5<1400::AID-IMMU1400>3.0.CO;2-J

McCurley, T. L., Abe, T., Carter, C. E., & Colley, D. G. (1986). Studies of tolerance in schistosomiasis. *Cellular Immunology, 99*(2), 411–421. https://doi.org/10.1016/0008-8749(86)90249-2

McFarlane, E., Carter, K. C., McKenzie, A. N., Kaye, P. M., Brombacher, F., & Alexander, J. (2011). Endogenous IL-13 Plays a Crucial Role in Liver Granuloma Maturation During Leishmania donovani Infection, Independent of IL-4Rα–Responsive Macrophages and Neutrophils. *The Journal of Infectious Diseases*, *204*(1), 36–43. https://doi.org/10.1093/INFDIS/JIR080

McMahon-Pratt, D., & Alexander, J. (2004). Does the Leishmania major paradigm of pathogenesis and protection hold for New World cutaneous leishmaniases or the visceral disease? *Immunological Reviews*, *201*, 206–224. https://doi.org/10.1111/J.0105-2896.2004.00190.X

Michel, M.-L., Mendes-da-Cruz, D., Keller, A. C., Lochner, M., Schneider, E., Dy, M., Eberl, G., & Leite-de-Moraes, M. C. (2008). Critical role of ROR-γt in a new thymic pathway leading to IL-17-producing invariant NKT cell differentiation. *Proceedings of the National Academy of Sciences*, *105*(50), 19845–19850. https://doi.org/10.1073/PNAS.0806472105

Miles, S. A., Conrad, S. M., Alves, R. G., Jeronimo, S. M. B., & Mosser, D. M. (2005). A role for IgG immune complexes during infection with the intracellular pathogen Leishmania. *Journal of Experimental Medicine*, *201*(5), 747–754. https://doi.org/10.1084/jem.20041470

Miyamoto-Shinohara, Y., Imaizumi, T., Sukenobe, J., Murakami, Y., Kawamura, S., & Komatsu, Y. (2000). Survival Rate of Microbes after Freeze-Drying and Long-Term Storage. *Cryobiology*, *41*(3), 251–255. https://doi.org/10.1006/CRYO.2000.2282

Mohrs, M., Ledermann, B., Köhler, G., Dorfmüller, A., Gessner, A., & Brombacher, F. (1999). Differences between IL-4- and IL-4 receptor alpha-deficient mice in chronic leishmaniasis reveal a protective role for IL-13 receptor signaling. *Journal of Immunology (Baltimore, Md. : 1950)*, *162*(12), 7302–7308. http://www.ncbi.nlm.nih.gov/pubmed/10358179

Moreira-Teixeira, L., Resende, M., Coffre, M., Devergne, O., Herbeuval, J.-P., Hermine, O., Schneider, E., Rogge, L., Ruemmele, F. M., Dy, M., Cordeiro-

da-Silva, A., & Leite-de-Moraes, M. C. (2011). Proinflammatory Environment Dictates the IL-17–Producing Capacity of Human Invariant NKT Cells. *The Journal of Immunology*, *186*(10), 5758–5765. https://doi.org/10.4049/JIMMUNOL.1003043

Moreira-Teixeira, L., Resende, M., Devergne, O., Herbeuval, J.-P., Hermine, O., Schneider, E., Dy, M., Cordeiro-da-Silva, A., & Leite-de-Moraes, M. C. (2012). Rapamycin Combined with TGF-β Converts Human Invariant NKT Cells into Suppressive Foxp3+ Regulatory Cells. *The Journal of Immunology*, *188*(2), 624–631. https://doi.org/10.4049/JIMMUNOL.1102281

Müller, K., Zandbergen, G., Hansen, B., Laufs, H., Jahnke, N., Solbach, W., & Laskay, T. (2001). Chemokines, natural killer cells and granulocytes in the early course of Leishmania major infection in mice. *Medical Microbiology and Immunology*, *190*(1–2), 73–76. https://doi.org/10.1007/S004300100084

Munder, M., Eichmann, K., & Modolell, M. (1998). Alternative Metabolic States in Murine Macrophages Reflected by the Nitric Oxide Synthase/Arginase Balance: Competitive Regulation by CD4 + T Cells Correlates with Th1/Th2 Phenotype. *The Journal of Immunology*, *160*(11), 5347–5354.

Muxel, S. M., Aoki, J. I., Fernandes, J. C. R., Laranjeira-Silva, M. F., Zampieri, R. A., Acuña, S. M., Müller, K. E., Vanderlinde, R. H., & Floeter-Winter, L. M. (2018). Arginine and polyamines fate in leishmania infection. *Frontiers in Microbiology*, *8*(JAN), 2682. https://doi.org/10.3389/FMICB.2017.02682/BIBTEX

Nandakumar, R., Tschismarov, R., Meissner, F., Prabakaran, T., Krissanaprasit, A., Farahani, E., Zhang, B. cun, Assil, S., Martin, A., Bertrams, W., Holm, C. K., Ablasser, A., Klause, T., Thomsen, M. K., Schmeck, B., Howard, K. A., Henry, T., Gothelf, K. V., Decker, T., & Paludan, S. R. (2019). Intracellular bacteria engage a STING–TBK1–MVB12b pathway to enable paracrine cGAS–STING signalling. In *Nature Microbiology* (Vol. 4, Issue 4). https://doi.org/10.1038/s41564-019-0367-z

Nashed, B. F., Maekawa, Y., Takashima, M., Zhang, T., Ishii, K., Dainichi, T., Ishikawa, H., Sakai, T., Hisaeda, H., & Himeno, K. (2000). Different cytokines are required for induction and maintenance of the Th2 type response in DBA/2 mice resistant to infection with Leishmania major. *Microbes and Infection*, *2*(12), 1435–1443. https://doi.org/10.1016/S1286-4579(00)01298-3

Natori, T., Morita, M., Akimoto, K., & Koezuka, Y. (1994). Agelasphins, novel antitumor and immunostimulatory cerebrosides from the marine sponge Agelas mauritianus. *Tetrahedron*, *50*(9), 2771–2784. https://doi.org/10.1016/S0040-4020(01)86991-X

Newcomb, D. C., Zhou, W., Moore, M. L., Goleniewska, K., Hershey, G. K. K., Kolls, J. K., & Peebles, R. S. (2009). A functional IL-13 receptor is expressed on polarized murine CD4+ Th17 cells and IL-13 signaling attenuates Th17 cytokine production. *Journal of Immunology (Baltimore, Md. : 1950)*, *182*(9), 5317–5321. https://doi.org/10.4049/JIMMUNOL.0803868

Noben-Trauth, N., Kropf, P., & Müller, I. (1996). Susceptibility to Leishmania major infection in interleukin-4-deficient mice. *Science (New York, N.Y.)*, *271*(5251), 987–990. https://doi.org/10.1126/SCIENCE.271.5251.987

O'Garra, A., & Vieira, P. (2007). T(H)1 cells control themselves by producing interleukin-10. *Nature Reviews. Immunology*, *7*(6), 425–428. https://doi.org/10.1038/NRI2097

Oliveira, P. R. S., Dessein, H., Romano, A., Cabantous, S., de Brito, M. E. F., Santoro, F., Pitta, M. G. R., Pereira, V., Pontes-de-Carvalho, L. C., Rodrigues, V., Rafati, S., Argiro, L., & Dessein, A. J. (2015). IL2RA genetic variants reduce IL-2-dependent responses and aggravate human cutaneous leishmaniasis. *Journal of Immunology (Baltimore, Md. : 1950)*, *194*(6), 2664–2672. https://doi.org/10.4049/JIMMUNOL.1402047

Pacheco-Fernandez, T., Volpedo, G., Gannavaram, S., Bhattacharya, P., Dey, R., Satoskar, A., Matlashewski, G., & Nakhasi, H. L. (2021). Revival of Leishmanization and Leishmanin. *Frontiers in Cellular and Infection*

Microbiology, *11*(March), 1–11. https://doi.org/10.3389/fcimb.2021.639801

Pacheco-Soares, C., Gaziri, L. C. J., Loyola, W., & Felipe, I. (1992). Phagocytosis of enteropathogenic Escherichia coli and Candida albicans by lectin-like receptors. *Brazilian Journal of Medical and Biological Research*, *25*(10), 1015–1024. https://pubmed.ncbi.nlm.nih.gov/1342822/

Pal, D. S., Abbasi, M., Mondal, D. K., Varghese, B. A., Paul, R., Singh, S., & Datta, R. (2017). Interplay between a cytosolic and a cell surface carbonic anhydrase in pH homeostasis and acid tolerance of Leishmania. *Journal of Cell Science*, *130*(4), 754–766. https://doi.org/10.1242/jcs.199422

Parish, C. R., Lang, P. G., & Ada, G. L. (1967). Tolerance in Adult Rats to a Purified Protein, Flagellin, from Salmonella adelaide. *Nature 1967 215:5106*, *215*(5106), 1202–1203. https://doi.org/10.1038/2151202a0

Parish, Christopher R. (1996). Immune deviation: a historical perspective. *Immunology and Cell Biology*, *74*(5), 449–456. https://doi.org/10.1038/ICB.1996.75

Pasparakis, M., Haase, I., & Nestle, F. O. (2014). Mechanisms regulating skin immunity and inflammation. *Nature Reviews. Immunology*, *14*(5), 289–301. https://doi.org/10.1038/NRI3646

Peiser, L., Gough, P. J., Kodama, T., & Gordon, S. (2000). Macrophage class A scavenger receptor-mediated phagocytosis of Escherichia coli: Role of cell heterogeneity, microbial strain, and culture conditions in vitro. *Infection and Immunity*, *68*(4), 1953–1963. https://doi.org/10.1128/IAI.68.4.1953-1963.2000

Peters, N. C., Egen, J. G., Secundino, N., Debrabant, A., Kamhawi, S., Lawyer, P., Fay, M. P., Germain, R. N., & Sacks, D. (2009). In vivo imaging reveals an essential role for neutrophils in Leishmaniasis transmitted by sand flies. *Science*, *321*(5891), 970–974. https://doi.org/10.1126/science.1159194.In

Peters, N. C., Pagán, A. J., Lawyer, P. G., Hand, T. W., Henrique Roma, E.,

Stamper, L. W., Romano, A., & Sacks, D. L. (2014). Chronic Parasitic Infection Maintains High Frequencies of Short-Lived Ly6C+CD4+ Effector T Cells That Are Required for Protection against Re-infection. *PLoS Pathogens*, *10*(12). https://doi.org/10.1371/journal.ppat.1004538

Platanias, L. C. (2005). Mechanisms of type-I- and type-II-interferon-mediated signalling. *Nature Reviews. Immunology*, *5*(5), 375–386. https://doi.org/10.1038/NRI1604

Prajeeth, C. K., Haeberlein, S., Sebald, H., Schleicher, U., & Bogdan, C. (2011). Leishmania-infected macrophages are targets of NK cell-derived cytokines but not of NK cell cytotoxicity. *Infection and Immunity*, *79*(7), 2699–2708. https://doi.org/10.1128/IAI.00079-11

Prina, E., Lang, T., Glaichenhaus, N., & Antoine, J. C. (1996). Presentation of the protective parasite antigen LACK by Leishmania-infected macrophages. *The Journal of Immunology*, *156*(11).

Radwanska, M., Cutler, A. J., Hoving, J. C., Magez, S., Holscher, C., Bohms, A., Arendse, B., Kirsch, R., Hunig, T., Alexander, J., Kaye, P., & Brombacher, F. (2007). Deletion of IL-4Rα on CD4 T Cells Renders BALB/c Mice Resistant to Leishmania major Infection. *PLOS Pathogens*, *3*(5), e68. https://doi.org/10.1371/JOURNAL.PPAT.0030068

Raymond, F., Boisvert, S., Roy, G., Ritt, J. F., Légaré, D., Isnard, A., Stanke, M., Olivier, M., Tremblay, M. J., Papadopoulou, B., Ouellette, M., & Corbeil, J. (2012). Genome sequencing of the lizard parasite Leishmania tarentolae reveals loss of genes associated to the intracellular stage of human pathogenic species. *Nucleic Acids Research*, *40*(3), 1131–1147. https://doi.org/10.1093/NAR/GKR834

Reguera, R. M., Balaña-Fouce, R., Showalter, M., Hickerson, S., & Beverley, S. M. (2009). Leishmania major lacking arginase (ARG) are auxotrophic for polyamines but retain infectivity to susceptible BALB/c mice. *Molecular and Biochemical Parasitology*, *165*(1), 48–56.

https://doi.org/10.1016/J.MOLBIOPARA.2009.01.001

Ribeiro-Gomes, F. L., Romano, A., Lee, S., Roffê, E., Peters, N. C., Debrabant, A., & Sacks, D. (2015). Apoptotic cell clearance of Leishmania major-infected neutrophils by dendritic cells inhibits $CD8^+$ T-cell priming in vitro by Mer tyrosine kinase-dependent signaling. *Cell Death & Disease*, *6*(12). https://doi.org/10.1038/CDDIS.2015.351

Ribeiro-Gomes, Flavia L., Moniz-de-Souza, M. C. A., Alexandre-Moreira, M. S., Dias, W. B., Lopes, M. F., Nunes, M. P., Lungarella, G., & DosReis, G. A. (2007). Neutrophils activate macrophages for intracellular killing of Leishmania major through recruitment of TLR4 by neutrophil elastase. *Journal of Immunology (Baltimore, Md. : 1950)*, *179*(6), 3988–3994. https://doi.org/10.4049/JIMMUNOL.179.6.3988

Ribeiro-Gomes, Flavia L., Peters, N. C., Debrabant, A., & Sacks, D. L. (2012). Efficient Capture of Infected Neutrophils by Dendritic Cells in the Skin Inhibits the Early Anti-Leishmania Response. *PLOS Pathogens*, *8*(2), e1002536. https://doi.org/10.1371/JOURNAL.PPAT.1002536

Rogers, M. E. (2012). The Role of Leishmania Proteophosphoglycans in Sand Fly Transmission and Infection of the Mammalian Host. *Frontiers in Microbiology*, *3*(JUN). https://doi.org/10.3389/FMICB.2012.00223

Ross, G. D., Cain, J. A., Myones, B. L., Newman, S. L., & Lachmann, P. J. (1987). Specificity of membrane complement receptor type three (CR3) for beta-glucans. *Complement (Basel, Switzerland)*, *4*(2), 61–74. https://doi.org/10.1159/000463010

Rostamian, M., Sohrabi, S., Kavosifard, H., & Niknam, H. M. (2017). Lower levels of IgG1 in comparison with IgG2a are associated with protective immunity against Leishmania tropica infection in BALB/c mice. *Journal of Microbiology, Immunology and Infection*, *50*(2), 160–166. https://doi.org/10.1016/J.JMII.2015.05.007

Roy, S., Kumar, G. A., Jafurulla, M., Mandal, C., & Chattopadhyay, A. (2014).

Integrity of the actin cytoskeleton of host macrophages is essential for Leishmania donovani infection. *Biochimica et Biophysica Acta - Biomembranes*, *1838*(8), 2011–2018. https://doi.org/10.1016/j.bbamem.2014.04.017

Sacks, D. L., & Perkins, P. V. (1984). *Identification of an Infective Stage of Leishmania Promastigotes*. *223*(4643), 1417–1419.

Sacks, D., & Noben-Trauth, N. (2002). The immunology of susceptibility and resistance to Leishmania major in mice. *Nature Reviews. Immunology*, *2*(11), 845–858. https://doi.org/10.1038/NRI933

Scharton, T. M., & Scott, P. (1993). Natural killer cells are a source of interferon gamma that drives differentiation of CD4+ T cell subsets and induces early resistance to Leishmania major in mice. *The Journal of Experimental Medicine*, *178*(2), 567–578. https://doi.org/10.1084/JEM.178.2.567

Schleicher, U., Mattner, J., Blos, M., Schindler, H., Röllinghoff, M., Karaghiosoff, M., Müller, M., Werner-Felmayer, G., & Bogdan, C. (2004). Control of Leishmania major in the absence of Tyk2 kinase. *European Journal of Immunology*, *34*(2), 519–529. https://doi.org/10.1002/eji.200324465

Scianimanico, S., Desrosiers, M., Dermine, J. F., Méresse, S., Descoteaux, A., & Desjardins, M. (1999). Impaired recruitment of the small GTPase rab7 correlates with the inhibition of phagosome maturation by Leishmania donovani promastigotes. *Cellular Microbiology*, *1*(1), 19–32. https://doi.org/10.1046/j.1462-5822.1999.00002.x

Scott, P., Natovitz, P., Coffman, R. L., Pearce, E., & Sher, A. (1988). Immunoregulation of cutaneous leishmaniasis. T cell lines that transfer protective immunity or exacerbation belong to different T helper subsets and respond to distinct parasite antigens. *The Journal of Experimental Medicine*, *168*(5), 1675–1684. https://doi.org/10.1084/JEM.168.5.1675

Scott, P., & Novais, F. O. (2016). Cutaneous leishmaniasis: Immune responses in protection and pathogenesis. *Nature Reviews Immunology*, *16*(9), 581–592.

https://doi.org/10.1038/nri.2016.72

Scumpia, P. O., Botten, G. A., Norman, J. S., Kelly-Scumpia, K. M., Spreafico, R., Ruccia, A. R., Purbey, P. K., Thomas, B. J., Modlin, R. L., & Smale, S. T. (2017). Opposing roles of Toll-like receptor and cytosolic DNA-STING signaling pathways for Staphylococcus aureus cutaneous host defense. *PLoS Pathogens*, *13*(7). https://doi.org/10.1371/JOURNAL.PPAT.1006496

Sen, S., Roy, K., Mukherjee, S., Mukhopadhyay, R., & Roy, S. (2011). Restoration of IFNγR subunit assembly, IFNγ signaling and parasite clearance in Leishmania donovani infected macrophages: role of membrane cholesterol. *PLoS Pathogens*, *7*(9). https://doi.org/10.1371/JOURNAL.PPAT.1002229

Serafim, T. D., Coutinho-Abreu, I. V., Oliveira, F., Meneses, C., Kamhawi, S., & Valenzuela, J. G. (2018). Sequential blood meals promote Leishmania replication and reverse metacyclogenesis augmenting vector infectivity. *Nature Microbiology*, *3*(5), 548–555. https://doi.org/10.1038/s41564-018-0125-7

Sharma, S., DeOliveira, R. B., Kalantari, P., Parroche, P., Goutagny, N., Jiang, Z., Chan, J., Bartholomeu, D. C., Lauw, F., Hall, J. P., Barber, G. N., Gazzinelli, R. T., Fitzgerald, K. A., & Golenbock, D. T. (2011). Innate immune recognition of an AT-rich stem-loop DNA motif in the Plasmodium falciparum genome. *Immunity*, *35*(2), 194–207. https://doi.org/10.1016/J.IMMUNI.2011.05.016

Shaw, M. H., Freeman, G. J., Scott, M. F., Fox, B. A., Bzik, D. J., Belkaid, Y., & Yap, G. S. (2006). Tyk2 Negatively Regulates Adaptive Th1 Immunity by Mediating IL-10 Signaling and Promoting IFN-γ-Dependent IL-10 Reactivation. *The Journal of Immunology*, *176*(12), 7263–7271. https://doi.org/10.4049/jimmunol.176.12.7263

Sisquella, X., Ofir-Birin, Y., Pimentel, M. A., Cheng, L., Abou Karam, P., Sampaio, N. G., Penington, J. S., Connolly, D., Giladi, T., Scicluna, B. J., Sharples, R. A., Waltmann, A., Avni, D., Schwartz, E., Schofield, L., Porat,

Z., Hansen, D. S., Papenfuss, A. T., Eriksson, E. M., … Regev-Rudzki, N. (2017). Malaria parasite DNA-harbouring vesicles activate cytosolic immune sensors. *Nature Communications*, *8*(1). https://doi.org/10.1038/s41467-017-02083-1

Smelt, S. C., Cotterell, S. E. J., Engwerda, C. R., & Kaye, P. M. (2000). B cell-deficient mice are highly resistant to Leishmania donovani infection, but develop neutrophil-mediated tissue pathology. *Journal of Immunology (Baltimore, Md. : 1950)*, *164*(7), 3681–3688. https://doi.org/10.4049/JIMMUNOL.164.7.3681

Snapper, C. M., & Paul, W. E. (1987). Interferon-gamma and B cell stimulatory factor-1 reciprocally regulate Ig isotype production. *Science (New York, N.Y.)*, *236*(4804), 944–947. https://doi.org/10.1126/SCIENCE.3107127

Srivastav, S., Kar, S., Chande, A. G., Mukhopadhyaya, R., & Das, P. K. (2012). Leishmania donovani exploits host deubiquitinating enzyme A20, a negative regulator of TLR signaling, to subvert host immune response. *Journal of Immunology (Baltimore, Md. : 1950)*, *189*(2), 924–934. https://doi.org/10.4049/JIMMUNOL.1102845

Stäger, S., Alexander, J., Carter, K. C., Brombacher, F., & Kaye, P. M. (2003). Both interleukin-4 (IL-4) and IL-4 receptor alpha signaling contribute to the development of hepatic granulomas with optimal antileishmanial activity. *Infection and Immunity*, *71*(8), 4804–4807. https://doi.org/10.1128/IAI.71.8.4804-4807.2003

Stäger, S., Alexander, J., Kirby, A. C., Botto, M., Van Rooijen, N., Smith, D. F., Brombacher, F., & Kaye, P. M. (2003). Natural antibodies and complement are endogenous adjuvants for vaccine-induced CD8+ T-cell responses. *Nature Medicine*, *9*(10), 1287–1292. https://doi.org/10.1038/NM933

Stäger, S., Maroof, A., Zubairi, S., Sanos, S. L., Kopf, M., & Kaye, P. M. (2006). Distinct roles for IL-6 and IL-12p40 in mediating protection against Leishmania donovani and the expansion of IL-10+CD4+ T Cells. *European*

Journal of Immunology, *36*(7), 1764. https://doi.org/10.1002/EJI.200635937

Stanley, A. C., de Labastida Rivera, F., Haque, A., Sheel, M., Zhou, Y., Amante, F. H., Bunn, P. T., Randall, L. M., Pfeffer, K., Scheu, S., Hickey, M. J., Saunders, B. M., Ware, C., Hill, G. R., Tamada, K., Kaye, P. M., & Engwerda, C. R. (2011). Critical roles for light and its receptors in generating T cell-mediated immunity during Leishmania Donovani infection. *PLoS Pathogens*, *7*(10). https://doi.org/10.1371/journal.ppat.1002279

Stanley, A. C., Zhou, Y., Amante, F. H., Randall, L. M., Haque, A., Pellicci, D. G., Hill, G. R., Smyth, M. J., Godfrey, D. I., & Engwerda, C. R. (2008). Activation of invariant NKT cells exacerbates experimental visceral leishmaniasis. *PLoS Pathogens*, *4*(2), 1–14. https://doi.org/10.1371/journal.ppat.1000028

Strazzulla, A., Cocuzza, S., Pinzone, M. R., Postorino, M. C., Cosentino, S., Serra, A., Cacopardo, B., & Nunnari, G. (2013). Mucosal leishmaniasis: An underestimated presentation of a neglected disease. *BioMed Research International*, *2013*. https://doi.org/10.1155/2013/805108

Sun, R., Hedl, M., & Abraham, C. (2021). TNFSF15 Promotes Antimicrobial Pathways in Human Macrophages and These Are Modulated by TNFSF15 Disease-Risk Variants. *Cmgh*, *11*(1), 249–272. https://doi.org/10.1016/j.jcmgh.2020.08.003

Sun, Y., & Cheng, Y. (2020). STING or Sting: cGAS-STING-Mediated Immune Response to Protozoan Parasites. *Trends in Parasitology*, *36*(9), 773–784. https://doi.org/10.1016/j.pt.2020.07.001

Sundar, S., Reed, S. G., Singh, V. P., Kumar, P. C. K., & Murray, H. W. (1998). Rapid accurate field diagnosis of Indian visceral leishmaniasis. *Lancet (London, England)*, *351*(9102), 563–565. https://doi.org/10.1016/S0140-6736(97)04350-X

Sung, S. S. J., Nelson, R. S., & Silverstein, S. C. (1983). Yeast mannans inhibit binding and phagocytosis of zymosan by mouse peritoneal macrophages.

Journal of Cell Biology, *96*(1), 160–166. https://doi.org/10.1083/jcb.96.1.160

Sypek, J. P., Chung, C. L., Mayor, S. E. H., Subramanyam, J. M., Goldman, S. J., Sieburth, D. S., Wolf, S. F., & Schaub, R. G. (1993). Resolution of cutaneous leishmaniasis: interleukin 12 initiates a protective T helper type 1 immune response. *The Journal of Experimental Medicine*, *177*(6), 1797–1802. https://doi.org/10.1084/JEM.177.6.1797

Taylor, M. E., Conary, J. T., Lennartz, M. R., Stahl, P. D., & Drickamer, K. (1990). Primary structure of the mannose receptor contains multiple motifs resembling carbohydrate-recognition domains. *Journal of Biological Chemistry*, *265*(21), 12156–12162. https://doi.org/10.1016/s0021-9258(19)38325-5

Teixeira, M. J., Dumet Fernandes, J., Romero Teixeira, C., Bezerril Andrade, B., Lima Pompeu, M., Santana Da Silva, J., Brodskyn, C. I., Barral-Netto, M., & Barral, A. (2005). Distinct Leishmania braziliensis isolates induce different paces of chemokine expression patterns. *Infection and Immunity*, *73*(2), 1191–1195. https://doi.org/10.1128/IAI.73.2.1191-1195.2005

Thomas, B. N., & Buxbaum, L. U. (2008). FcgammaRIII mediates immunoglobulin G-induced interleukin-10 and is required for chronic Leishmania mexicana lesions. *Infection and Immunity*, *76*(2), 623–631. https://doi.org/10.1128/IAI.00316-07

Titus, R. G., Dekrey, G. K., Morris, R. V., & Soares, M. B. P. (2001). Interleukin-6 deficiency influences cytokine expression in susceptible BALB mice infected with Leishmania major but does not alter the outcome of disease. *Infection and Immunity*, *69*(8), 5189–5192. https://doi.org/10.1128/IAI.69.8.5189-5192.2001

Titus, R. G., Marchand, M., Boon, T., & Louis, J. A. (1985). A limiting dilution assay for quantifying Leishmania major in tissues of infected mice. *Parasite Immunology*, *7*(5), 545–555. https://doi.org/10.1111/j.1365-3024.1985.tb00098.x

Toellner, K. M., Luther, S. A., Sze, D. M. Y., Choy, R. K. W., Taylor, D. R.,

MacLennan, I. C. M., & Acha-Orbea, H. (1998). T Helper 1 (Th1) and Th2 Characteristics Start to Develop During T Cell Priming and Are Associated with an Immediate Ability to Induce Immunoglobulin Class Switching. *The Journal of Experimental Medicine*, *187*(8), 1193. https://doi.org/10.1084/JEM.187.8.1193

Tolouei, S., Hejazi, S. H., Ghaedi, K., Khamesipour, A., & Hasheminia, S. J. (2013). TLR2 and TLR4 in Cutaneous Leishmaniasis Caused by Leishmania major. *Scandinavian Journal of Immunology*, *78*(5), 478–484. https://doi.org/10.1111/sji.12105

Tomiotto-Pellissier, F., Bortoleti, B. T. da S., Assolini, J. P., Gonçalves, M. D., Carloto, A. C. M., Miranda-Sapla, M. M., Conchon-Costa, I., Bordignon, J., & Pavanelli, W. R. (2018). Macrophage Polarization in Leishmaniasis: Broadening Horizons. *Frontiers in Immunology*, *0*, 2529. https://doi.org/10.3389/FIMMU.2018.02529

Ueno, N., Bratt, C. L., Rodriguez, N. E., & Wilson, M. E. (2009). Differences in human macrophage receptor usage, lysosomal fusion kinetics and survival between logarithmic and metacyclic Leishmania infantum chagasi promastigotes. *Cellular Microbiology*, *11*(12), 1827–1841. https://doi.org/10.1111/j.1462-5822.2009.01374.x

Ueno, N., & Wilson, M. E. (2012). Receptor-mediated phagocytosis of Leishmania: Implications for intracellular survival. *Trends in Parasitology*, *28*(8), 335–344. https://doi.org/10.1016/j.pt.2012.05.002

Uzonna, J. E., Joyce, K. L., & Scott, P. (2004). Low dose Leishmania major promotes a transient T helper cell type 2 response that is down-regulated by interferon gamma-producing CD8+ T cells. *The Journal of Experimental Medicine*, *199*(11), 1559–1566. https://doi.org/10.1084/JEM.20040172

Van Bockstal, L., Bulté, D., Van den Kerkhof, M., Dirkx, L., Mabille, D., Hendrickx, S., Delputte, P., Maes, L., & Caljon, G. (2020). Interferon Alpha Favors Macrophage Infection by Visceral Leishmania Species Through

Upregulation of Sialoadhesin Expression. *Frontiers in Immunology*, *11*(June), 1–11. https://doi.org/10.3389/fimmu.2020.01113

van der Laan, L. J., Döpp, E. A., Haworth, R., Pikkarainen, T., Kangas, M., Elomaa, O., Dijkstra, C. D., Gordon, S., Tryggvason, K., & Kraal, G. (1999). Regulation and functional involvement of macrophage scavenger receptor MARCO in clearance of bacteria in vivo. *Journal of Immunology (Baltimore, Md. : 1950)*, *162*(2), 939–947. http://www.ncbi.nlm.nih.gov/pubmed/9916718

van Zandbergen, G., Klinger, M., Mueller, A., Dannenberg, S., Gebert, A., Solbach, W., & Laskay, T. (2004). Cutting Edge: Neutrophil Granulocyte Serves as a Vector for Leishmania Entry into Macrophages. *The Journal of Immunology*, *173*(11), 6521–6525. https://doi.org/10.4049/jimmunol.173.11.6521

Van Zandbergen, Ger, Bollinger, A., Wenzel, A., Kamhawi, S., Voll, R., Klinger, M., Müller, A., Hölscher, C., Herrmann, M., Sacks, D., Solbach, W., & Laskay, T. (2006). Leishmania disease development depends on the presence of apoptotic promastigotes in the virulent inoculum. *Proceedings of the National Academy of Sciences of the United States of America*, *103*(37), 13837–13842. https://doi.org/10.1073/pnas.0600843103

Verma, J. K., Rastogi, R., & Mukhopadhyay, A. (2017). Leishmania donovani resides in modified early endosomes by upregulating Rab5a expression via the downregulation of miR-494. *PLoS Pathogens*, *13*(6), 1–25. https://doi.org/10.1371/journal.ppat.1006459

Vinet, A. F., Fukuda, M., Turco, S. J., & Descoteaux, A. (2009). The Leishmania donovani lipophosphoglycan excludes the vesicular proton-ATPase from phagosomes by impairing the recruitment of Synaptotagmin V. *PLoS Pathogens*, *5*(10). https://doi.org/10.1371/journal.ppat.1000628

Volpedo, G., Pacheco-Fernandez, T., Holcomb, E. A., Cipriano, N., Cox, B., & Satoskar, A. R. (2021). Mechanisms of Immunopathogenesis in Cutaneous Leishmaniasis And Post Kala-azar Dermal Leishmaniasis (PKDL). *Frontiers*

in Cellular and Infection Microbiology, 11, 512. https://doi.org/10.3389/FCIMB.2021.685296/BIBTEX

Von Stebut, E., Ehrchen, J. M., Belkaid, Y., Kostka, S. L., Mölle, K., Knop, J., Sunderkötter, C., & Udey, M. C. (2003). Interleukin 1α Promotes Th1 Differentiation and Inhibits Disease Progression in Leishmania major–susceptible BALB/c Mice. *The Journal of Experimental Medicine, 198*(2), 191. https://doi.org/10.1084/JEM.20030159

Wang, P., Li, S., Zhao, Y., Zhang, B., Li, Y., Liu, S., Du, H., Cao, L., Ou, M., Ye, X., Li, P., Gao, X., Wang, P., Jing, C., Shao, F., Yang, G., & You, F. (2019). The GRA15 protein from Toxoplasma gondii enhances host defense responses by activating the interferon stimulator STING. *Journal of Biological Chemistry*, *294*(45), 16494–16508. https://doi.org/10.1074/JBC.RA119.009172

Wang, X., & Mosmann, T. (2001). In vivo priming of CD4 T cells that produce interleukin (IL)-2 but not IL-4 or interferon (IFN)-gamma, and can subsequently differentiate into IL-4- or IFN-gamma-secreting cells. *The Journal of Experimental Medicine, 194*(8), 1069–1080. https://doi.org/10.1084/JEM.194.8.1069

Whitaker, S. M., Colmenares, M., Pestana, K. G., & McMahon-Pratt, D. (2008). Leishmania pifanoi proteoglycolipid complex P8 induces macrophage cytokine production through Toll-like receptor 4. *Infection and Immunity*, *76*(5), 2149–2156. https://doi.org/10.1128/IAI.01528-07

World Health Organziation. Leishmaniasis. (2022). https://www.who.int/news-room/fact-sheets/detail/leishmaniasis

Wu, J., Tian, L., Yu, X., Pattaradilokrat, S., Li, J., Wang, M., Yu, W., Qi, Y., Zeituni, A. E., Nair, S. C., Crampton, S. P., Orandle, M. S., Bolland, S. M., Qi, C. F., Long, C. A., Myers, T. G., Coligan, J. E., Wang, R., & Su, X. Z. (2014). Strain-specific innate immune signaling pathways determine malaria parasitemia dynamics and host mortality. *Proceedings of the National*

Academy of Sciences of the United States of America, *111*(4), E511–E520. https://doi.org/10.1073/PNAS.1316467111/-/DCSUPPLEMENTAL

Xu, G., Liu, D., Okwor, I., Wang, Y., Korner, H., Kung, S. K. P., Fu, Y.-X., & Uzonna, J. E. (2007). LIGHT Is Critical for IL-12 Production by Dendritic Cells, Optimal CD4 + Th1 Cell Response, and Resistance to Leishmania major . *The Journal of Immunology*, *179*(10), 6901–6909. https://doi.org/10.4049/jimmunol.179.10.6901

Yu, X., Cai, B., Wang, M., Tan, P., Ding, X., Wu, J., Li, J., Li, Q., Liu, P., Xing, C., Wang, H. Y., Su, X. zhuan, & Wang, R. F. (2016). Cross-Regulation of Two Type I Interferon Signaling Pathways in Plasmacytoid Dendritic Cells Controls Anti-malaria Immunity and Host Mortality. *Immunity*, *45*(5), 1093–1107. https://doi.org/10.1016/J.IMMUNI.2016.10.001

Zamboni, D. S., & Sacks, D. L. (2019). Inflammasomes and Leishmania: in good times or bad, in sickness or in health. *Current Opinion in Microbiology*, *52*, 70–76. https://doi.org/10.1016/j.mib.2019.05.005

Zhang, W. W., Karmakar, S., Gannavaram, S., Dey, R., Lypaczewski, P., Ismail, N., Siddiqui, A., Simonyan, V., Oliveira, F., Coutinho-Abreu, I. V., DeSouza-Vieira, T., Meneses, C., Oristian, J., Serafim, T. D., Musa, A., Nakamura, R., Saljoughian, N., Volpedo, G., Satoskar, M., … Nakhasi, H. L. (2020). A second generation leishmanization vaccine with a markerless attenuated Leishmania major strain using CRISPR gene editing. *Nature Communications*, *11*(1), 1–14. https://doi.org/10.1038/s41467-020-17154-z

APPENDICES

A. Culture, collection and freezing media recipes

Table A.1. Leishmania Growth Medium

Component	Final Concentration	Company	Cat no:
Heat Inactivated FBS	20% (v/v)	Biological Industries, Israel	04-127-1A
HEPES buffer 1M	20 mM	Biological Industries, Israel	03-025-1B
Penicillin/Streptomycin (Pen/Strep) Solution	Pen: 100 units/ml Strep: 100 µg/ml	Biological Industries, Israel	03-031-1B
RPMI 1640 Medium with L-glutamine and Phenol Red	-	Biological Industries, Israel	01-100-1A

Table A.2. Leishmania Freezing Medium

Component	Final Concentration	Company	Cat no:
Heat Inactivated FBS	40% (v/v)	Biological Industries, Israel	04-127-1A
Dimethyl Sulfoxide (DMSO)	20% (v/v)	Merck, Germany	D8418

Table A.2. (continued) *Leishmania* Freezing Medium

RPMI 1640 Medium with L-glutamine and Phenol Red	-	Biological Industries, Israel	01-100-1A

Table A.3. 2% Regular RPMI Medium

Component	**Final Concentration**	**Company**	**Cat no:**
Heat Inactivated FBS	2% (v/v)	Biological Industries, Israel	04-127-1A
HEPES buffer 1M	20 mM	Biological Industries, Israel	03-025-1B
Penicillin/Streptomycin (Pen/Strep) Solution	Pen: 100 units/ml Strep: 100 µg/ml	Biological Industries, Israel	03-031-1B
MEM Non-Essential Amino Acids Solution (100X)	1X	Biological Industries, Israel	01-340-1B
Sodium Pyruvate Solution	0.11 mg/ml	Biological Industries, Israel	03-042-1B
RPMI 1640 Medium with L-glutamine and Phenol Red	-	Biological Industries, Israel	01-100-1A

Table A.4. Exosome-free Medium

Component	Final Concentration	Company	Cat no:
Heat Inactivated FBS	10% (v/v)	Biological Industries, Israel	04-127-1A
HEPES buffer 1M	20 mM	Biological Industries, Israel	03-025-1B
Penicillin/Streptomycin (Pen/Strep) Solution	Pen: 100 units/ml Strep: 100 µg/ml	Biological Industries, Israel	03-031-1B
RPMI 1640 Medium with L-glutamine and Phenol Red	-	Biological Industries, Israel	01-100-1A

Table A.5. Exosome Collection Medium (pH: ≈5)

Component	Final Concentration	Company	Cat no:
Exosome-Free Medium (Table A.4., Appendix A)	-	-	-
MES Buffer (250mM)	25mM	Sigma- Aldrich, Germany	M1317
HCl (1N)	0.016N	Sigma- Aldrich, Germany	1003171000

Table A.6. 10% Regular RPMI Medium

Component	Final Concentration	Company	Cat no:
Heat Inactivated FBS	10% (v/v)	Biological Industries, Israel	04-127-1A
HEPES buffer 1M	20 mM	Biological Industries, Israel	03-025-1B
Penicillin/Streptomycin (Pen/Strep) Solution	Pen: 100 units/ml Strep: 100 µg/ml	Biological Industries, Israel	03-031-1B
MEM Non-Essential Amino Acids Solution (100X)	1X	Biological Industries, Israel	01-340-1B
Sodium Pyruvate Solution	0.11 mg/ml	Biological Industries, Israel	03-042-1B
RPMI 1640 Medium with L-glutamine and Phenol Red	-	Biological Industries, Israel	01-100-1A

Table A.7. THP1-Dual Freezing Medium

Component	Final Concentration	Company	Cat no:
Heat Inactivated FBS	80% (v/v)	Biological Industries, Israel	04-127-1A
Dimethyl Sulfoxide (DMSO)	20% (v/v)	Merck, Germany	D8418

Table A.8. THP1-Dual™ KO-TBK1 Freezing Medium

Component	**Final Concentration**	**Company**	**Cat no:**
Heat Inactivated FBS	90% (v/v)	Biological Industries, Israel	04-127-1A
Dimethyl Sulfoxide (DMSO)	10% (v/v)	Merck, Germany	D8418

B. Buffers for Zymography and ELISA

Table B.1. Separating Gel for Zymography for 1.0 mm plates

Component	Required Volume of Component
1.5 M Tris pH 8.8	2 mL
30% acrylamide	2 mL
dH_2O	2 mL
Gelatin (4 mg/mL)	2 mL
10% SDS	80 µL
10% APS	80 µL
TEMED	10 µL

Table B.2. Stacking Gel for Zymography for 1.0 mm plates

Component	Required Volume of Component
0.5 M Tris pH 6.8	1.25 mL
30% acrylamide	0.670 mL
dH_2O	3.075 mL
10 % SDS	50 µL
10 % APS	50 µL
TEMED	10 µL

Table B.3. Washing Buffer for Zymography

Component	Final Concentration	For 250 ml
Triton X-100	2.5%	6.25 mL of 100% stock
Tris-HCl, pH 7.5	50 mM	12.5 mL of 1 M stock
$CaCl_2$	5 mM	625 µL of 2 M stock
$ZnCl_2$	1 µM	2.5 µL of 0.1 M stock
dH_2O	-	Fill up to 250 ml

Table B.4. Incubation Buffer for Zymography

Component	Final Concentration	For 250 ml
Triton X-100	1%	2.5 mL of 100% stock
Tris-HCl, pH 7.5	50 mM	12.5 mL of 1 M stock
$CaCl_2$	5 mM	625 µL of 2 M stock
$ZnCl_2$	1 µM	2.5 µL of 0.1 M stock
dH_2O	--	Fill up to 250 ml

Table B.5. Staining Solution for Zymography

Component	For 100 ml
Methanol	40 mL
Acetic acid	10 mL
dH_2O	50 mL
Coomassie Blue	0.5 g

Table B.6. Destaining Solution for Zymography

Component	For 1 l
Methanol	400 mL
Acetic acid	100 mL
dH_2O	500 mL

Table B.7. Coating Buffer for IgG ELISA

Component	For 1 l
$NaHCO_3$	8.4 g
Na_2CO_3	3.56 g
dH_2O	Fill up to 1 l

Table B.8. Blocking Buffer for ELISA

Component	For 500 ml
1X PBS	500 ml
Bovine Serum Albumin	5 g
Tween 20	250 µl

Table B.9. ELISA Wash Buffer

Component	For 10 l
10X PBS	1 l
dH_2O	9 l
Tween-20	5 ml

Table B.10. PNPP Substrate Solution for ELISA

Component	**Required Amount (for 1 plate)**	**Company**	**Cat no:**
pNPP substrate 5 mg, tablets	1 tablet	VWR, U.S.A.	0405-100T
Diethanolamine Substrate Buffer 5X Concentrate	1 ml	Thermo Fisher Scientific, U.S.A	34064
dH_2O	4 ml	-	-

C. Buffers for PAGE

Table C.1. 10X Running Buffer for PAGE

Component	For 1 l
Tris base	30 g
Glycine	144 g
SDS	10 g
dH_2O	Fill up to 1 l

Table C.2. 1X Running Buffer for PAGE

Component	For 1 l
10X Running Buffer (Table C.1., Appendix C)	100 ml
dH_2O	900 ml

D. Assessment of Parasite Limiting Effect of Amlexanox in cGAS-KO THP1 Cells

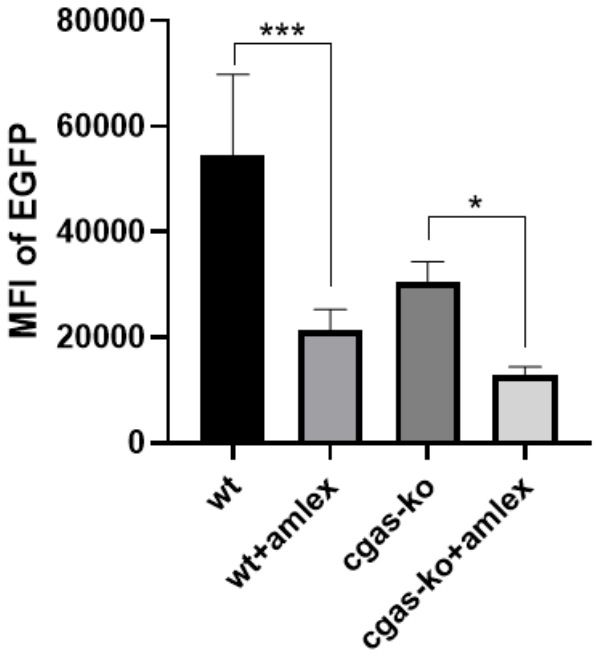

Figure D.1. Assessment of parasite limiting effect of Amlexanox in cGAS-KO THP1 cells.

Differentiated THP1 cells were infected with eGFP expressing *L. major* parasites at a MOI of 1:10 (macrophage:parasite) ratio. At 24th hour post-infection, infection percentages and parasite loads were quantified using a flow cytometer. Amlexanox addition was done 1 hour prior to infection. The graphs were constructed based on two independent experiments. The groups were statistically compared to each other using ordinary one-way ANOVA followed by Tukey's multiple comparison test (*: p=0.0403, ***: p=0.0005)